

ND-R106 811

DESIGN OF SURVIVABLE SHIPBOARD HF MAST ANTENNA MODELS 1/2

USING THE NUMERICAL ELECTROMAGNETICS CODE(U) NAVAL

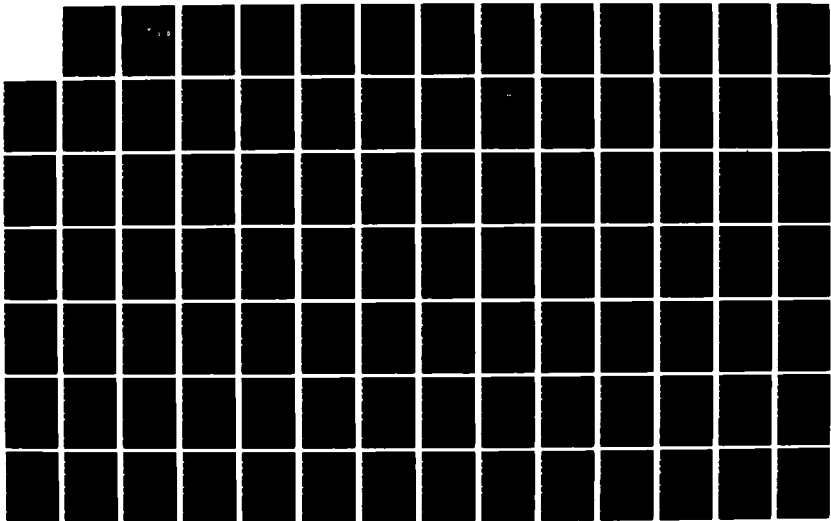
POSTGRADUATE SCHOOL MONTEREY CA I V CHOI SEP 87

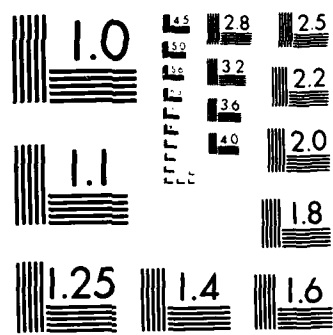
UNCLASSIFIED

NPS62-87-015

F/G 9/1

ML





MICROCOPY RESOLUTION TEST CHART  
NATIONAL BUREAU OF STANDARDS 1963-A

DTIC FILE COPY

(2)

# NAVAL POSTGRADUATE SCHOOL

## Monterey, California

AD-A186 811



DTIC  
SELECTED  
DEC 14 1987  
**S D**  
g D

# THESIS

DESIGN OF SURVIVABLE SHIPBOARD HF  
MAST ANTENNA MODELS USING THE  
NUMERICAL ELECTROMAGNETICS CODE

by

Il Yong, Choi

September 1987

Thesis Advisor

Richard W. Adler

Approved for public release; distribution is unlimited.

Prepared for: Naval Ocean Systems Center,  
San Diego, California 92152

87 11 3

NAVAL POSTGRADUATE SCHOOL

Monterey, CA 93943-5000

Rear Admiral R. C. Austin

K. T. Marshall

Superintendent

Acting Provost

This thesis is prepared in conjunction with research sponsored in part by Naval Ocean Systems Center under N6600186WR00516.

Reproduction of all or part of this report is authorized.

Released by:



Gordon E. Schacher

Dean of Science and Engineering

## REPORT DOCUMENTATION PAGE

1a REPORT SECURITY CLASSIFICATION UNCLASSIFIED		1b RESTRICTIVE MARKINGS					
2a SECURITY CLASSIFICATION AUTHORITY		3 DISTRIBUTION/AVAILABILITY OF REPORT Approved for public release; distribution is unlimited.					
2b DECLASSIFICATION/DOWNGRADING SCHEDULE							
4 PERFORMING ORGANIZATION REPORT NUMBER(S) NPS-62-87-015		5 MONITORING ORGANIZATION REPORT NUMBER(S)					
6a NAME OF PERFORMING ORGANIZATION Naval Postgraduate School	6b OFFICE SYMBOL (if applicable) 62	7a NAME OF MONITORING ORGANIZATION Naval Postgraduate School					
6c ADDRESS (City, State, and ZIP Code) Monterey, California 93943-4600		7b ADDRESS (City, State, and ZIP Code) Monterey, California 93943-5000					
8a NAME OF FUNDING/SPONSORING ORGANIZATION Naval Ocean Systems Ctr	8b OFFICE SYMBOL (if applicable) NOSC	9 PROCUREMENT INSTRUMENT IDENTIFICATION NUMBER N660186WR00516					
8c ADDRESS (City, State, and ZIP Code) San Diego, California 92152		10 SOURCE OF FUNDING NUMBERS <table border="1"> <tr> <td>PROGRAM ELEMENT NO 62121N</td> <td>PROJECT NO</td> <td>TASK NO</td> <td>WORK UNIT ACCESSION NO</td> </tr> </table>		PROGRAM ELEMENT NO 62121N	PROJECT NO	TASK NO	WORK UNIT ACCESSION NO
PROGRAM ELEMENT NO 62121N	PROJECT NO	TASK NO	WORK UNIT ACCESSION NO				

11 TITLE (Include Security Classification)

DESIGN OF SURVIVABLE SHIPBOARD HF MAST ANTENNA MODELS USING THE  
NUMERICAL ELECTROMAGNETICS CODE12 PERSONAL AUTHOR(S)  
CHOI, IL YONG13 TYPE OF REPORT  
Master's Thesis      13b TIME COVERED  
FROM \_\_\_\_\_ TO \_\_\_\_\_14 DATE OF REPORT (Year, Month Day)  
1987 September15 PAGE COUNT  
134

16 SUPPLEMENTARY NOTATION

17 COSATI CODES			18 SUBJECT TERMS (Continue on reverse if necessary and identify by block number) survivable shipboard HF mast antenna models	
FIELD	GROUP	SUB-GROUP		

19 ABSTRACT (Continue on reverse if necessary and identify by block number)

Modern combat ships are crucially dependent on electromagnetic systems including numerous and varied types of antennas. There are many shipboard communication antenna parameters such as location, number, type, and survivability of given antenna systems. Each of these parameters can be varied to determine the overall optimal system. This thesis investigates computer numerical models to improve combat survivability for HF shipboard antenna systems. Future generations of ships will have low profile combat survivable antennas. Possible improvements for present ships might be the elimination of fragile HF antennas by exciting existing mast structures. Two mast configurations resembling an FFG-45 class ship are investigated for various heights: (1) a simplified rectangular column representing a forward mast, and (2) a tapered

20 DISTRIBUTION/AVAILABILITY OF ABSTRACT <input checked="" type="checkbox"/> UNCLASSIFIED/UNLIMITED <input type="checkbox"/> SAME AS RPT <input type="checkbox"/> DTIC USERS			21 ABSTRACT SECURITY CLASSIFICATION UNCLASSIFIED	
22a NAME OF RESPONSIBLE INDIVIDUAL R. W. Adler			22b TELEPHONE (Include Area Code) 408-646-2352	22c OFFICE SYMBOL 62Ab

## UNCLASSIFIED

SECURITY CLASSIFICATION OF THIS PAGE (When Data Entered)

## 19. continued

column containing more details and closely resembling an after mast. The masts are modeled by using surface patches and wire grids. Six computer models of the given masts are developed by the Numerical Electromagnetics Code (NEC). Average power gain, input impedance, and radiation patterns of driven antennas are presented and the results between surface patch models and wire grid models are compared for frequencies from 2 MHz through 16 MHz. It is seen that good performance is possible, for several different feed methods, when using existing mast structures for 2-16 MHz. Some feeding techniques and NEC modeling options that were tried were unsuccessful and yielded non-physical results.



Accession For	
NTIS CRA&I	<input checked="" type="checkbox"/>
OVIC TAB	<input type="checkbox"/>
Unannounced	<input type="checkbox"/>
Justification	
By _____	
Distribution/	
Availability Codes	
1 Day	<input type="checkbox"/> Standard
A-1	

S N 0102-LF-014-6601

UNCLASSIFIED

Approved for public release; distribution is unlimited.

Design of Survivable Shipboard HF  
Mast Antenna Models Using The  
Numerical Electromagnetics Code

by

Il Yong, Choi  
Lieutenant, Republic of Korean Navy  
B.S., Korean Naval Academy, 1981

Submitted in partial fulfillment of the  
requirements for the degree of

MASTER OF SCIENCE IN ELECTRICAL ENGINEERING

from the

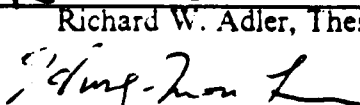
NAVAL POSTGRADUATE SCHOOL  
September 1987

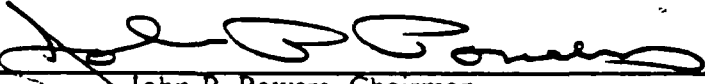
Author:

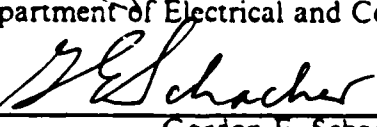
  
Il Yong, Choi

Approved by:

  
Richard W. Adler, Thesis Advisor

  
Hung-Mou Lee, Second Reader

  
John P. Powers, Chairman,  
Department of Electrical and Computer Engineering

  
Gordon E. Schacher,  
Dean of Science and Engineering

## ABSTRACT

Modern combat ships are crucially dependent on electromagnetic systems including numerous and varied types of antennas. There are many shipboard communication antenna parameters such as location, number, type, and survivability of given antenna systems. Each of these parameters can be varied to determine the overall optimal system. This thesis investigates computer numerical models to improve combat survivability for HF shipboard antenna systems. Future generations of ships will have low profile combat survivable antennas. Possible improvements for present ships might be the elimination of fragile HF antennas by exciting existing mast structures. Two mast configurations resembling an FFG-45 class ship are investigated for various heights: (1) a simplified rectangular column representing a forward mast, and (2) a tapered column containing more details and closely resembling an after mast. The masts are modeled by using surface patches and wire grids. Six computer models of the given masts are developed by the Numerical Electromagnetics Code (NEC). Average power gain, input impedance, and radiation patterns of driven antennas are presented and the results between surface patch models and wire grid models are compared for frequencies from 2 MHz through 16 MHz. It is seen that good performance is possible, for several different feed methods, when using existing mast structures for 2-16 MHz. Some feeding techniques and NEC modeling options that were tried were unsuccessful and yielded non-physical results.

## TABLE OF CONTENTS

I.	INTRODUCTION .....	13
A.	NEED FOR THE STUDY .....	13
B.	STATEMENT OF THE PROBLEM .....	15
C.	HISTORICAL BACKGROUND .....	15
D.	SCOPE AND LIMITATIONS .....	16
1.	Scope of the Study .....	16
2.	Limitation of the Study .....	16
II.	COMPUTER MODEL DEVELOPMENT .....	18
A.	OVERVIEW OF MODELING TECHNIQUES .....	18
B.	MODEL 1 (SUB-MAST SURFACE PATCH MODEL) .....	22
C.	MODEL 2 (SUB-MAST WIRE GRID MODEL) .....	22
D.	MODEL 3 (MAIN-MAST SURFACE PATCH MODEL) .....	26
E.	MODEL 4 (MAIN-MAST WIRE GRID MODEL) .....	31
III.	COMPUTER MODEL RESULTS .....	34
A.	OVERVIEW OF RESULTS .....	34
B.	MODEL 1 RESULTS .....	38
1.	Average Power Gain of Model 1 .....	38
2.	Input Impedance of Model 1 .....	40
3.	Radiation Patterns of Model 1 .....	40
4.	Voltage Standing Wave Ratio of Model 1 .....	44
C.	MODEL 2 RESULTS .....	44
1.	Average Power Gain of Model 2 .....	44
2.	Input Impedance of Model 2 .....	47
3.	Radiation Patterns of Model 2 .....	48
4.	Voltage Standing Wave Ratio of Model 2 .....	48
D.	MODEL 3 RESULTS .....	53
1.	Average Power Gain of Model 3 .....	53

2.	Input Impedance of Model 3 .....	57
3.	Radiation Patterns of Model 3 .....	57
4.	Voltage Standing Wave Ratio of Model 3 .....	57
E.	<b>MODEL 4 RESULTS .....</b>	<b>65</b>
1.	Average Power Gain of Model 4 .....	65
2.	Input Impedance of Model 4 .....	65
3.	Radiation Patterns of Model 4 .....	65
4.	Voltage Standing Wave Ratio of Model 4 .....	65
IV.	<b>SUMMARY .....</b>	<b>75</b>
A.	<b>CONCLUSIONS .....</b>	<b>75</b>
B.	<b>RECOMMENDATIONS .....</b>	<b>77</b>
<b>APPENDIX A: GEOMETRY DATA SETS .....</b>		<b>79</b>
a.	Model 1 Geometry Data Set .....	79
b.	Model 2 Geometry Data Set .....	80
c.	Model 2A Geometry Data Set .....	80
d.	Model 2B Geometry Data Set .....	81
e.	Model 3 Geometry Data Set .....	82
f.	Model 4 Geometry Data Set .....	83
<b>APPENDIX B: MODEL 2 RESULTS FOR DIFFERENT FEED METHODS. ....</b>		<b>85</b>
<b>APPENDIX C: MODEL 3 RESULTS FOR DIFFERENT FEED METHODS. ....</b>		<b>106</b>
<b>APPENDIX D: MODEL 4 RESULTS FOR DIFFERENT FEED METHODS. ....</b>		<b>112</b>
<b>LIST OF REFERENCES .....</b>		<b>127</b>
<b>INITIAL DISTRIBUTION LIST .....</b>		<b>128</b>

## LIST OF TABLES

1. CONFIGURATION FOR EACH MODEL .....	22
2. MODEL 1 FREQUENCY AND GEOMETRY DATA IN WAVELENGTHS .....	24
3. MODEL 2 FREQUENCY AND GEOMETRY DATA IN WAVELENGTHS .....	26
4. MODEL 3 FREQUENCY AND GEOMETRY DATA IN WAVELENGTHS .....	30
5. MODEL 4 FREQUENCY AND GEOMETRY DATA IN WAVELENGTHS .....	33
6. MODEL 1 AVERAGE POWER GAIN IN FREQUENCY 2-10 MHZ .....	40
7. MODEL 1 3:1 VSWR AND MATCHABLE REGIONS .....	47
8. MODEL 2 AVERAGE POWER GAIN IN FREQUENCY 2-10 MHZ .....	48
9. MODEL 2A AND 2B AVERAGE POWER GAIN IN FREQUENCY 2-10 MHZ .....	49
10. MODEL 2 3:1 VSWR AND MATCHABLE REGIONS .....	53
11. MODEL 3 AVERAGE POWER GAIN IN FREQUENCY 2-16 MHZ .....	56
12. MODEL 3 3:1 VSWR AND MATCHABLE REGIONS .....	62
13. MODEL 4 AVERAGE POWER GAIN IN FREQUENCY 2-8 MHZ .....	66
14. MODEL 4 AVERAGE POWER GAIN IN FREQUENCY 8-16 MHZ .....	67
15. MODEL 4 3:1 VSWR AND MATCHABLE REGIONS .....	72
16. MODEL 2 INPUT IMPEDANCE IN FREQUENCY 2-10 MHZ FOR FOUR BASE FEEDS .....	85
17. MODEL 2 INPUT IMPEDANCE IN FREQUENCY 2-10 MHZ FOR THREE BASE FEEDS .....	87
18. MODEL 2 INPUT IMPEDANCE IN FREQUENCY 2-10 MHZ FOR TWO DIAGONAL BASE FEEDS .....	89
19. MODEL 2 INPUT IMPEDANCE IN FREQUENCY 2-10 MHZ FOR ONE BASE FEED .....	91
20. MODEL 2A INPUT IMPEDANCE IN FREQUENCY 2-10 MHZ FOR FOUR EXTERNAL SHUNT FEEDS .....	93

21. MODEL 3 INPUT IMPEDANCE IN FREQUENCY 2-16 MHZ FOR FOUR EXTERNAL SHUNT FEEDS .....	107
22. MODEL 3 INPUT IMPEDANCE IN FREQUENCY 2-16 MHZ FOR TWO EXTERNAL SHUNT FEEDS .....	108
23. MODEL 4 INPUT IMPEDANCE IN FREQUENCY 2-8 MHZ FOR FOUR BASE FEEDS .....	112
24. MODEL 4 INPUT IMPEDANCE IN FREQUENCY 8-16 MHZ FOR FOUR BASE FEEDS .....	113
25. MODEL 4 INPUT IMPEDANCE IN FREQUENCY 2-8 MHZ FOR THREE BASE FEEDS .....	115
26. MODEL 4 INPUT IMPEDANCE IN FREQUENCY 8-16 MHZ FOR THREE BASE FEEDS .....	117
27. MODEL 4 INPUT IMPEDANCE IN FREQUENCY 2-8 MHZ FOR ONE BASE FEED .....	119
28. MODEL 4 INPUT IMPEDANCE IN FREQUENCY 8-16 MHZ FOR ONE BASE FEED .....	121

## LIST OF FIGURES

2.1	Sub-Mast Area of FFG-45 Frigate .....	18
2.2	Main-Mast Area of FFG-45 Frigate .....	19
2.3	Different Feed Types and Connection .....	21
2.4	Model 1 (Sub-Mast Surface Patch Model) .....	23
2.5	Model 2 (Sub-Mast Wire Grid Model) .....	25
2.6	Model 2A (Sub-Mast Wire Grid Model) for 4 External Shunt Feeds .....	27
2.7	Model 2B (Sub-Mast Wire Grid Model) for 1 Internal Shunt Feed .....	28
2.8	Model 3 (Main-Mast Surface Patch Model) .....	29
2.9	Model 4 (Main-Mast Wire Grid Model) .....	32
3.1	E-Field Azimuth Pattern of a 9 Meter Monopole at 2 MHz .....	35
3.2	E-Field Elevation Pattern of a 9 Meter Monopole at 10 MHz .....	36
3.3	E-Field Elevation Pattern of a 18 Meter Monopole at 16 MHz .....	37
3.4	3:1 VSWR Matchable Region in Smith Chart .....	39
3.5	Model 1 Input Impedance in Frequency 2-10 MHz for 4 External Shunt Feeds .....	41
3.6	Model 1 E-Field Azimuth Pattern at 2 MHz for 4 External Shunt Feeds .....	42
3.7	Model 1 E-Field Elevation Pattern at 10 MHz for 4 External Shunt Feeds .....	43
3.8	Model 1 Impedance Plot in Frequency 2-10 MHz for 4 External Shunt Feeds: $Z_0 = 50 \text{ Ohm}$ .....	45
3.9	Model 1 Impedance Plot in Frequency 2-10 MHz for 4 External Shunt Feeds: $Z_0 = 200 \text{ Ohm}$ .....	46
3.10	Model 2 Input Impedance in Frequency 2-10 MHz for 4 Base Feeds .....	50
3.11	Model 2 E-Field Azimuth Pattern at 2 MHz for 4 Base Feeds .....	51
3.12	Model 2 E-Field Elevation Pattern at 10 MHz for 4 Base Feeds .....	52
3.13	Model 2 Impedance Plot in Frequency 2-10 MHz for 4 Base Feeds: $Z_0 = 50 \text{ Ohm}$ .....	54
3.14	Model 2 Impedance Plot in Frequency 2-10 MHz for 4 Base Feeds: $Z_0 = 150 \text{ Ohm}$ .....	55

3.15	Model 3 Input Impedance in Frequency 2-16 MHz for 4 External Shunt Feeds .....	58
3.16	Model 3 E-Field Elevation Pattern at 2 MHz for 4 External Shunt Feeds .....	59
3.17	Model 3 E-Field Azimuth Pattern at 16 MHz for 4 External Shunt Feeds .....	60
3.18	Model 3 E-Field Elevation Pattern at 16 MHz for 4 External Shunt Feeds .....	61
3.19	Model 3 Impedance Plot in Frequency 2-16 MHz for 4 External Shunt Feeds: $Z_0 = 50 \text{ Ohm}$ .....	63
3.20	Model 3 Impedance Plot in Frequency 2-16 MHz for 4 External Shunt Feeds: $Z_0 = 150 \text{ Ohm}$ .....	64
3.21	Model 4 Input Impedance in Frequency 2-8 MHz for 4 Base Feeds .....	68
3.22	Model 4 Input Impedance in Frequency 8-16 MHz for 4 Base Feeds .....	69
3.23	Model 4 E-Field Azimuth Pattern at 2 MHz for 4 Base Feeds .....	70
3.24	Model 4 E-Field Elevation Pattern at 16 MHz for 4 Base Feeds .....	71
3.25	Model 4 Impedance Plot in Frequency 2-16 MHz for 4 Base Feeds: $Z_0 = 50 \text{ Ohm}$ .....	73
3.26	Model 4 Impedance Plot in Frequency 2-16 MHz for 4 Base Feeds: $Z_0 = 300 \text{ Ohm}$ .....	74
B.1	Model 2 Input Impedance in Frequency 2-10 MHz for 3 Base Feeds .....	86
B.2	Model 2 Input Impedance in Frequency 2-10 MHz for 2 Diagonal Base Feeds .....	88
B.3	Model 2 Input Impedance in Frequency 2-10 MHz for 1 Base Feed .....	90
B.4	Model 2A Input Impedance in Frequency 2-10 MHz for 4 External Shunt Feeds .....	92
B.5	Model 2 E-Field Azimuth Pattern at 2 MHz for 3 Base Feeds .....	94
B.6	Model 2 E-Field Elevation Pattern at 10 MHz for 3 Base Feeds .....	94
B.7	Model 2 E-Field Azimuth Pattern at 10 MHz for 3 Base Feeds .....	95
B.8	Model 2 E-Field Azimuth Pattern at 2 MHz for 1 Base Feed .....	96
B.9	Model 2 E-Field Elevation Pattern at 2 MHz for 1 Base Feed .....	97
B.10	Model 2 E-Field Azimuth Pattern at 10 MHz for 1 Base Feed .....	98
B.11	Model 2 E-Field Elevation Pattern at 10 MHz for 1 Base Feed .....	99
B.12	Model 2A E-Field Azimuth Pattern at 2 MHz for 4 External Shunt Feeds .....	101
B.13	Model 2 Impedance Plot in Frequency 2-10 MHz for 3 Base Feeds: $Z_0 = 150 \text{ Ohm}$ .....	101

B.14	Model 2 Impedance Plot in Frequency 2-10 MHz for 2 Diagonal Base Feeds: $Z_0 = 50 \text{ Ohm}$ .....	102
B.15	Model 2 Impedance Plot in Frequency 2-10 MHz for 1 Base Feed: $Z_0 = 50 \text{ Ohm}$ .....	103
B.16	Model 2A Impedance Plot in Frequency 2-10 MHz for 4 External Shunt feeds: $Z_0 = 50 \text{ Ohm}$ .....	104
C.1	Model 3 Input Impedance in Frequency 2-16 MHz for 2 External Shunt Feeds .....	106
C.2	Model 3 E-Field Azimuth Pattern at 16 MHz for 2 External Shunt Feeds .....	109
C.3	Model 3 E-Field Elevation Pattern at 16 MHz for 2 External Shunt Feeds .....	110
C.4	Model 3 Impedance Plot in Frequency 2-16 MHz for 2 External Shunt Feeds: $Z_0 = 300 \text{ Ohm}$ .....	111
D.1	Model 4 Input Impedance in Frequency 2-8 MHz for 3 Base Feeds .....	114
D.2	Model 4 Input Impedance in Frequency 8-16 MHz for 3 Base Feeds .....	116
D.3	Model 4 Input Impedance in Frequency 2-8 MHz for 1 Base Feed .....	118
D.4	Model 4 Input Impedance in Frequency 8-16 MHz for 1 Base Feed .....	120
D.5	Model 4 E-Field Azimuth Pattern at 16 MHz for 3 Base Feeds .....	122
D.5	Model 4 E-Field Elevation Pattern at 16 MHz for 3 Base Feeds .....	122
D.6	Model 4 E-Field Azimuth Pattern at 16 MHz for 1 Base Feed .....	123
D.7	Model 4 Impedance Plot in Frequency 2-16 MHz for 3 Base Feeds: $Z_0 = 300 \text{ Ohm}$ .....	124
D.8	Model 4 Impedance Plot in Frequency 2-16 MHz for 1 Base Feed: $Z_0 = 300 \text{ Ohm}$ .....	125

## ACKNOWLEDGEMENT

I would like to express my sincere appreciation to Dr. Richard W. Adler, my thesis advisor, and to Hung-Mou Lee, my second reader, both of whom are from the Department of Electrical and Computer Engineering of the Naval Postgraduate School.

I thank my wife, Yong-Mi, and my son, Won Sang, for their support and patience away from our home during two years in United States.

Finally, I wish to thank the 40,000,000 Korean taxpayers for having paid for my course of studies.

## I. INTRODUCTION

### A. NEED FOR THE STUDY

In recent years, as the development of electromagnetic systems has rapidly progressed, modern combat ships have employed more of these systems. Many employments of electromagnetic systems have caused problems, in that the numerous and varied types of antennas must be installed in limited available space aboard navy surface ships. These problems include interference, coupling, blockade, and isolation between the antennas and the other superstructures of a combat ship. Before trying to solve these problems, it is important to consider the overall factors in the design and modeling procedures of shipboard antenna systems.

In the search for optimum shipboard antenna designs, the designer is constantly faced with two basic facts:

- No rigorous algorithms can be developed for selecting antenna locations until all factors influencing the desirability of an antenna have been determined. Initially, a designer has to consider the location of a shipboard antenna system.
- All factors influencing antenna desirability can not be determined until all antennas are located.

The fact that these two statements are incompatible indicates that it is not possible to develop rigorous methodologies for locating an antenna on a ship. Therefore, in the first step, a designer has to test the given antenna using computer modeling procedures.

Electromagnetic radiation problems can always be represented by an integral expression with an inhomogeneous source term which can not be readily solved. The 'Method of Moments' [Ref. 1: p. 306] essentially involves a reduction of the associated integral equation to linear algebraic equations where coefficients in some appropriate expansion of the current are unknown. The resulting matrix equation can be solved for current by a high speed digital computer, and then the current can be used to solve for the far-field, near-field, impedance, and average power gain. The computer programs based on 'Method of Moments' have been developed to use computer modeling procedures. The output data of a computer model are functions of frequency, physical location, and given environments. To make the error of approximation as small as possible, the number of linear algebraic equations must be

increased. To calculate with small errors requires much computer CPU time. The amount of computer time required is dependent on the number of linear algebraic equations.

When a ship computer model is completed and good results are verified for a limited number of frequencies, the designer next resorts to brass scale modeling. The basic approach to scale modeling is to make a series of measurements on a scale model antenna installed on a brass scale ship. Frequencies are selected so that the ratio of wavelength to model size is the same as would exist on a full-sized ship. With accurately scaled models the measured antenna parameters such as patterns, impedance, and isolation will closely match those of antennas installed on full-sized ships. There are no clearly defined theoretical limitations associated with scale modeling. However, there are some practical considerations which influence the time, cost, and accuracy associated with this empirical approach. Measurements of near-fields and current distribution are very difficult on conducting surfaces, but gain and input impedance are easily obtained at all frequencies by using sweep frequency test equipment.

On the other hand, in communication systems that use the atmosphere for the transmission channel, interference and propagation conditions are strongly dependent on the transmission frequency. Theoretically, any type of modulation (e.g., A.M, F.M, SSB, PSK, FSK, etc.) could be used at any transmission frequency. However, to provide some semblance of order and for political reasons, modulation type, bandwidth, and type of information to be transmitted over designated frequency bands must be regulated. Lower frequencies such as HF are used for longer range over-the-horizon communications.

There are limiting factors in designing a shipboard communication antenna system. The amount of available space in a combat ship is limited and isolation from other antennas or from other superstructures of a ship is required. An antenna system cannot be installed in the firing zones of weapon systems, the visual navigation zones, the boat handling area, the helicopter operation area, or the fuel supplying area. The best installation areas are on masts, yardarms, and bulkheads, but because other systems are also required to be installed on these kinds of structures, the installation area is limited.

Consequently, location, number, and types of antennas are critical. Other important factors to consider in designing shipboard communication antenna systems

are survivability and vulnerability of shipboard communication antennas during combat situations. Because improved survivability of shipboard communication antennas increases the ship's fighting capabilities, survivability of communication antennas is a very important factor.

### B. STATEMENT OF THE PROBLEM

Survivability is defined as the capability of an antenna to avoid and/or endure a hostile environment. There are several kinds of survivable shipboard antenna designs that can improve the survivability of shipboard HF communication antennas. Most of them require low-profile structures. Since no low-profile combat ships are in use, this feature applies only to new ship designs and is not a short-term solution. It is possible to use slot antennas or to use the existing superstructures of a present ship. Present combat ships have available tall superstructures such as masts, stacks, bulkheads, and turrets. This thesis concentrates on survivable shipboard HF antenna designs modeled by the existing mast structures of a combat ship. The excitation of existing superstructures in the form of a mast may provide the electrical performance characteristics of an antenna for the HF frequency range. The mast structures can be developed with numerical models by using the all methods available for the surfaces with connecting wires or wire grid segments.

The purpose of this thesis is to determine the usefulness of NEC [Ref. 2] in solving this problem and to investigate the electrical performance characteristics of the mast structures when used as antennas.

### C. HISTORICAL BACKGROUND

The following studies about survivable shipboard communication antennas have been conducted at the Naval Postgraduate School:

- In September 1983, D. D. Thomson calculated the electromagnetic near-field of a broadcast monopole [Ref. 3] using the Numerical Electromagnetics Code (NEC).
- In March 1986, James C. Tertocha investigated the feasibility of electromagnetic performance characteristics for a rectangular volume [Ref. 4]
  - excited by a square patch atop a monopole centered at one of the volume's faces.
- In June 1986, George L. Lyberopoulos investigated the feasibility of a survivable HF communication antenna [Ref. 5] by exciting existing wire grid masts.

- In June 1986, Mario Cabral Neiva investigated the electromagnetic performance characteristics of a broadband shipboard HF slot antenna [Ref. 6] to improve survivability of HF communications in a combat ship.
- In December 1986, Ioannis G. Vorrias investigated the feasibility of two shipboard combat survivable HF communication antennas [Ref. 7]: one excited by a square patch atop a monopole, and the other excited by a wire connected between the center of a face that is created by a rectangular shaped notch.
- In March 1987, Constantious Theofanopoulos evaluated the performance of a half-wave resonant slot antenna over perfect ground [Ref. 8] using Numerical Electromagnetics Code.

#### D. SCOPE AND LIMITATIONS

##### 1. Scope of the Study

This thesis concentrates on survivable shipboard HF antenna designs. The ideal shipboard HF antenna is a quarter wave vertical antenna. The HF spectrum is from 2-30 MHz, so the 2 MHz frequency requires an antenna of 37.5 meters. This type of antenna is too large to be installed on a ship. The reduction of tall and large structures increases survivability of antennas during combat and the excitation of existing masts decreases the number of antennas installed in a combat ship.

Two types of masts are investigated, one for a sub-mast and the other for a main-mast of a combat ship. The sub-mast is shaped like a quadrangular pole measuring 3 x 3 x 9 meters. The main-mast is shaped like a quadrangular pole with dimensions of 4 x 4 meters at the base, 2 x 2 meters at the top, and 18 meters in height. Additional wire structures model the yardarm. (See Figures 2.1 and 2.2.) Two kinds of modeling procedures are applied in developing the survivable shipboard HF antennas using each mast: one for the surface patch models, including the feed wires, and the other for the wire grid models.

##### 2. Limitation of the Study

This thesis develops six different mast computer models as survivable shipboard HF communication antennas by using the Numerical Electromagnetics Code. Each mast computer model is independently tested by the several different feed methods without considering the interference from structures which are located near each mast.

The frequency range is limited to 2-10 MHz for all sub-mast models and 2-16 MHz for all main-mast models due to computer storage and processing time. As frequency increases, the wavelength decreases, and the required number of segments to

model an antenna increases. All mast computer models are driven over a perfect ground plane.

The validity of a numerical model is determined in part by calculating the average power gain of the antenna. An average power gain of 2.0 dBi is used to represent a theoretical antenna radiating in a half space over a perfect ground plane.

In Chapter II, six different mast models are developed by using the Numerical Electromagnetics Code (NEC). An attempt to look for the most favorable feed method is another goal of this thesis.

Chapter III presents results for average power gain, input impedance, radiation patterns, and VSWR characteristics with 3:1 standard criteria for the most favorable feeding method of the driven survivable mast communication antennas.

The final chapter, Chapter IV, summarizes the results and compares surface patch models and wire grid models. Discussions, conclusions, and recommendations for future study are presented.

The appendices include the simulation data such as geometry cards for each model, input impedance, radiation patterns, and VSWR characteristics for the different feed methods.

## II. COMPUTER MODEL DEVELOPMENT

### A. OVERVIEW OF MODELING TECHNIQUES

This chapter develops six different mast computer models. All models are chosen to improve survivability for an HF shipboard antenna system using the existing masts instead of a number of fragile HF antennas. Four sub-mast models and two main-mast models are made by using two types of FFG-45 frigate masts. Figure 2.1 and Figure 2.2, from Naval Electronic Systems Command [Ref. 9: p. 10-13] illustrate the sub-mast and main-mast area of a FFG-45 frigate.

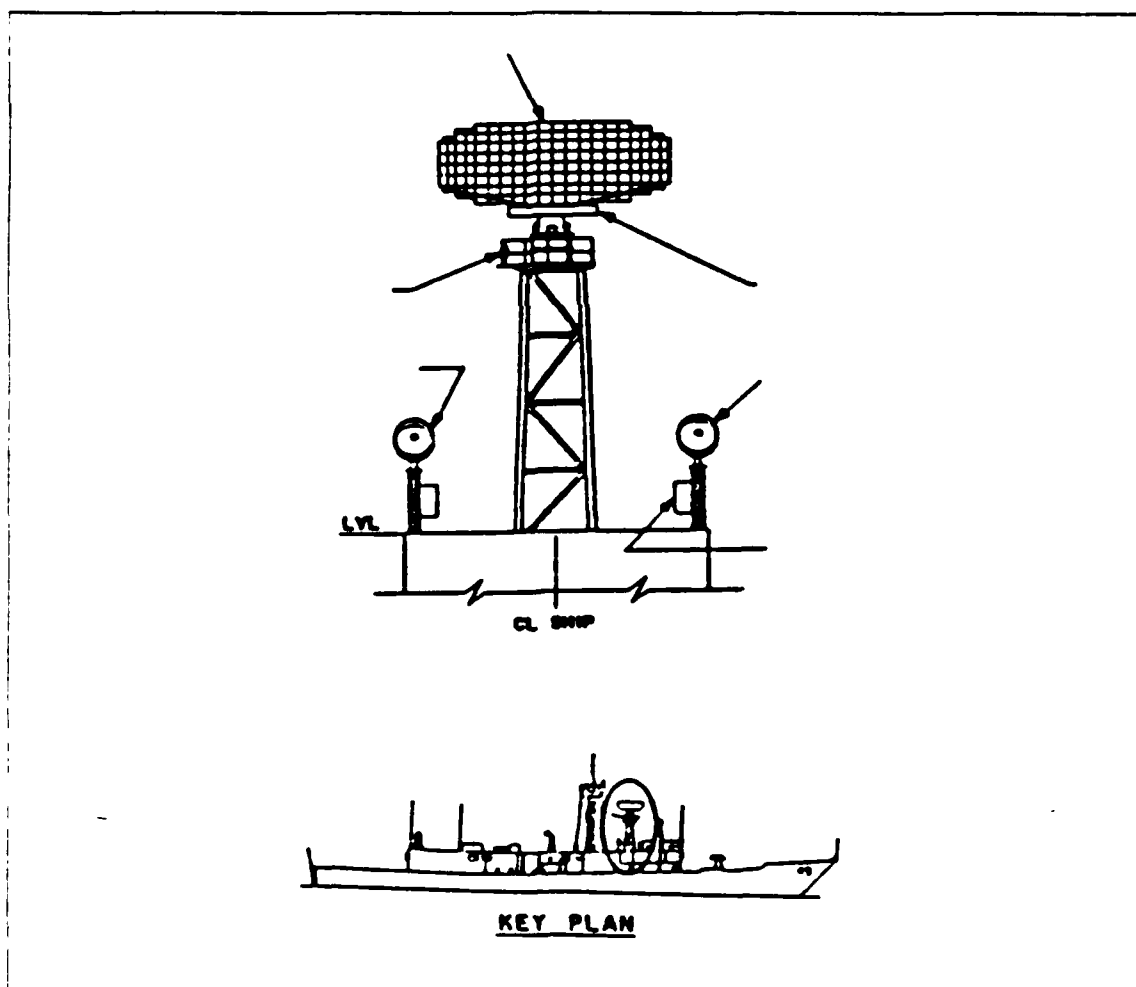


Figure 2.1 Sub-Mast Area of FFG-45 Frigate.

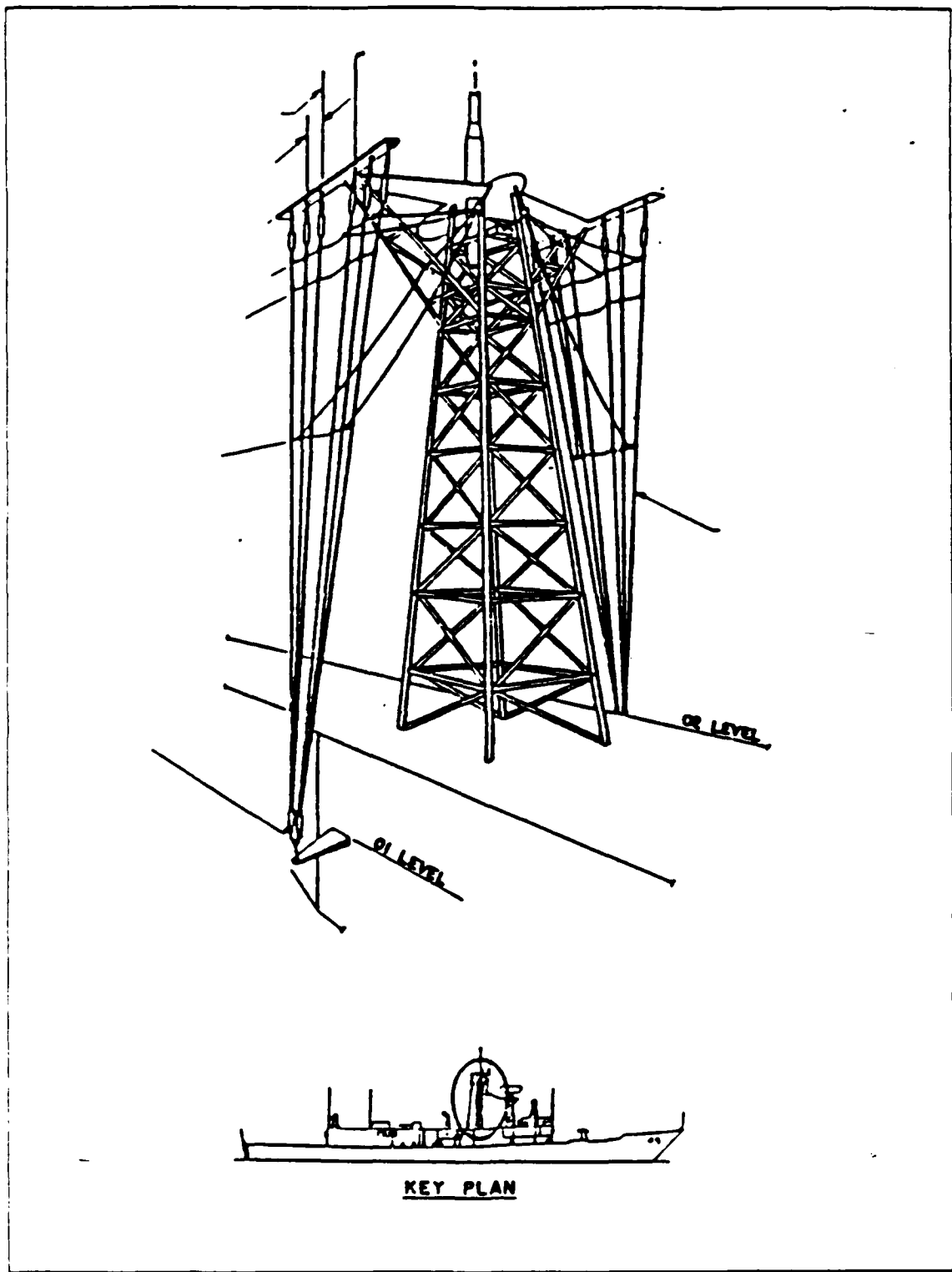


Figure 2.2 Main-Mast Area of FFG-45 Frigate.

The quadrangular sub-mast has dimensions of 3 x 3 x 9 meters. The quadrangular main-mast is 18 meters tall, tapering from 4 x 4 meters at the base to 2 x 2 meters at the top, with additional wire structures. Each mast is modeled by two different procedures: the wire grid method and the surface patch method, with connecting wires, in some instances, providing excitation of the masts.

For the wire modeling, the main electrical consideration is segment length,  $\Delta$ , relative to the wavelength,  $\lambda$ . For accurate results,  $\Delta$  should be less than approximately  $0.1\lambda$  at the desired frequency. The wire radius,  $a$ , is limited, in that the relationship  $2\pi a/\lambda < < 1$  must hold. For surface patch modeling, a minimum of 25 patches should be used per square wavelength of surface. The shape of patches does not affect the solution since there is no integration over the patch unless a wire is connected to the patch center. Very long narrow patches should be avoided when subdividing the surface and the use of surface patches is restricted to modeling voluminous bodies, those with closed continuous surfaces.

Each model is driven by several different feed methods. Figure 2.3 shows the three different feed techniques used.

For the base feed, all feed positions are located at the base segments of the mast stem without adding any additional wires. The base feed in this thesis is subdivided with five different feed methods:

- Four base feeds,
- Three base feeds,
- Two diagonal base feeds,
- Two adjacent base feeds,
- One base feed.

The base feed is used for the wire grid models and cannot apply to surface patch models.

For the external shunt feed, all feed positions are located at the base segments of feed wires. The external shunt feed is used for surface patch models or wire grid models. The external shunt feed is subdivided into two different patch methods, such as four external shunt feeds and two external shunt feeds, by the number of the feed wires of the mast. For the internal shunt feed, a feed is located at the base segments of a inside feed wire.

All sub-mast computer models are modeled and run for the frequency range 2-10 MHz and all main-mast computer models are modeled and run for 2-16 MHz. Table 1 compares the summarized data for each model in this thesis.

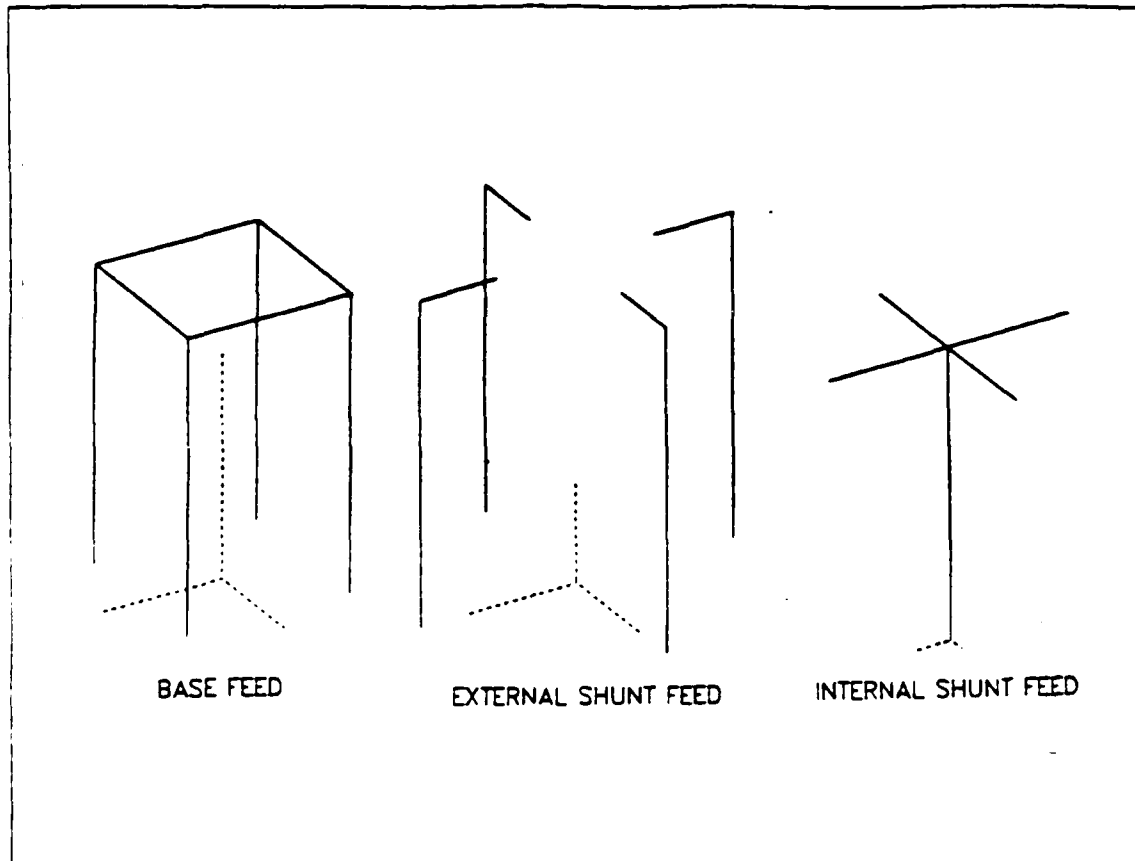


Figure 2.3 Different Feed Types and Connection.

For convenience, the sub-mast surface patch computer model is represented by 'Model 1' and the sub-mast wire grid computer model is represented by 'Model 2'. For the sub-mast wire grid model, two additional models are developed by using the four external shunt feeds and the one internal shunt feed. The modified model, with four external shunt feeds, is represented by 'Model 2A' and the other modified model, with one internal shunt feed, is represented by 'Model 2B'. The main-mast computer models are represented by 'Model 3' for the surface patch model and 'Model 4' for the wire grid model.

The MVS batch system [Ref. 10: p. 29] was used on the main frame of the IBM 3033 Network. NEC is designed for a 64 bit computer, and the IBM 3033 has 32 bits, so double precision is often needed for the low frequency range from 2 MHz to 3 MHz. Each model is briefly explained in the following sections.

TABLE 1  
CONFIGURATION FOR EACH MODEL

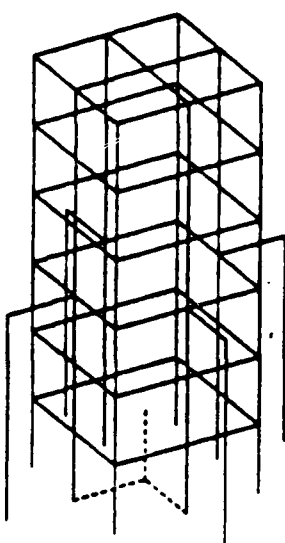
Model Name	Mast	Drive Method	Frequency Range
Model 1	Sub-Mast	Wire Grid + Surface	2-10 MHz
Model 2	Sub-Mast	Wire Grid	2-10 MHz
Model 2A	Sub-Mast	Wire Grid	2-10 MHz
Model 2B	Sub-Mast	Wire Grid	2-10 MHz
Model 3	Main-Mast	Wire Grid + Surface	2-16 MHz
Model 4	Main-Mast	Wire Grid	2-16 MHz

#### B. MODEL 1 (SUB-MAST SURFACE PATCH MODEL)

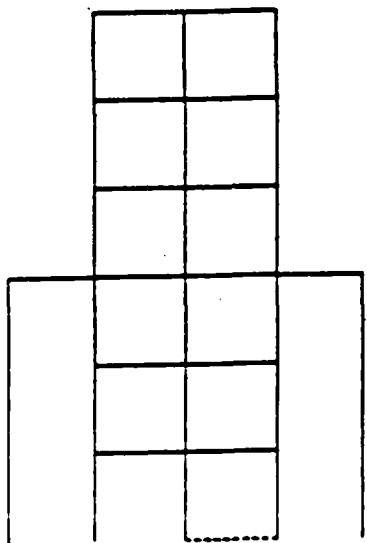
Model 1 is a surface patch mast model with dimensions 3 x 3 x 9 meters and four feed wires. Each wire has the same shape : 4.5 meter height, 0.05 meter radius, and 1.5 meter separation from the each side of the driven sub-mast surface. Figure 2.4 shows the sub-mast surface patch computer model, Model 1, and Table 2 provides the geometry data for nine different frequencies. Because the segment length is less than  $0.1\lambda$  and  $2\pi a/\lambda$  is much less than one, the wire geometry of Model 1 is adequate for the wire grid modeling procedures of NEC. Because Model 1 has fifty-two surface patches, the surface geometry is acceptable at the design frequency range. Detailed data are provided in Appendix A. Model 1 is excited by four external shunt feeds for the frequency range 2-10 MHz.

#### C. MODEL 2 (SUB-MAST WIRE GRID MODEL)

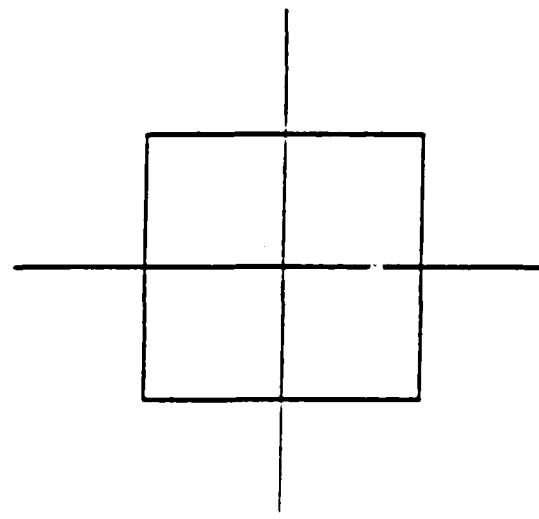
Model 2 is the sub-mast wire grid model with dimensions 3 x 3 x 9 meters. Because four base feed points are located at the base segments of the stem of the sub-mast, feed wires are not necessary. The radii of all wires are 0.05 meters and the



THETA = 60.00 PHI = 60.00 ETA = 90.00



THETA = 90.00 PHI = 0.00 ETA = 90.00



THETA = 0.00 PHI = 0.00 ETA = 90.00

Figure 2.4 Model 1 (Sub-Mast Surface Patch Model).

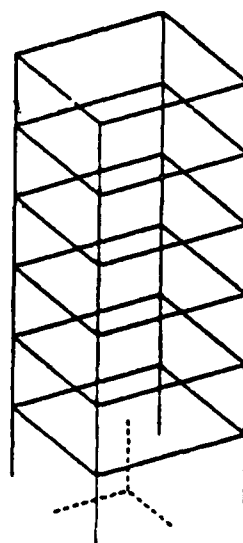
TABLE 2  
MODEL 1 FREQUENCY AND GEOMETRY DATA IN WAVELENGTHS

Frequency in MHz	Number of Patches	Number of Segments	Patches Area in Sq. meters	Seg. Len. in Wavelengths
2	52	12	2.25	0.010
3	52	12	2.25	0.015
4	52	12	2.25	0.020
5	52	12	2.25	0.025
6	52	12	2.25	0.030
7	52	12	2.25	0.035
8	52	12	2.25	0.040
9	52	12	2.25	0.045
10	52	12	2.25	0.050

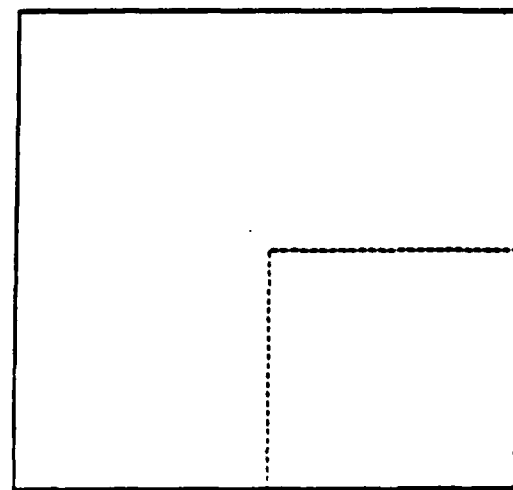
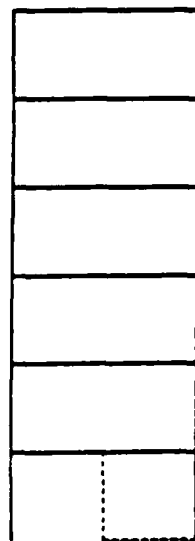
lengths of all segments are 1.5 meters. The grid is 1.5 meters high (one segment) and 3 meters wide (two segments).

Figure 2.5 shows Model 2, the sub-mast wire grid model, and Table 3 presents geometry data for nine different frequencies. Segment length is less than  $0.1\lambda$  and  $2\pi\alpha\lambda$  is much less than one,  $\lambda$  and  $\alpha$  of Model 2 are adequate. Detailed geometry data is provided in Appendix A.

To evaluate performance and find the most favorable feed method, the model is fed by two different methods. One is four external shunt feeds, located outside of the wire grid mast, as in a sleeve antenna. This was previously presented as 'Model 2A'. The other excitation is via one internal shunt feed, located inside of the wire grid sub-mast. This internal shunt wire is split into four wires to feed the source at each side of the mast. This was previously presented as 'Model 2B'. Figure 2.6 and Figure 2.7 show Model 2A and Model 2B.



THETA = 60.00 PHI = 60.00 ETA = 90.00



THETA = 90.00 PHI = 0.00 ETA = 90.00

THETA = 0.00 PHI = 0.00 ETA = 90.00

Figure 2.5 Model 2 (Sub-Mast Wire Grid Model).

TABLE 3  
MODEL 2 FREQUENCY AND GEOMETRY DATA IN WAVELENGTHS

Frequency in MHz	Number of Segments	Seg. length in Wavelengths	Grid Height in Wavelengths	Grid Width in Wavelengths
2	72	0.01000	0.01000	0.02000
3	72	0.01500	0.01500	0.03000
4	72	0.02001	0.02001	0.04001
5	72	0.02501	0.02501	0.05002
6	72	0.03002	0.03002	0.06004
7	72	0.03501	0.03501	0.07001
8	72	0.04003	0.04003	0.08004
9	72	0.04500	0.04500	0.09001
10	72	0.05003	0.05003	0.10007

Model 2 is excited by seven different feed methods for the frequency range 2-10 MHz: four base feeds, three base feeds, two diagonal base feeds, two adjacent base feeds, one base feed, four external shunt feeds, and one internal shunt feed.

#### D. MODEL 3 (MAIN-MAST SURFACE PATCH MODEL)

Model 3 is modeled by a surface main-mast with additional wire grid structures. The surface main-mast is a tapered quadrangular pole. A wire, 6 meters high and 0.3 meters in radius, stands at the center of the top surface. The yardarm is modeled by wire grids at two sides of the surface sub-mast. The radius of all wires, except the top wire, is 0.05 meters. Four feed wires are used, similar to Model 1. The surface patch size decreases as the height of the mast increases.

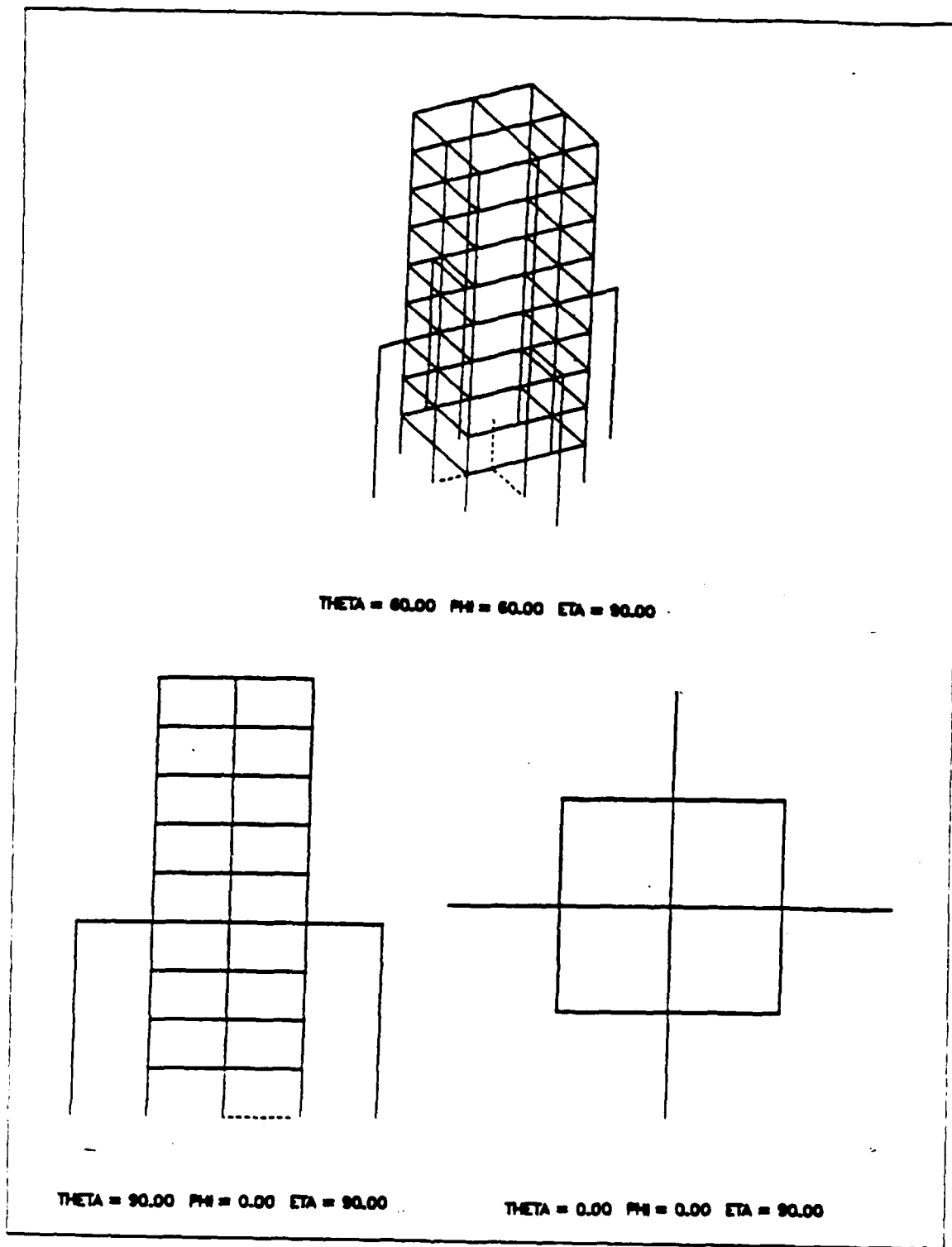
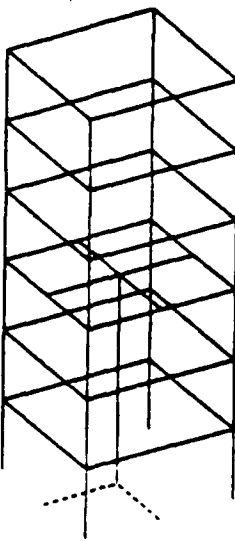
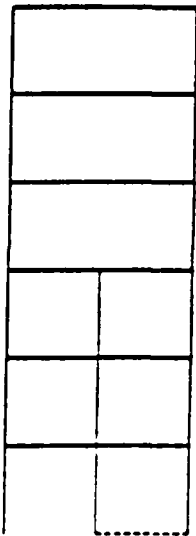


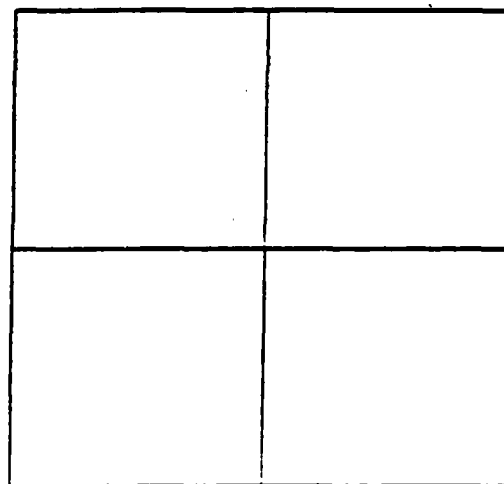
Figure 2.6 Model 2A (Sub-Mast Wire Grid Model)  
for 4 External Shunt Feeds.



THETA = 60.00 PHI = 60.00 ETA = 90.00

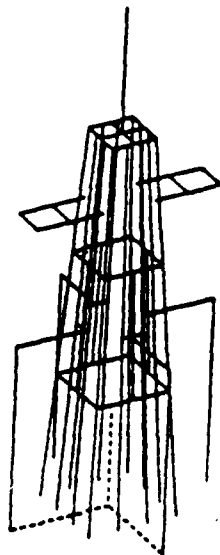


THETA = 90.00 PHI = 0.00 ETA = 90.00

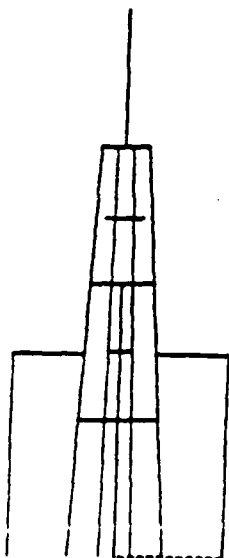


THETA = 0.00 PHI = 0.00 ETA = 90.00

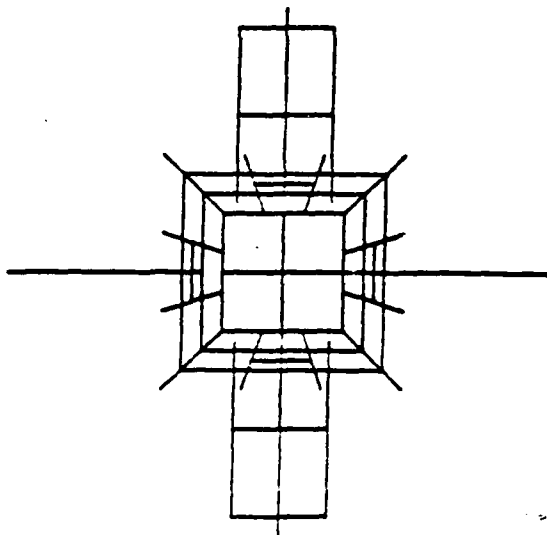
Figure 2.7 Model 2B (Sub-Mast Wire Grid Model)  
for 1 Internal Shunt Feed.



THETA = 60.00 PHI = 60.00 ETA = 90.00



THETA = 90.00 PHI = 0.00 ETA = 90.00



THETA = 0.00 PHI = 0.00 ETA = 90.00

Figure 2.8 Model 3 (Main-Mast Surface Patch Model).

TABLE 4  
MODEL 3 FREQUENCY AND GEOMETRY DATA IN WAVELENGTHS

Frequency in MHz	Number of Patches	Number of Segments	Min. Seg. in Wavelengths	Max. Seg. in Wavelengths
2	58	32	0.00988	0.01045
3	58	32	0.01482	0.01566
4	58	32	0.01977	0.02090
5	58	32	0.02470	0.02611
6	58	32	0.02965	0.03134
7	58	32	0.03457	0.03655
8	58	32	0.03953	0.04179
9	58	32	0.04445	0.04699
10	58	32	0.04942	0.05224
11	58	32	0.05433	0.05743
12	58	32	0.05928	0.06267
13	58	32	0.06413	0.06780
14	58	32	0.06913	0.07308
15	58	32	0.07415	0.07839
16	58	32	0.07901	0.08353

Figure 2.8 shows Model 3, the main-mast surface patch model, and Table 4 lists geometry data for fifteen different frequencies. As seen in Table 4, the segment length, the radius of the wire, the number of the patches of Model 3 are chosen to meet modeling guidelines. The detailed geometry data are in Appendix A.

Model 3 is fed by two different methods for the frequency range 2-16 MHz: four external shunt feeds and the two external shunt feeds.

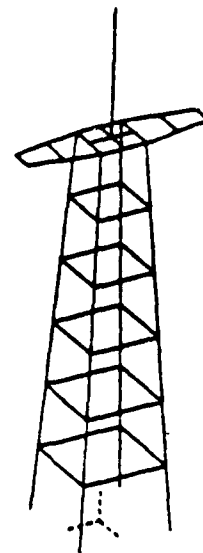
#### E. MODEL 4 (MAIN-MAST WIRE GRID MODEL)

Model 4 changes the surface model of Model 3 to a wire grid with additional structures moved to the top of the main-mast with the same geometry. The four feed wires used in Model 3 are removed, and four base feeds are used in their place. The grid height is fixed at 3 meters, but the width of the grid cells decreases as the height of the main-mast increases.

Figure 2.9 shows Model 4, and Table 5 presents geometry data for fifteen different frequencies. As seen in Table 5, the segmentation length of Model 4 is adequate for frequency range 2-14 MHz but is slightly over  $0.1\lambda$  for the frequency range 15-16 MHz. The radius of the wires is such that  $2\pi a/\lambda < < 1$ . The detailed data are in Appendix A.

Model 4 is excited by five different feed methods: four base feeds, three base feeds, two diagonal base feeds, two adjacent base feeds, and one base feed.

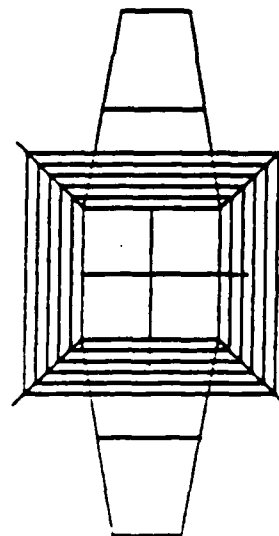
The next step was to energize the mast computer models, using each of the different source feeding methods, to study the change of the mast input impedance with frequency variation, and to evaluate average power gain and azimuth and elevation radiation patterns. The VSWR characteristic will be obtained from the Smith Chart plots by plotting the input impedance with the frequency variation.



THETA = 60.00 PHI = 60.00 ETA = 90.00



THETA = 90.00 PHI = 0.00 ETA = 90.00



THETA = 0.00 PHI = 0.00 ETA = 90.00

Figure 2.9 Model 4 (Main-Mast Wire Grid Model).

TABLE 5  
MODEL 4 FREQUENCY AND GEOMETRY DATA IN WAVELENGTHS

Frequency in MHz	Number of Segments	Min. Seg. in Wavelengths	Max. Seg. in Wavelengths	Grid Height in Wavelengths
2	119	0.00500	0.01333	0.02000
3	119	0.00750	0.02000	0.03000
4	119	0.01001	0.02668	0.04001
5	119	0.01250	0.03333	0.05000
6	119	0.01501	0.04002	0.06004
7	119	0.01750	0.04667	0.07001
8	119	0.02001	0.05336	0.08004
9	119	0.02250	0.06001	0.09001
10	119	0.02500	0.06671	0.10007
11	119	0.02750	0.07334	0.11001
12	119	0.03001	0.08003	0.12005
13	119	0.03250	0.08658	0.12787
14	119	0.03500	0.09333	0.13999
15	119	0.03750	0.10010	0.15015
16	119	0.04000	0.10667	0.16000

### III. COMPUTER MODEL RESULTS

This chapter presents the results of the computer models developed in Chapter II. Each model was tested by using several different feed techniques to find the most favorable feeding method. All models in this thesis have the same performance as a monopole antenna over a perfect ground plane.

#### A. OVERVIEW OF RESULTS

A common criterion applied to antenna computer models is to check the validity of the model via average power gain. An average power gain of 2.0 represents an antenna radiating in a half space over a perfect ground plane. The average power gain is obtained by integrating the radiated power density over all space to find the total radiated power, then comparing that to the total input power at the feed points. These should be equal for a valid solution and provides a necessary (but not sufficient) conditional test of the numerical model. The average power gain was calculated for a quarter of the rectangular coordinates to save computer time.

The data sets were run to evaluate the variation of the input impedance of each computer model as functions of the feeding methods and frequency. The results are indicated on two different curves, one for resistance ( $R$ ), the other for reactance ( $jX$ ). The reactance ( $jX$ ) is dominated by the capacitance of the surface patch models and the inductance of the wire grid models. When combining wire grid and surface patch models, the reactance ( $jX$ ) is controlled by both capacitive and inductive components.

Radiation patterns for each model were obtained in the frequency range 2-10 MHz for the sub-mast computer models and in the frequency range 2-16 MHz for the main-mast models for each feed method. Figures 3.1 and 3.2 show the azimuth pattern at 2 MHz and the elevation pattern at 10 MHz for a 9 meter monopole whip antenna with the same height sub-mast. Figure 3.3 shows the elevation pattern of an 18 meter monopole whip antenna with the same height of the main-mast at 16 MHz.

For the low frequency region (less than 10 MHz), the radiation patterns looked like the patterns of an equal height monopole antenna. The azimuth patterns were omnidirectional and the elevation patterns looked similar to those of an equal sized monopole whip antenna. For high frequency region (over 10 MHz), the azimuth patterns were still omnidirectional and the elevation patterns looked similar to those of an equal sized monopole whip antenna.

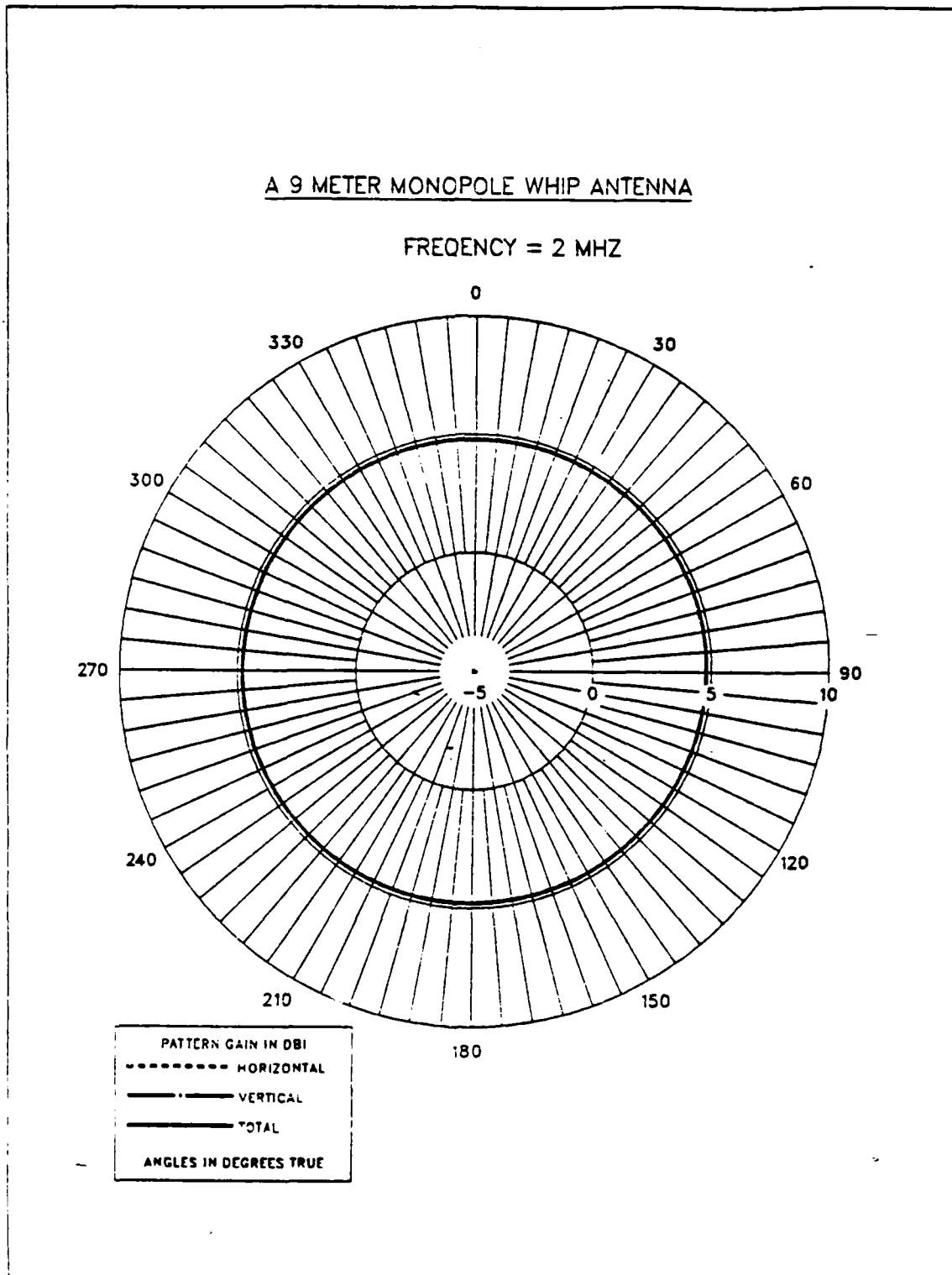
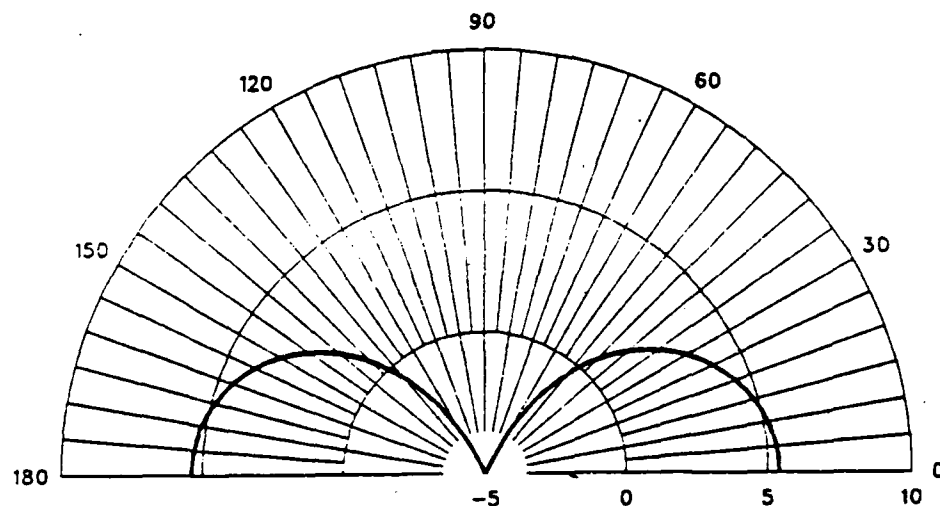


Figure 3.1 E-Field Azimuth Pattern of a 9 Meter Monopole at 2 MHz.

A 9 METER MONPOLE WHIP ANTENNA

FREQUENCY = 10 MHZ

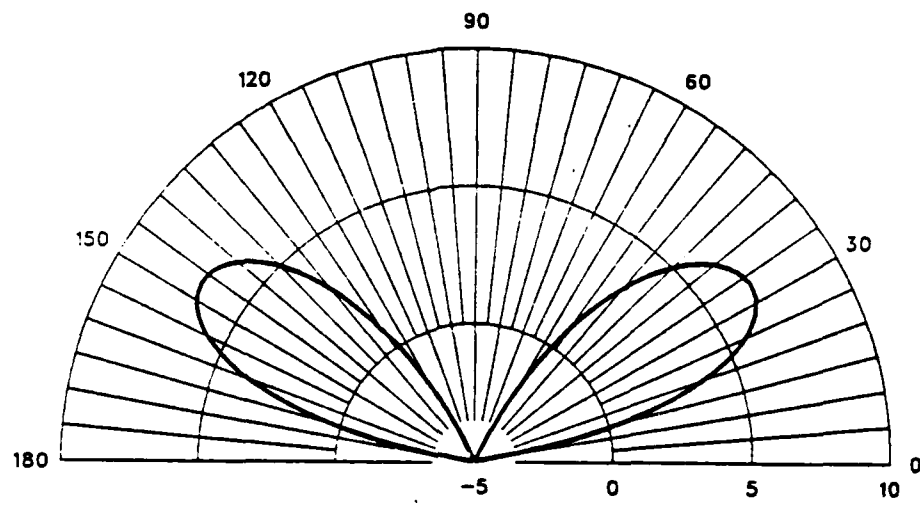


PATTERN GAIN IN DBI  
----- HORIZONTAL  
— VERTICAL  
— TOTAL  
— ELEVATION ANGLE

Figure 3.2 E-Field Elevation Pattern of a 9 Meter Monopole at 10 MHz.

A 18 METER MONOPOLE WHIP ANTENNA

FREQUENCY = 16 MHZ



PATTERN GAIN IN DBI  
----- HORIZONTAL  
— VERTICAL  
— TOTAL  
— ELEVATION ANGLE

Figure 3.3 E-Field Elevation Pattern of a 18 Meter Monopole at 16 MHz.

A 3:1 VSWR is considered a standard criterion for broadband shipboard antenna operation. Only a few antennas satisfy this criterion over an operating band of interest but many antennas may be brought into this region by use of a series inductance or capacitance. Figure 3.4 shows the 3:1 VSWR circle and the shaded region represents the impedance of the Smith Chart which may be moved into the 3:1 VSWR circle by use of series reactances.

This shaded region is called the 3:1 'VSWR matchable region'. This thesis will consider impedances calculated into the 3:1 VSWR region or 3:1 VSWR matchable region are acceptable impedances for operational requirements. Two kinds of Smith Chart plots will be presented at the design frequency range for each model. One is the Smith Chart plot using the 50 Ohm characteristic impedance of typical HF whip antennas; the other is the Smith chart plot using a characteristic impedance ( $Z_0$ ), selected differently for each model to magnify the 3:1 VSWR regions and their matchable regions. Usually, the characteristic impedance ( $Z_0$ ) can be shifted for an HF shipboard antenna system.

The remainder of this chapter is devoted to antenna terminology, including the simulation results for the best feed position for each model.

## B. MODEL 1 RESULTS

The only feed method used for Model 1 is the four external shunt feeds. The height of feed positions at the surface of the sub-mast can be adjusted to obtain the best results. In the case of combining the wire grid and surface patch model, it was observed that the separation between surfaces of the mast and the feed wires must be considered. If computer models driven by combining both modeling procedures of NEC do not have enough separation between connecting wire structures and the surface, reasonable and satisfying results cannot be obtained.

A data set of nine frequencies from 2-10 MHz with the equal spacing of 1 MHz was run to evaluate the average power gain, the input impedance, and the radiation patterns.

### - 1. Average Power Gain of Model 1

Table 6 lists the calculated average power gain for nine different frequencies. The average power gain is calculated at near 2.0 dBi with -0.01 to +0.07 errors and are acceptable.

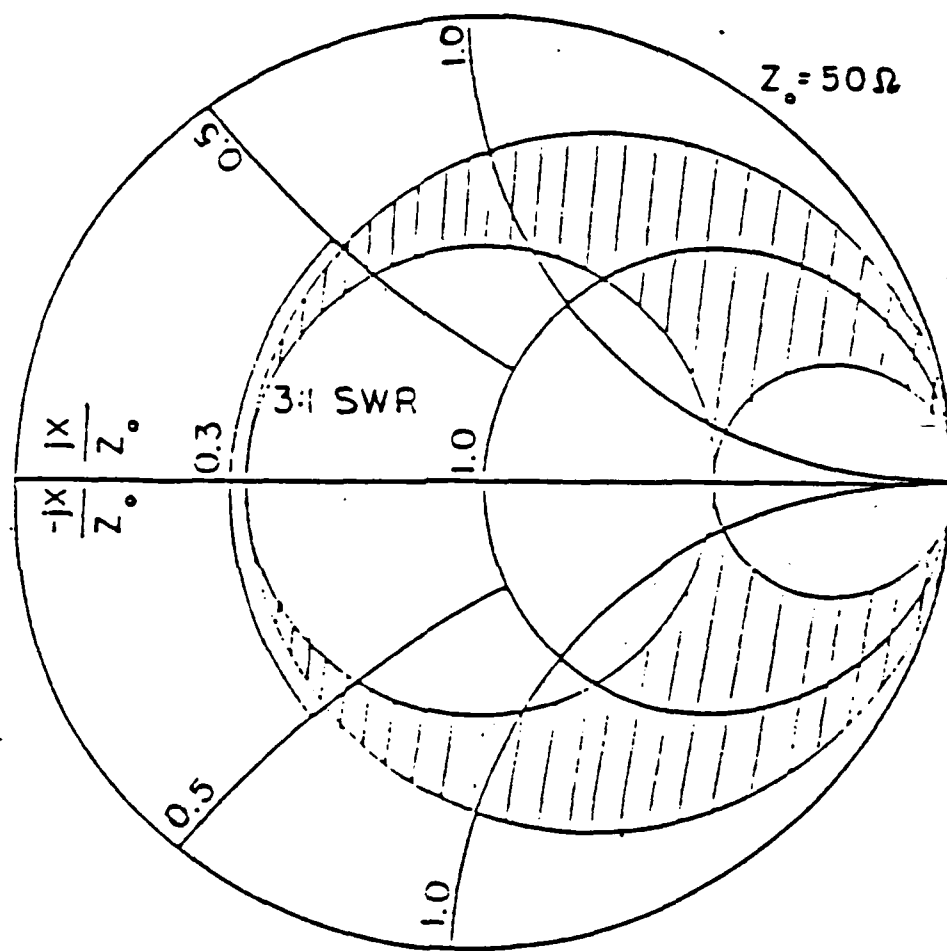


Figure 3.4 3:1 VSWR Matchable Region in Smith Chart.

TABLE 6  
MODEL 1 AVERAGE POWER GAIN IN FREQUENCY 2-10 MHZ

Frequency in MHz	Four External Shunt Feeds
2	2.03
3	2.07
4	2.04
5	2.01
6	2.00
7	2.00
8	1.99
9	1.99
10	1.99

## 2. Input Impedance of Model 1

Figure 3.5 shows two curves, one for the resistances ( $R$ ), and the other for the reactances ( $jX$ ) with frequency range 2-10 MHz. As seen in Figure 3.5, the resistances ( $R$ ) are very low values at the low frequency range 2-5 MHz. These resistances are hard to match into the 3:1 VSWR criteria. The reactances ( $jX$ ) are higher than the resistances ( $R$ ) in the entire frequency range 2-10 MHz due to the shortness of the mast in comparison to a wavelength.

## 3. Radiation Patterns of Model 1

The radiation patterns of Model 1, the sub-mast surface patch model, driven with E-gap voltage sources were obtained for the frequency range 2-10 MHz. A data set was run with the four external shunt feeds installed at the base segment of each feed wire for nine different frequencies. Figure 3.6 shows the azimuth pattern of Model 1 at 2 MHz and Figure 3.7 shows the elevation pattern of Model 1 at 10 MHz.

INPUT IMPEDANCE OF MODEL 1  
FOR 4 EXTERNAL SHUNT FEEDS

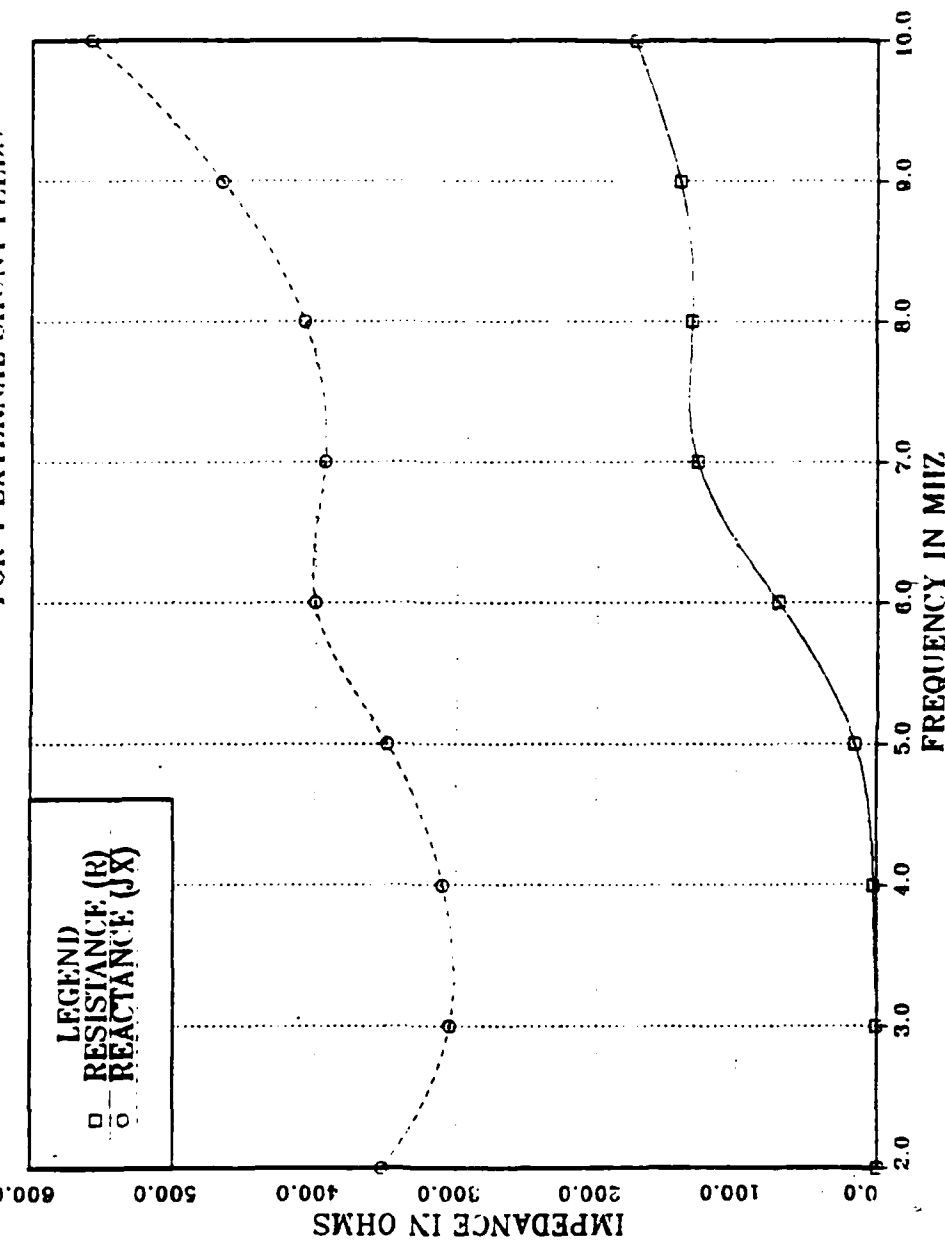


Figure 3.5 Model 1 Input Impedance in Frequency 2-10 MHz  
for 4 External Shunt Feeds.

MODEL 1 BY FOUR EXTERNAL SHUNT FEEDS

FREQUENCY = 2 MHZ

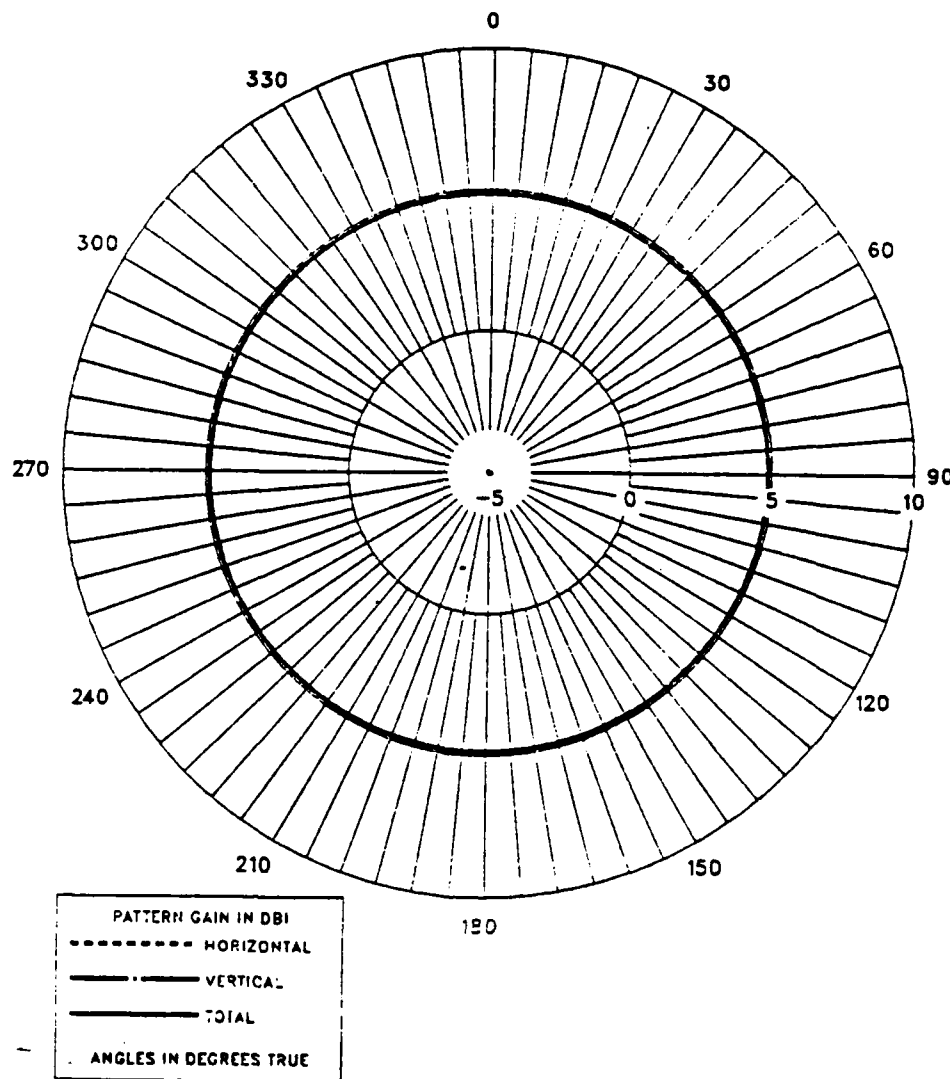
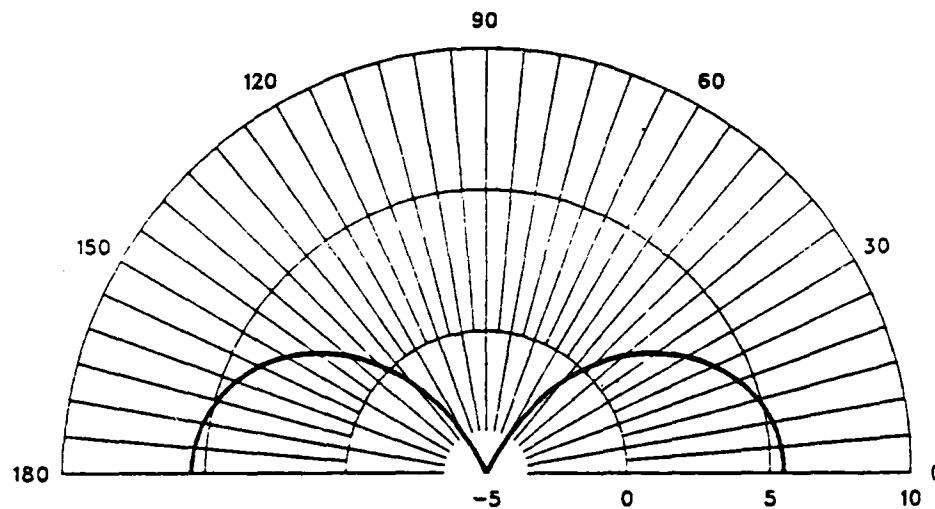


Figure 3.6 Model 1 E-Field Azimuth Pattern at 2 MHz  
for 4 External Shunt Feeds.

MODEL 1 BY FOUR EXTERNAL SHUNT FEEDS

FREQUENCY = .10 MHZ



PATTERN GAIN IN DBI  
----- HORIZONTAL  
— VERTICAL  
— TOTAL  
— ELEVATION ANGLE

Figure 3.7 Model 1 E-Field Elevation Pattern at 10 MHz  
for 4 External Shunt Feeds.

For frequencies less than 6 MHz, the radiation patterns are almost identical to those of an equal height monopole antenna. The azimuth pattern became perfectly omnidirectional with a directivity of 5 dBi and the elevation patterns looked similar to those of an equal sized monopole antenna.

In the frequency range 6-10 MHz, the radiation patterns still looked similar to those of an equal height monopole antenna. Because the beam width of the elevation patterns are narrower as frequency increases, the directivity is increased to slightly over 5 dBi. The half-power beamwidth of Model 1 is approximately 10 degrees less than that of a monopole antenna of the same height at the frequency 10 MHz.

#### 4. Voltage Standing Wave Ratio of Model 1

Two characteristic impedances were used to plot the impedances on a Smith Chart for nine frequencies. A characteristic impedance of 200 Ohms was chosen to broaden the 3:1 VSWR and the 3:1 VSWR matchable region in this case.

Figures 3.8 and 3.9 are the Smith Chart plots of the impedance characteristics for Model 1, the sub-mast surface patch model, and Table 7 lists the frequencies which fall in the 3:1 VSWR circle or are matchable by use of series of reactances to the 3:1 VSWR. Table 7 also reveals that even if the shifted characteristic impedance of 200 Ohms was used for this model, the VSWR does not fall in the 3:1 VSWR circle and the 3:1 VSWR matchable region is not appreciably increased.

These results show that Model 1, the sub-mast surface patch model is a feasible design for a shipboard HF communication antenna at frequency range 6-10 MHz.

### C. MODEL 2 RESULTS

This model was fed by five different methods: four base feeds, three base feeds, two adjacent base feeds, two diagonal base feeds, and one base feed. Two modified models, Model 2A and Model 2B, were run by four external shunt feeds and one internal shunt feed. All sub-mast wire grid models were excited for the frequency range 2-10 MHz at 1 MHz increments. This chapter presents the results of only the four base feeds; the results of other feed methods are provided in Appendix B.

#### 1. Average Power Gain of Model 2

Table 8 lists the calculated average power gain for nine different frequencies for five different feed methods, and Table 9 lists the calculated average power gain for two modified models, Model 2A and 2B, over the same frequency range.

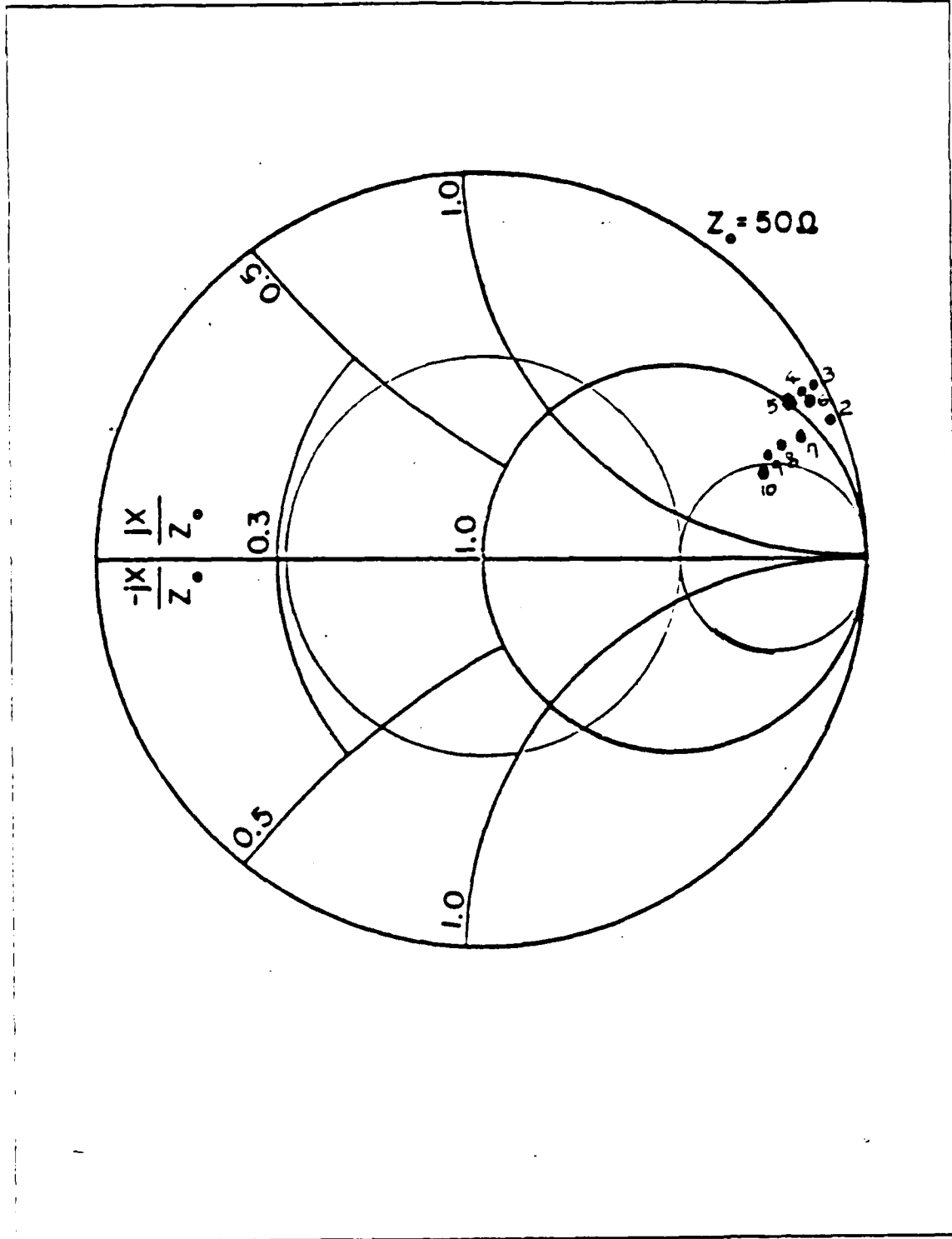


Figure 3.8 Model I Impedance Plot in Frequency 2-10 MHz  
for 4 External Shunt Feeds:  $Z_0 = 50 \Omega$ .

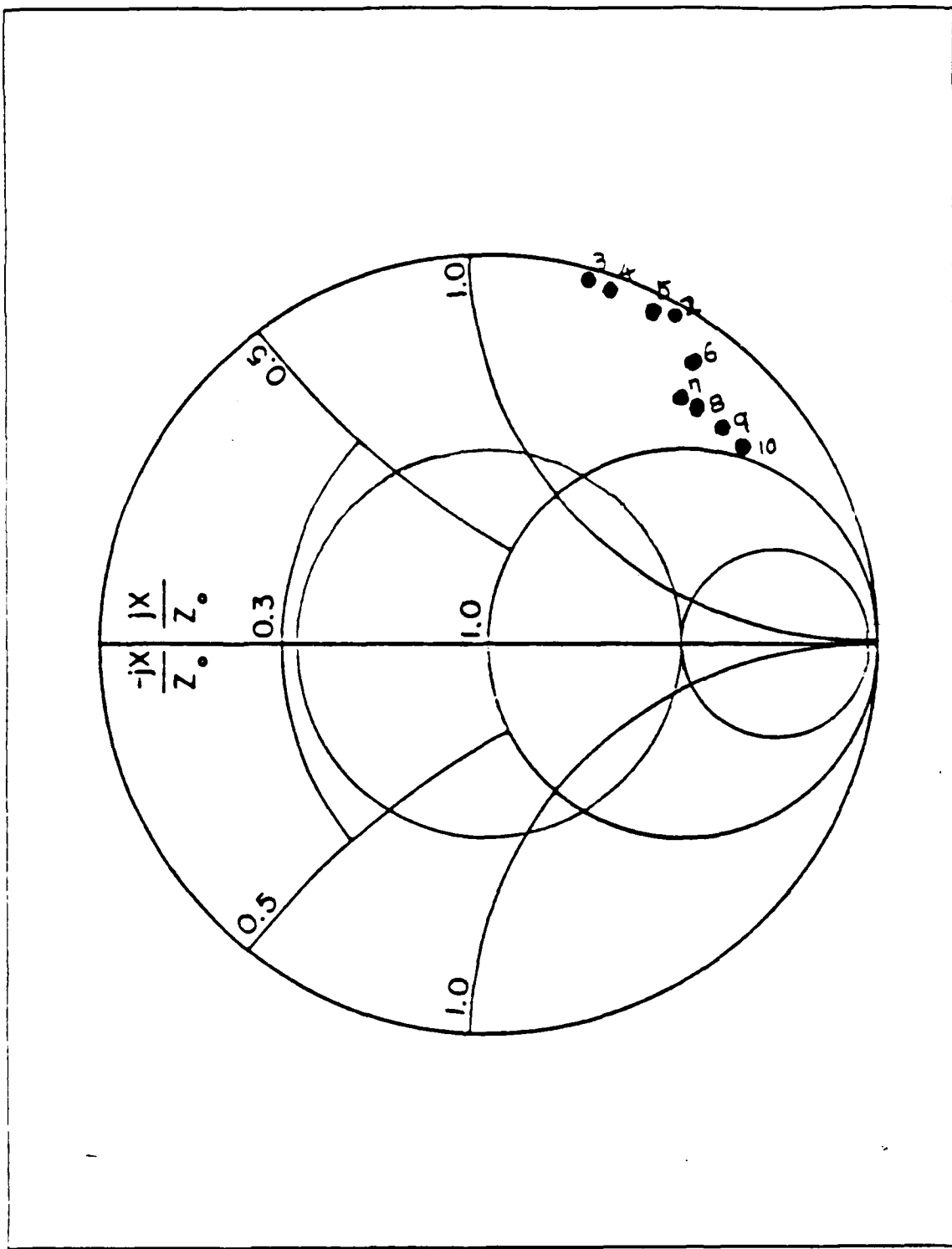


Figure 3.9 Model 1 Impedance Plot in Frequency 2-10 MHz  
for 4 External Shunt Feeds:  $Z_0 = 200$  Ohm.

TABLE 7  
MODEL 1 3:1 VSWR AND MATCHABLE REGIONS

for Frequency in MHz

Feeding Methods	4 External Shunt Feeds	
$Z_0$ (Ohm)	50	200
3: 1 VSWR Regions	None	None
3: 1 VSWR Matchable Regions	6-9	6-10

The four base feed model has a perfect average power gain of 2.0 dBi for the entire design range of 2-10 MHz. The three base feed model provides an acceptable average power gain with errors from -0.03 to -0.01 for the entire designed frequency range. The two adjacent base feed model provided unacceptable average power gains. The computer model is apparently not adequate for this case. Generally, an average power gain less than 0.1 or 0.15 error is acceptable. The two diagonal base feed and the one base feed model provided acceptable average power gains except at 2 MHz for the one feed model. For the two modified models, Model 2A provides an acceptable average power gain for the frequency range 3-10 MHz, but Model 2B does not provide an acceptable average power gain. In case of Model 2B, numerical errors were created for the entire frequency range.

## 2. Input Impedance of Model 2

Figure 3.10 illustrates input impedances with two curves, one for the resistances ( $R$ ), and the other for reactances ( $jX$ ) at the frequency range 2-10 MHz. As seen in Figure 3.10, the resistances ( $R$ ) monotonically increased as the frequency increased. The reactances ( $jX$ ) increased in the frequency range 2-8 MHz, and then slightly decreased over the frequency 8 MHz. In this case, most of reactances were negative or low positive region below 100 Ohms.

TABLE 8  
MODEL 2 AVERAGE POWER GAIN IN FREQUENCY 2-10 MHZ

Frequency in MHz	4 Base Feeds	3 Base Feeds	2 Adjacent Base Feeds	2 Diagonal Base Feeds	1 Base Feed
2	2.00	1.97	2.05	1.93	1.74
3	2.00	2.00	2.07	1.95	1.86
4	2.00	2.00	2.12	1.96	1.93
5	2.00	2.00	2.18	1.98	1.97
6	2.00	2.00	2.24	1.99	1.99
7	2.00	1.99	2.31	2.01	2.00
8	2.00	1.98	2.38	2.03	2.00
9	2.00	1.97	2.44	2.05	2.01
10	2.00	1.97	2.49	2.07	2.02

### 3. Radiation Patterns of Model 2

Figure 3.11 shows the azimuth pattern at 2 MHz for four base feeds. Radiation patterns of Model 2 are similar to those of a 9 meter monopole whip antenna. Figure 3.12 shows the elevation pattern for the same feed method at 10 MHz and reveals that the beamwidth is slightly decreased with directivity over 5 dBi. The half-power beamwidth of Model 2 is about 3 degrees less than that of a monopole antenna of equal height at 10 MHz. The four base feed model has omnidirectional azimuth patterns for 2-10 MHz.

### 4. Voltage Standing Wave Ratio of Model 2

Figures 3.13 and 3.14 are the Smith Chart plots of the Model 2 for the four base feeds. Table 10 lists the 3:1 VSWR and 3:1 VSWR matchable regions for each feed model and for the modified model, Model 2A. Each feed model used different

TABLE 9  
MODEL 2A AND 2B AVERAGE POWER GAIN IN FREQUENCY 2-10 MHZ

Frequency in MHz	4 External Shunt Feeds (Model 2A)	1 Internal Shunt Feed (Model 2B)
2	1.71	0.77
3	1.88	1.15
4	1.94	1.40
5	1.97	1.56
6	1.99	1.66
7	2.00	1.72
8	2.01	1.77
9	2.01	1.80
10	2.02	1.82

characteristic impedances ( $Z_0$ ). Model 2 driven by four base feeds has the largest 3:1 VSWR region, 6-10 MHz, without using a series of reactances ( $jX$ ). In case of using series reactances, the acceptable frequency region of 3:1 VSWR was increased to 4-10 MHz. This table also shows that Model 2 driven by other feed methods has a 3:1 VSWR matchable region over 5 MHz, but not for the frequencies below 5 MHz. If a smaller characteristic impedance ( $Z_0$ ) was used, it is possible to match into the 3:1 VSWR criteria for frequencies less than 5 MHz.

INPUT IMPEDANCE OF MODEL 2  
FOR 4 BASE FEEDS

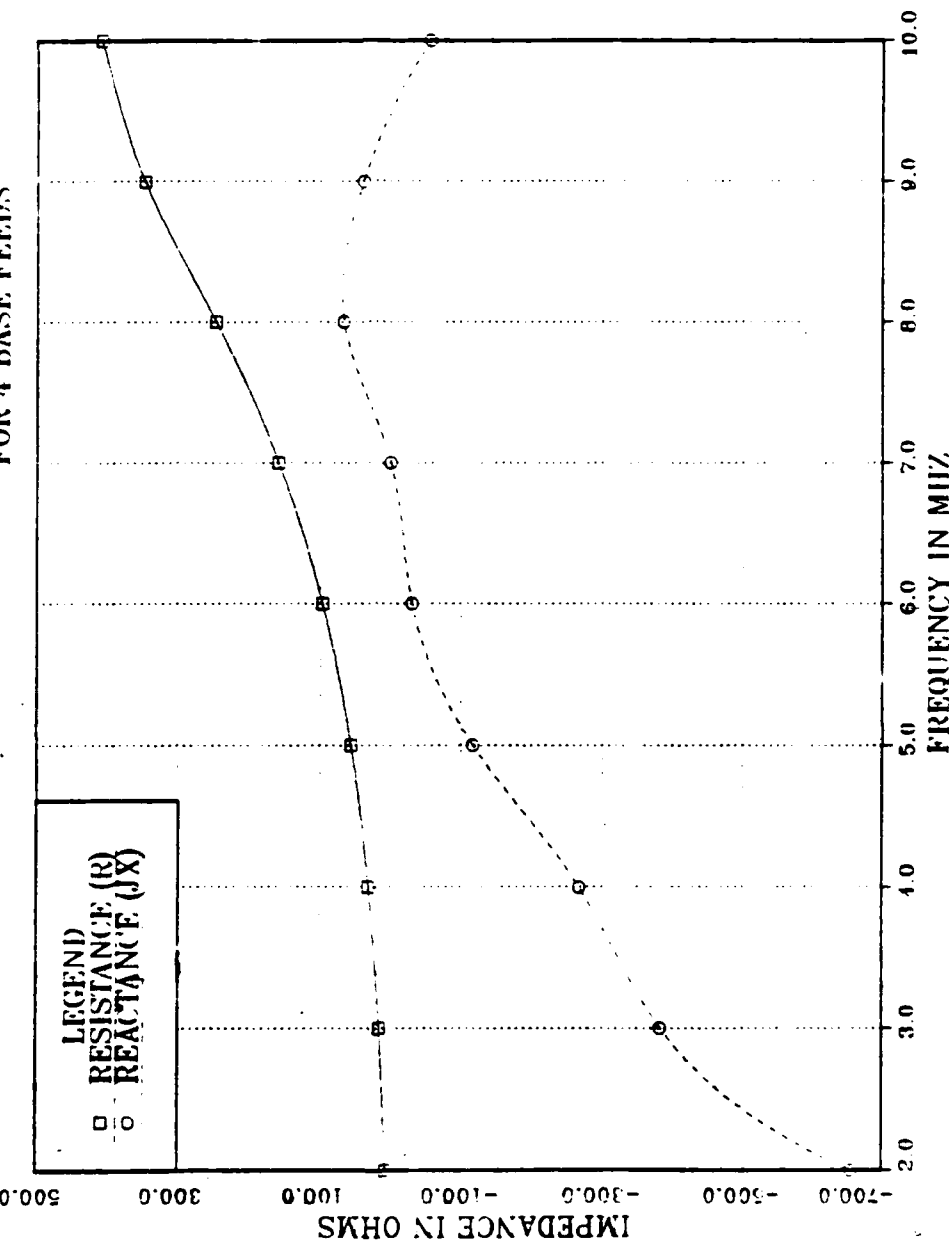


Figure 3.10 Model 2 Input Impedance in Frequency 2-10 MHz  
for 4 Base Feeds.

MODEL 2 BY FOUR BASE FEEDS

FREQUENCY = 2 MHZ

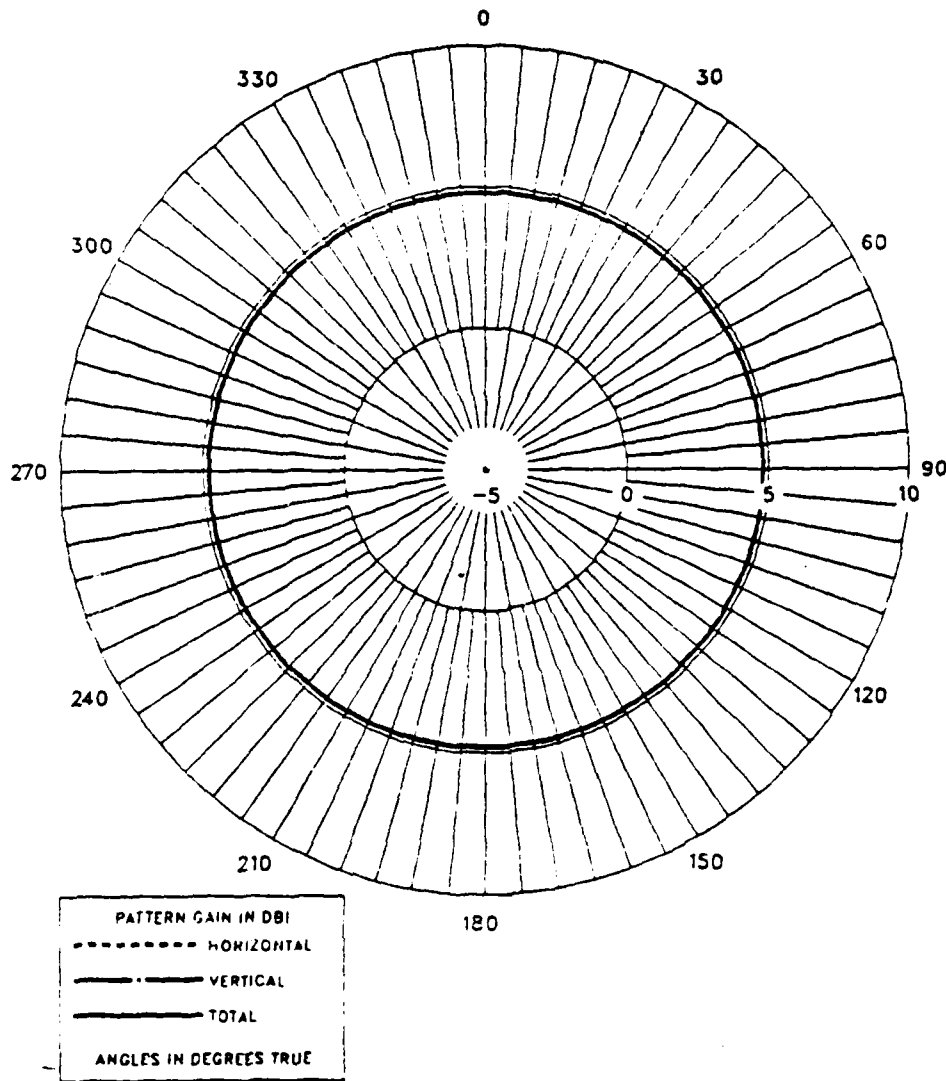
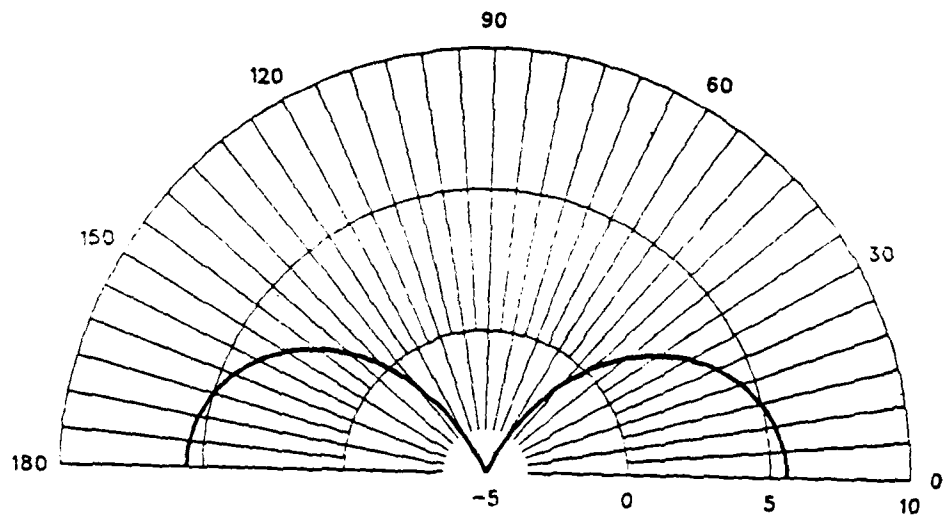


Figure 3.11 Model 2 E-Field Azimuth Pattern at 2 MHz  
for 4 Base Feeds.

MODEL 2 BY FOUR BASE FEEDS

FREQUENCY = 10 MHZ



PATTERN GAIN IN DBI  
----- HORIZONTAL  
----- VERTICAL  
----- TOTAL  
----- ELEVATION ANGLE

Figure 3.12 Model 2 E-Field Elevation Pattern at 10 MHz  
for 4 Base Feeds.

TABLE 10  
MODEL 2 3:1 VSWR AND MATCHABLE REGIONS  
for Frequency in MHz

Feeding Methods	4 Base Feeds		3 Base Feeds	2 Base Feeds	1 Base Feed	Model 2A
$Z_0$ (Ohm)	50	150	150	50	50	50
3: 1 VSWR Regions	6	6-10	5- 8	None	None	None
3: 1 VSWR Matchable Regions	3- 6	4- 6	4- 5	8-10	5-10	6-10

#### D. MODEL 3 RESULTS

As modeled in Chapter II, Model 3 was a surface main-mast with additional wire grid structures attached. Model 3 was driven by four external shunt feeds and two external shunt feeds. The height of a feed wire attachment point is 9 meters, half the height of the surface main-mast. To obtain better results, it is possible to adjust the height of feed positions, but these feed positions must be located at the centers of the model surface patches. Also, sufficient separation between the surfaces of the mast and the feed wires must be observed, as the results of Model 1 show.

Two data sets were run to evaluate the average power gains, the input impedances, and the radiation patterns for fifteen different frequencies from 2-16 MHz: one data set for four external shunt feeds, and the other for two external shunt feeds.

This chapter presents only the results of the four external shunt feeds; the results of the two external shunt feeds are provided in Appendix C.

##### 1. Average Power Gain of Model 3

Table 11 lists the calculated average power gain for two and four external shunt feeds for fifteen different frequencies. The average power gains were calculated at near 2.0 dBi with errors from -0.02 to + 0.06.

For four external shunt feeds, the average power gains are constant in the range of 2-16 MHz. For two external shunt feeds, the average power gains below 10

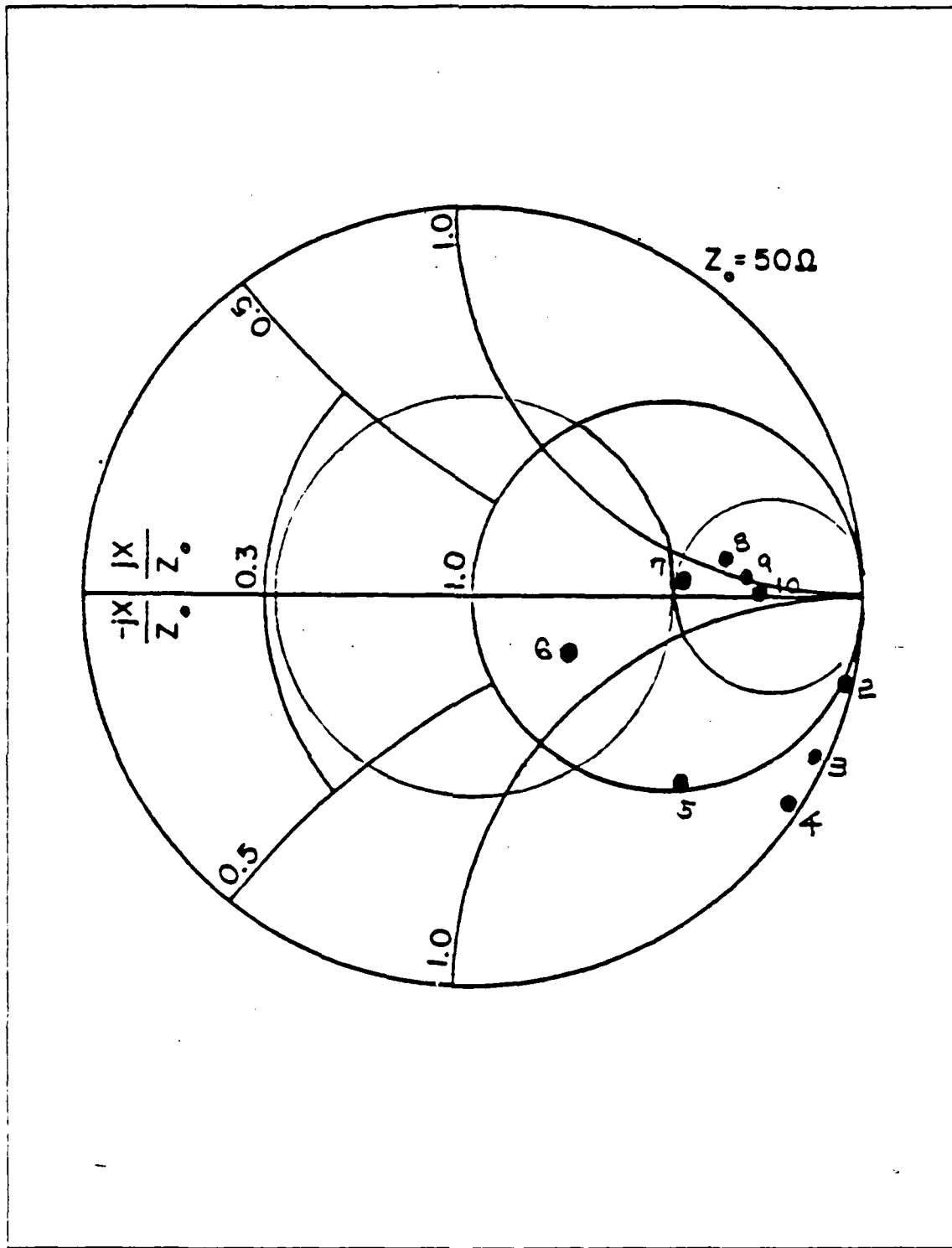


Figure 3.13 Model 2 Impedance Plot in Frequency 2-10 MHz  
for 4 Base Feeds:  $Z_0 = 50 \Omega$ .

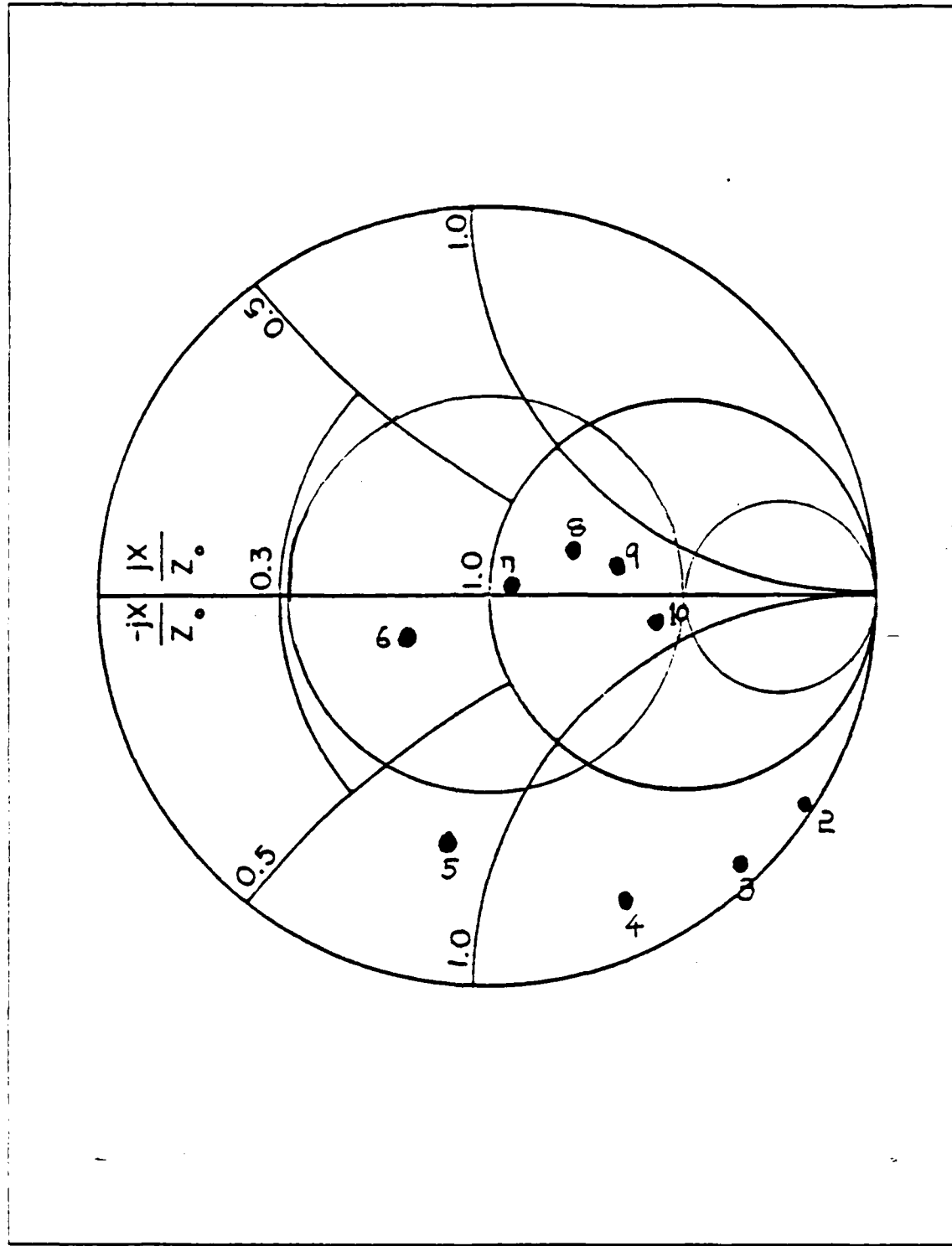


Figure 3.14 Model 2 Impedance Plot in Frequency 2-10 MHz  
for 4 Base Feeds:  $Z_0 = 150 \Omega$ .

MHz are constant, but the average power gains over 10 MHz are slightly increased. The average power gains for these two feed methods are acceptable for the entire frequency range 2-16 MHz.

TABLE 11  
MODEL 3 AVERAGE POWER GAIN IN FREQUENCY 2-16 MHZ

Frequency in MHz	4 External Shunt Feeds	2 External Shunt Feeds
2	1.98	1.97
3	1.98	1.97
4	1.98	1.97
5	1.98	1.97
6	1.98	1.97
7	1.98	1.97
8	1.98	1.97
9	1.98	1.97
10	1.98	1.97
11	1.98	1.98
12	1.98	2.00
13	1.98	2.06
14	1.98	2.06
15	1.98	2.06
16	1.98	2.06

## **2. Input Impedance of Model 3**

Figure 3.15 shows the input impedances at 2-16 MHz for the four external shunt feeds. The resistances ( $R$ ) smoothly increased as the frequency increased upto 12 MHz, but decreased above 14 MHz. For the low frequency range 2-5 MHz, resistance is relatively small, and is hard to match into the 3:1 VSWR criteria. Figure 3.15 also illustrates that there are three resonant frequencies: 6-7 MHz, 12-13 MHz, and 15-16 MHz.

## **3. Radiation Patterns of Model 3**

Figure 3.16 shows the elevation pattern at 2 MHz for four external shunt feeds. Radiation patterns of Model 3 at 2 MHz are almost the same as those of an 18 meter monopole whip antenna.

Figures 3.17 and 3.18 show azimuth and elevation patterns for the same feed method at 16 MHz and reveal that the beamwidth is considerably decreased with directivity at approximately 8.0 dBi. The radiation patterns of Model 3 are different from those of an 18 meter monopole whip antenna. The main lobe of Model 3 has a very low elevation angle, but that of an equal height monopole has a 45 degree elevation angle from the ground plane.

## **4. Voltage Standing Wave Ratio of Model 3**

Figures 3.19 and 3.20 are the Smith Chart plots of Model 3 for four external shunt feeds. Figure 3.19 is the Smith Chart plot for a  $Z_0$  of 50 Ohms and Figure 3.20 for 150 Ohms. Table 12 lists the 3:1 VSWR and 3:1 VSWR matchable regions by use of a series of reactances ( $jX$ ) for both feed methods, four external shunt feeds and two external shunt feeds. When a characteristic impedance of 150 Ohms was used, the frequency range 6-13 MHz was included into the 3:1 VSWR region without use of a series of reactances and the 3:1 VSWR is obtainable for 4-16 MHz by use of series of reactances ( $jX$ ). Therefore, the whole frequency range except for 2-3 MHz is included into the 3:1 VSWR criteria. This VSWR characteristic is a very good result for general shipboard HF communication antennas.

INPUT IMPEDANCE OF MODEL '3  
FOR 4 EXTERNAL SHUNT FEEDS

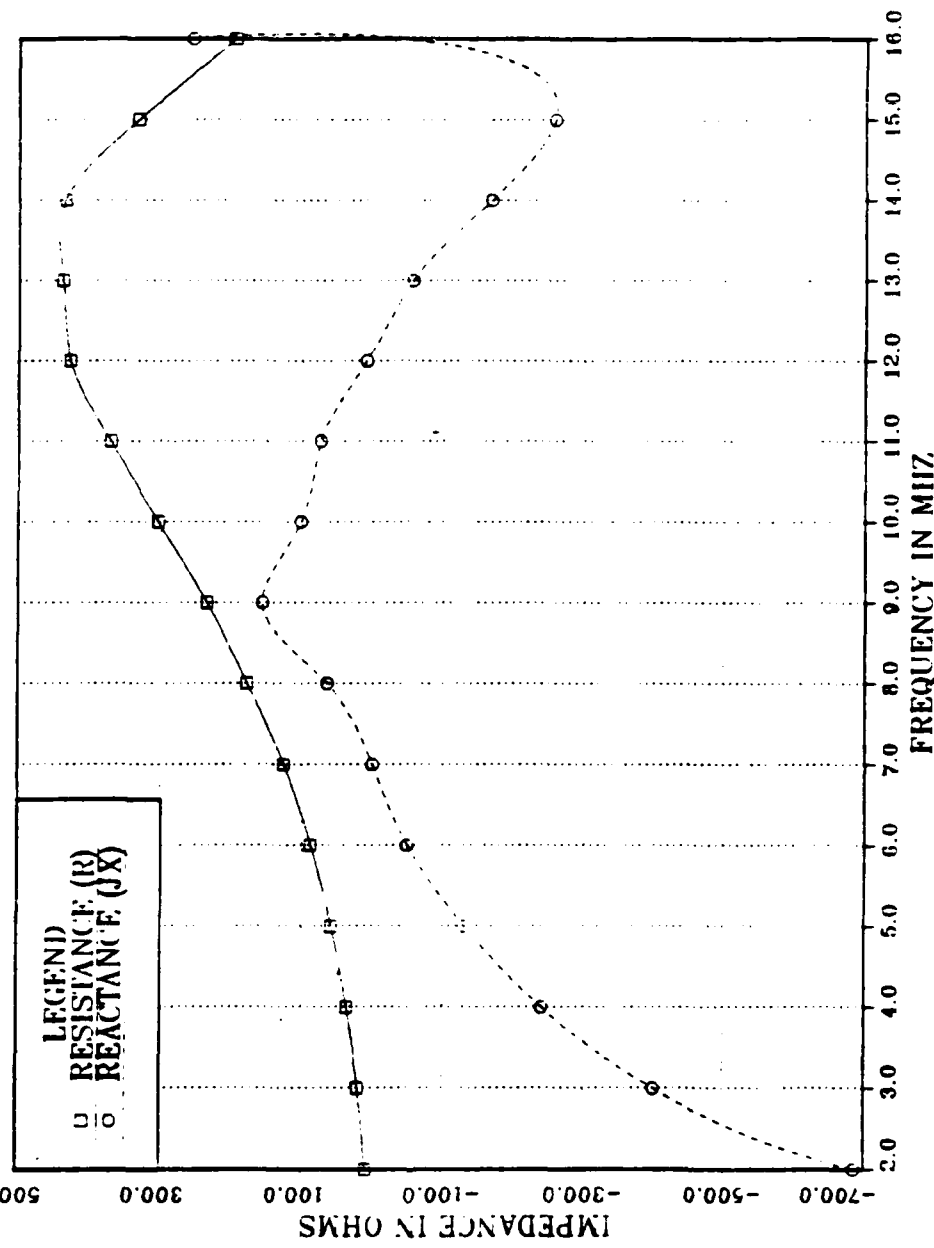


Figure 3.15 Model 3 Input Impedance in Frequency 2-16 MHz  
for 4 External Shunt Feeds.

MODEL 3 BY FOUR EXTERNAL SHUNT FEEDS

FREQUENCY = 2 MHZ

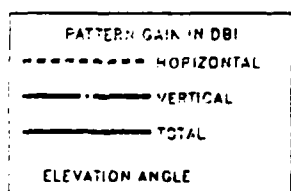
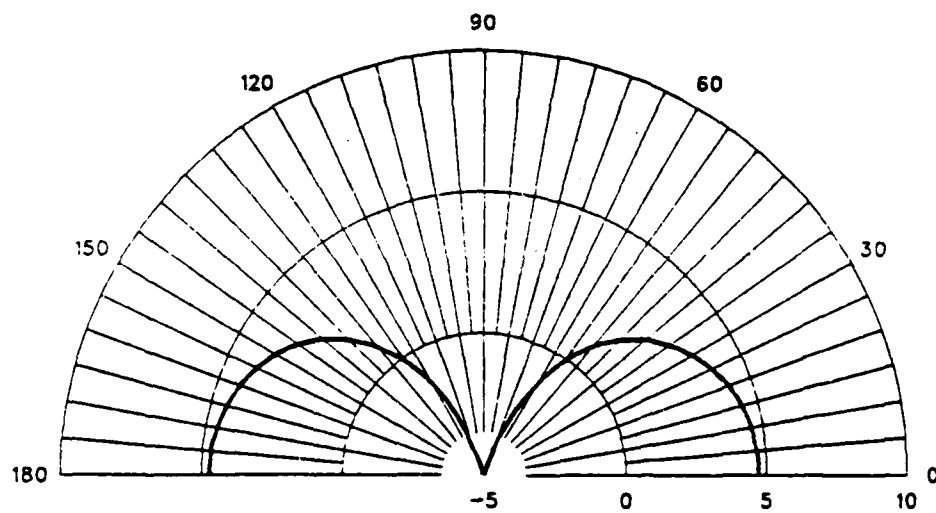


Figure 3.16 Model 3 E-Field Elevation Pattern at 2 MHz  
for 4 External Shunt Feeds.

MODEL 3 BY FOUR EXTERNAL SHUNT FEEDS

FREQUENCY = 16 MHZ

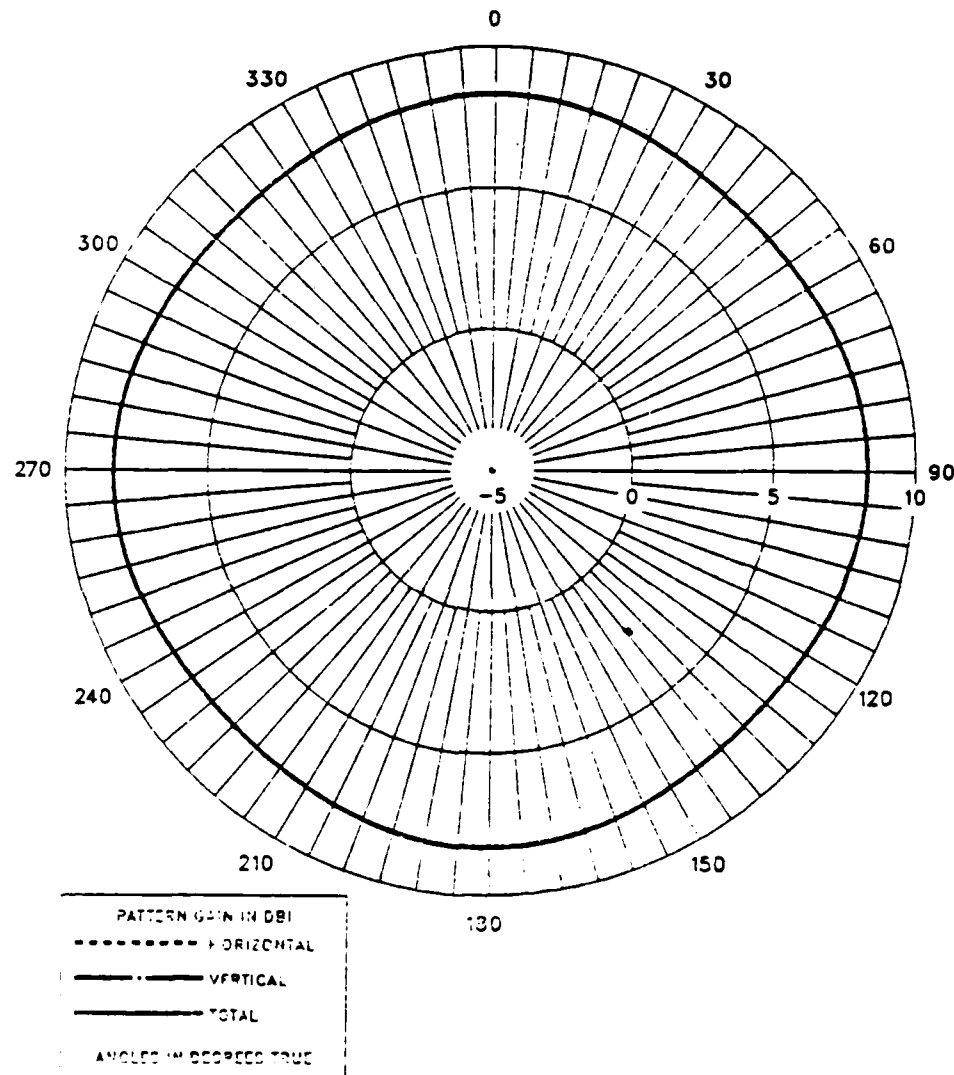


Figure 3.17 Model 3 E-Field Azimuth Pattern at 16 MHz  
for 4 External Shunt Feeds.

MODEL 3 BY FOUR EXTERNAL SHUNT FEEDS

FREQUENCY = 16 MHZ

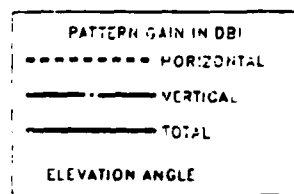
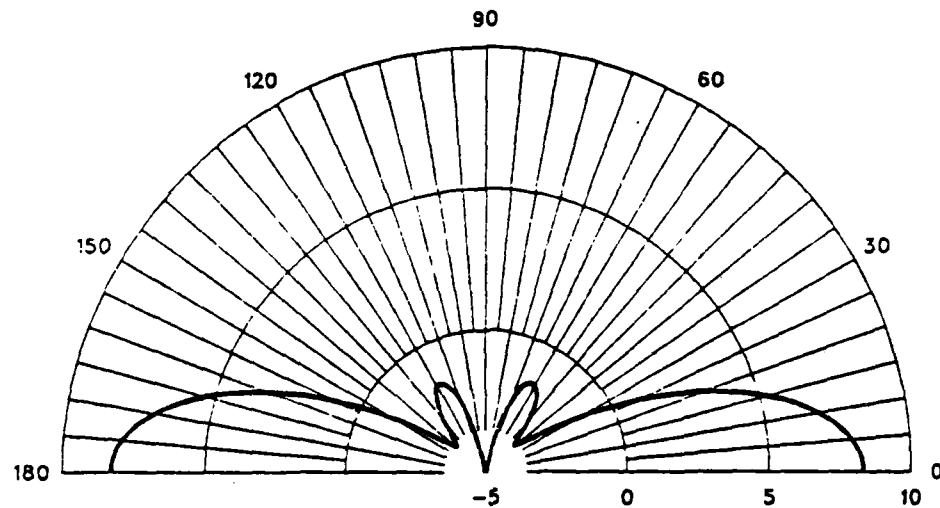


Figure 3.18 Model 3 E-Field Elevation Pattern at 16 MHz  
for 4 External Shunt Feeds.

**TABLE 12**  
**MODEL 3 3:1 VSWR AND MATCHABLE REGIONS**

for Frequency in MHz

Feeding Methods	4 External Shunt Feeds		2 External Shunt Feeds
Z <sub>o</sub> (Ohm)	50	150	300
3:1 VSWR Regions	6-7	6-13	9-11
3:1 VSWR Matchable Regions	5-6 7-8	4- 6 14-16	9-11 12-13

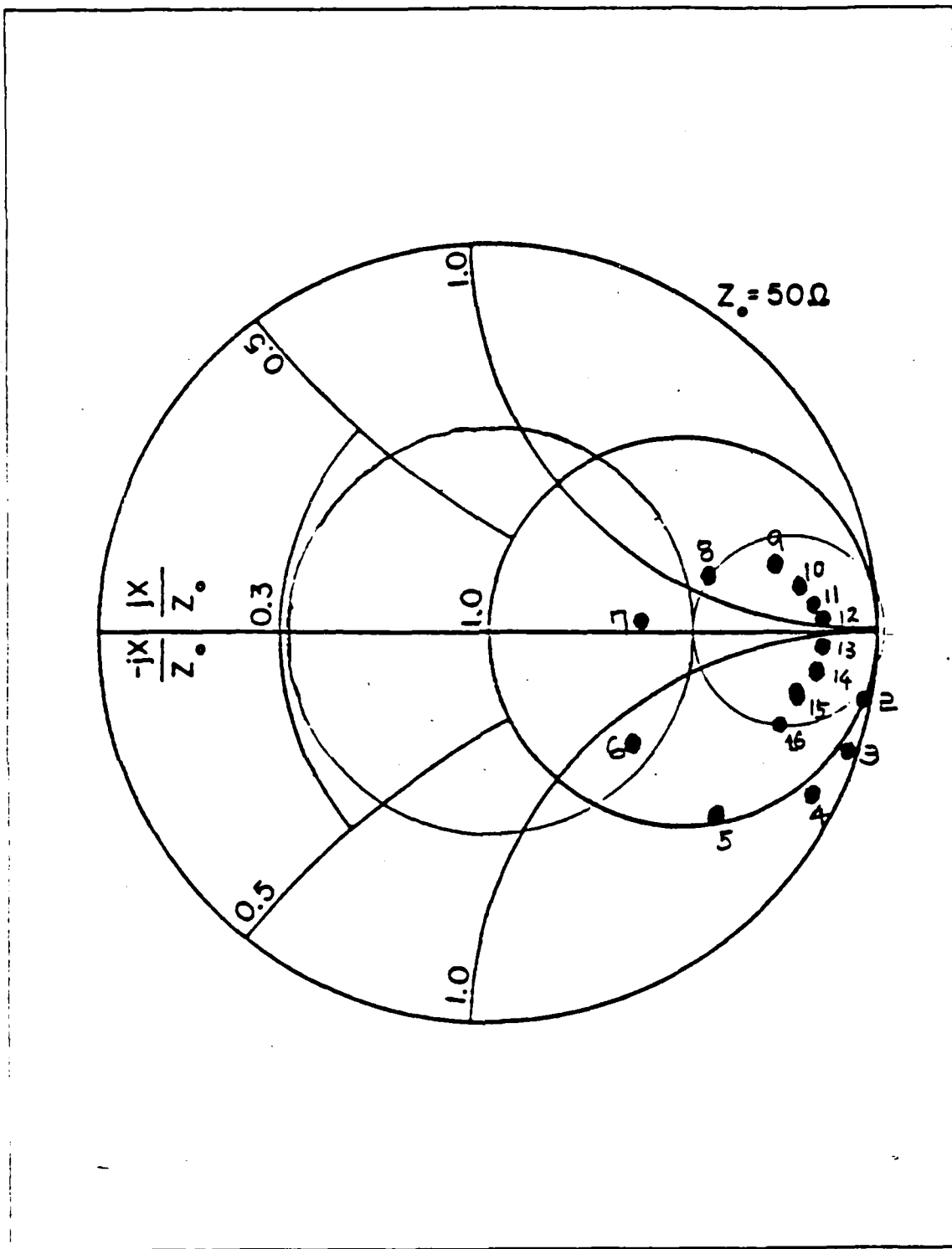


Figure 3.19 Model 3 Impedance Plot in Frequency 2-16 MHz  
for 4 External Shunt Feeds:  $Z_0 = 50$  Ohm.

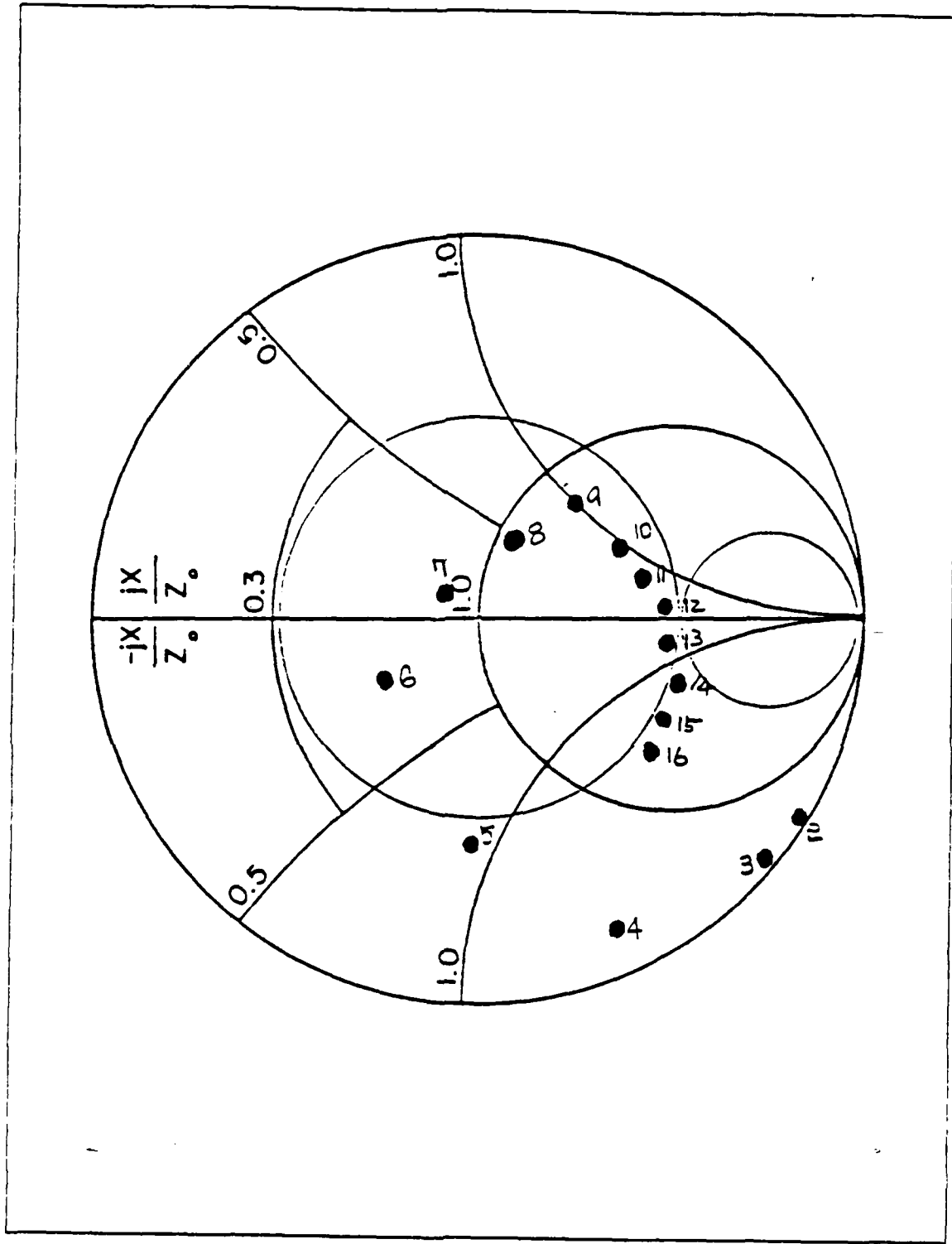


Figure 3.20 Model 3 Impedance Plot in Frequency 2-16 MHz  
for 4 External Shunt Feeds:  $Z_0 = 150 \text{ Ohm}$ .

## **E. MODEL 4 RESULTS**

This model was run for five different feed techniques: four base feeds, three base feeds, two diagonal base feeds, two adjacent feeds, and one base feed at twenty-two different frequencies in the range of 2-16 MHz. This chapter includes only the simulation results for four base feeds.

### **1. Average Power Gain of Model 4**

Tables 13 and 14 list the average power gain of Model 4 in the frequency range 2-16 MHz for the five different feed methods. The average power gains of the four base feed model have errors from -0.01 to +0.09 and are acceptable because Model 4 may be compared to a folded monopole antenna of the same height.

Even when the three and one base feed models have unsymmetrical patch positions, the average power gains are acceptable. But average power gains of the two adjacent and diagonal base feed models are not acceptable. The results of three and one base feed models are shown in Appendix D.

### **2. Input Impedance of Model 4**

Figure 3.21 shows the input impedance for 2-8 MHz and Figure 3.22 shows the input impedance for 8-16 MHz. As seen in Figures 3.21 and 3.22, most resistances are over 100 Ohms. Therefore, the relatively low resistances are hard to match into the 3:1 VSWR region without use of a series of reactances.

### **3. Radiation Patterns of Model 4**

Figure 3.23 shows the azimuth pattern at 2 MHz for four base feeds. When this pattern is compared with the radiation pattern of an 18 meter monopole whip antenna, the patterns are similar.

Figure 3.24 shows the elevation pattern of the same feed method at 16 MHz and reveals that the azimuth pattern gain is slightly over 5.0 dBi and the elevation pattern has main lobes at 45 degrees and 135 degrees.

### **4. Voltage Standing Wave Ratio of Model 4**

Figure 3.25 shows the Smith Chart plot for the four base feed model with a characteristic impedance of 50 Ohms. As seen in Figure 3.25, the input impedances are clustered on the right side of circle, due to high resistances and reactances. This means that if the proper characteristic impedance is chosen, it is possible to match the wide band frequency range into the 3:1 VSWR region.

Figure 3.26 shows the Smith Chart plot for a characteristic impedance of 300 Ohms. Several frequencies fall into the 3:1 VSWR region.

TABLE 13  
MODEL 4 AVERAGE POWER GAIN IN FREQUENCY 2-8 MHZ

Frequency in MHz	4 Base Feeds	3 Base Feeds	2 Adjacent Base Feeds	2 Diagonal Base Feeds	1 Base Feed
2.0	2.03	2.04	2.12	1.96	2.00
2.7	2.05	2.04	2.17	1.90	2.03
3.4	2.05	2.03	2.25	1.83	2.04
4.0	2.04	2.03	2.31	1.77	2.04
4.7	2.05	2.02	2.40	1.71	2.04
5.4	2.06	2.02	2.45	1.65	2.04
6.0	2.05	2.02	2.50	1.61	2.04
6.7	2.08	2.02	2.52	1.60	2.04
7.4	2.09	2.04	2.46	1.67	2.04
8.0	2.05	2.04	2.34	1.77	2.03

Table 15 shows the 3:1 VSWR and matchable regions for three different feed methods. For the four base feed model, large 3:1 VSWR regions are at 2.7-5.4 MHz and 8.0-14.7 MHz. In the case of using a series reactance the acceptable frequency regions of 3:1 VSWR may be increased to almost the entire frequency range of 2.7-15.4 MHz.

TABLE 14  
MODEL 4 AVERAGE POWER GAIN IN FREQUENCY 8-16 MHZ

Frequency in MHz	4 Base Feeds	3 Base Feeds	2 Adjacent Base Feeds	2 Diagonal Base Feeds	1 Base Feed
8.0	2.05	2.04	2.34	1.77	2.03
8.7	2.05	2.03	2.31	1.76	2.03
9.4	2.04	2.00	2.40	1.65	2.04
10.0	2.02	1.99	2.49	1.57	2.04
10.7	2.04	1.98	2.55	1.51	2.05
11.4	2.05	1.98	2.57	1.49	2.05
12.0	2.06	1.98	2.46	1.54	2.05
12.7	2.04	2.00	2.33	1.71	2.04
13.4	2.00	1.99	2.47	1.61	2.11
14.0	1.99	1.99	2.68	1.45	2.17
14.7	2.01	1.99	2.79	1.38	2.21
15.4	2.03	2.00	2.83	1.37	2.22
16.0	2.06	2.03	2.77	1.47	2.22

INPUT IMPEDANCE OF MODEL 4  
FOR 4 BASE FEEDS

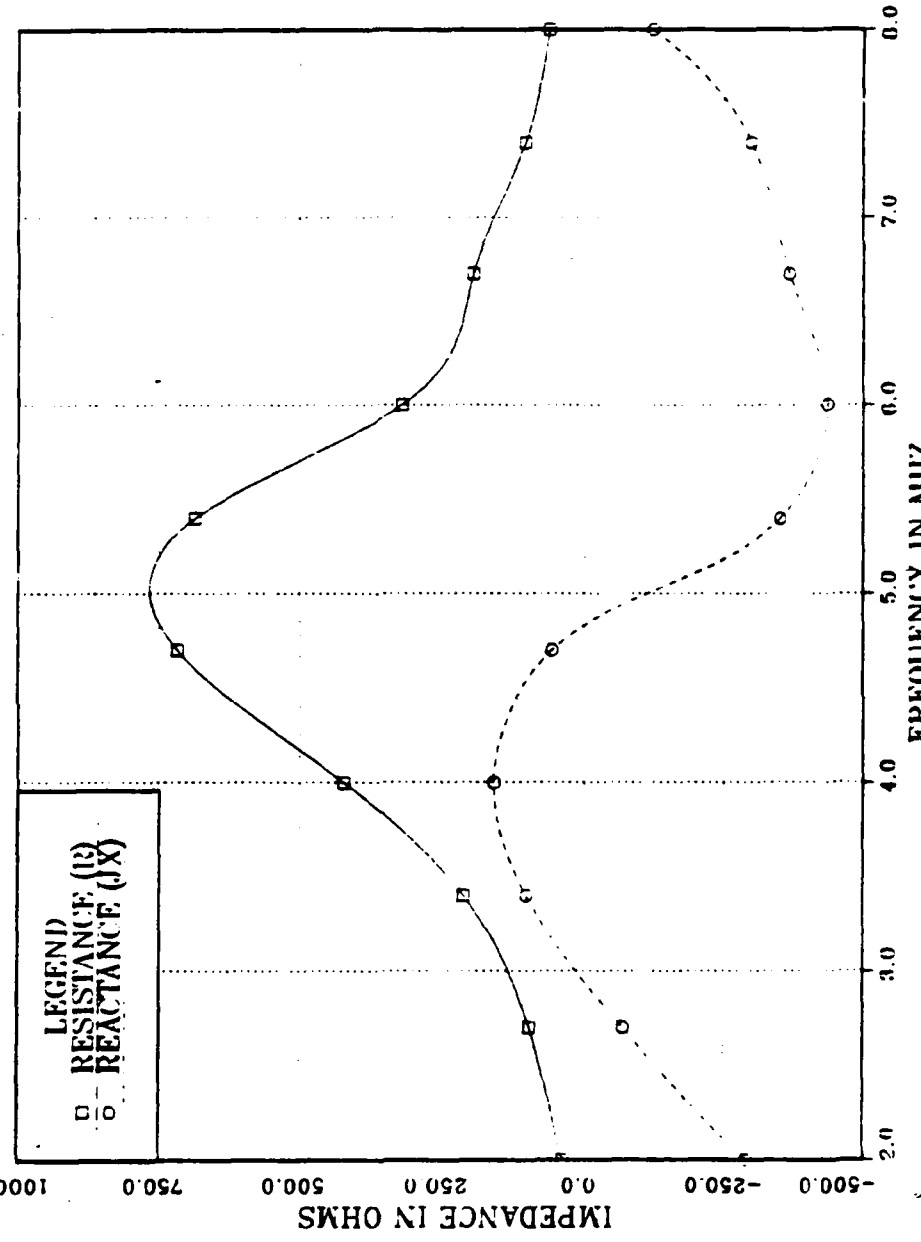


Figure 3.21 Model 4 Input Impedance in Frequency 2-8 MHz  
for 4 Base Feeds.

**INPUT IMPEDANCE OF MODEL 4  
for 4 BASE FEEDS**

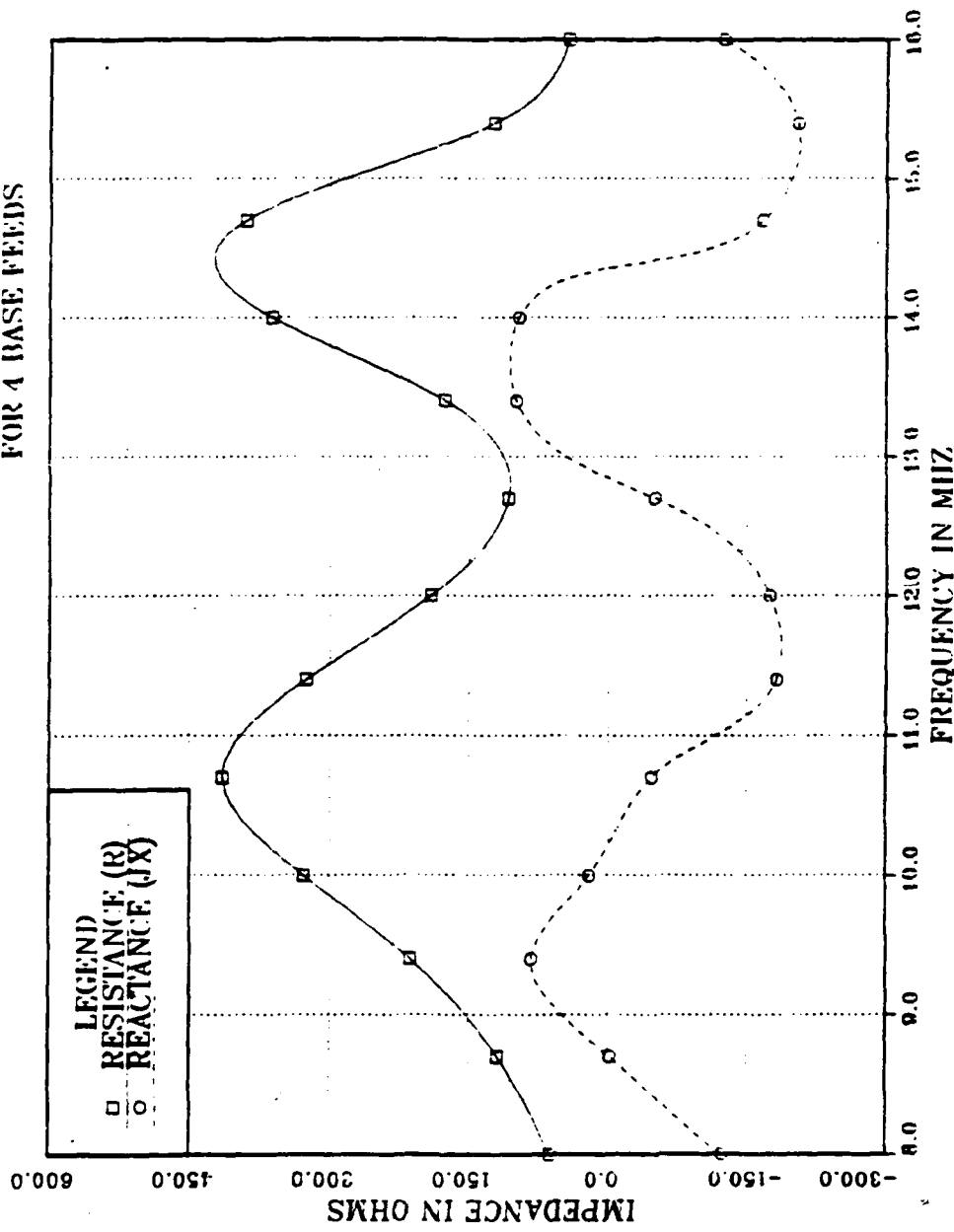


Figure 3.22 Model 4 Input Impedance in Frequency 8-16 MHz  
for 4 Base Feeds.

MODEL 4 BY FOUR BASE FEEDS

FREQUENCY = 2 MHZ

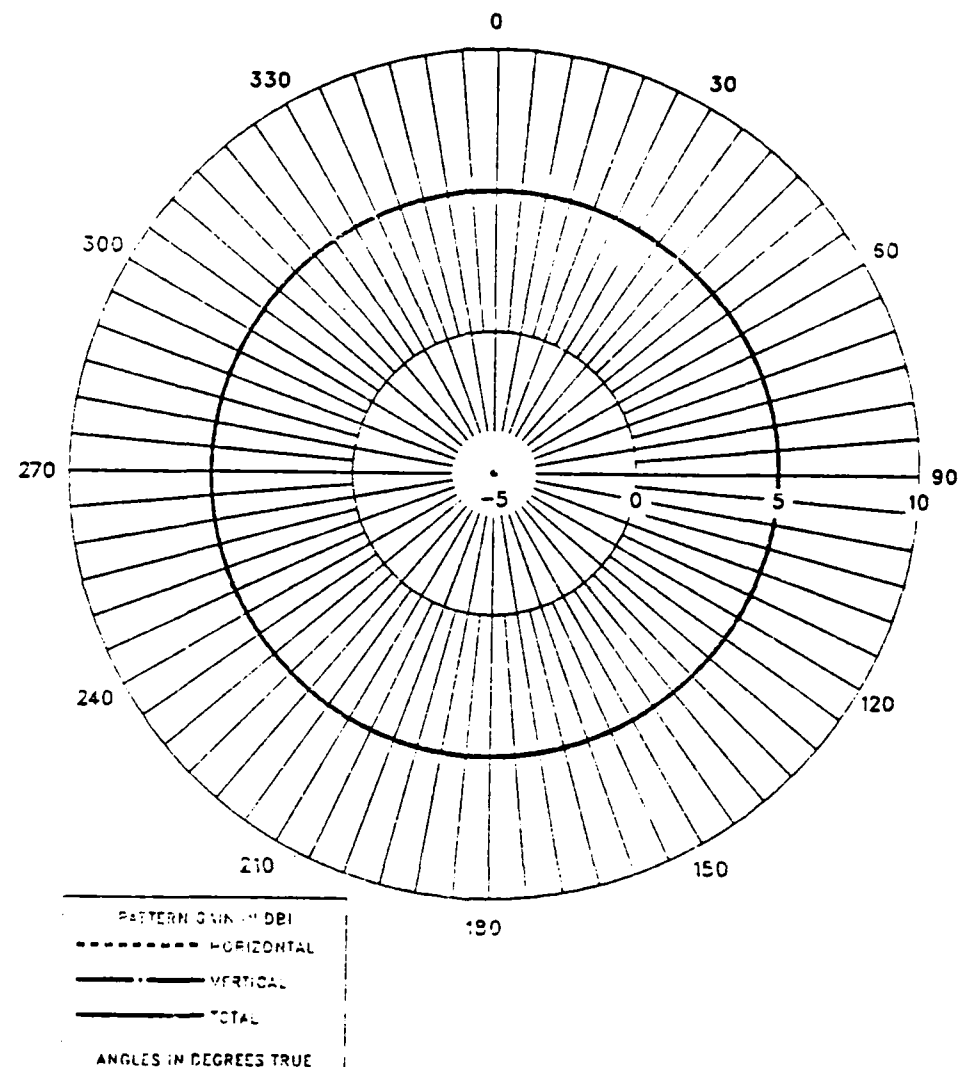
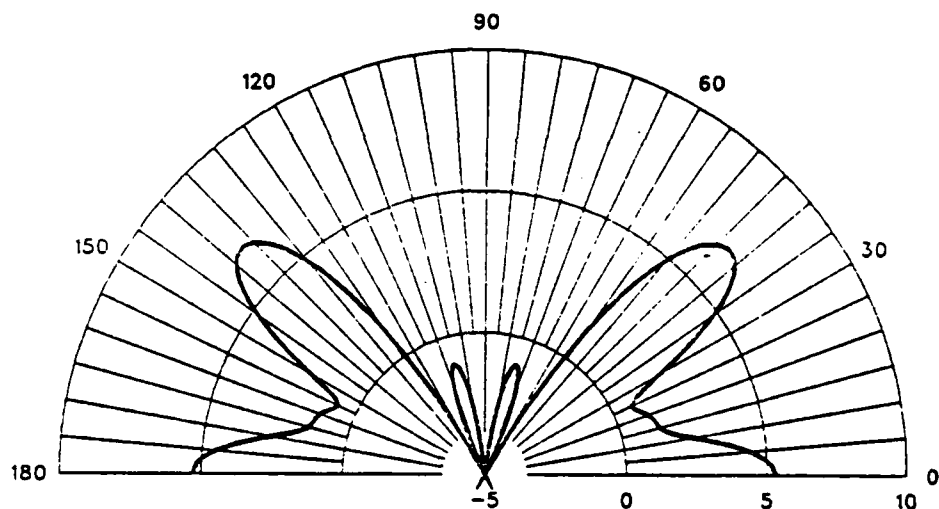


Figure 3.23 Model 4 E-Field Azimuth Pattern at 2 MHz  
for 4 Base Feeds.

MODEL 4 BY FOUR BASE FEEDS

FREQUENCY = 16 MHZ



PATTERN GAIN IN DBI  
----- HORIZONTAL  
— VERTICAL  
— TOTAL  
ELEVATION ANGLE

Figure 3.24 Model 4 E-Field Elevation Pattern at 16 MHz  
for 4 Base Feeds.

TABLE 15  
MODEL 4 3:1 VSWR AND MATCHABLE REGIONS  
for Frequency in MHz

Feeding Methods	4 Base Feeds		3 Base Feeds	1 Base Feed
Z <sub>o</sub> (Ohm)	50	300	300	300
3:1 VSWR	2.7- 3.4	2.7- 5.4	2.7 6.0- 6.7	8.0- 8.7
Regions	12.7-13.4	8.0-14.7	7.4-15.4	14.0
3:1 VSWR Matchable Regions	7.4- 9.4 12.0-13.4	5.4- 8.0	2.7- 6.0	7.4 8.7-14.7
	15.4-16.0	14.7-15.4		16.0

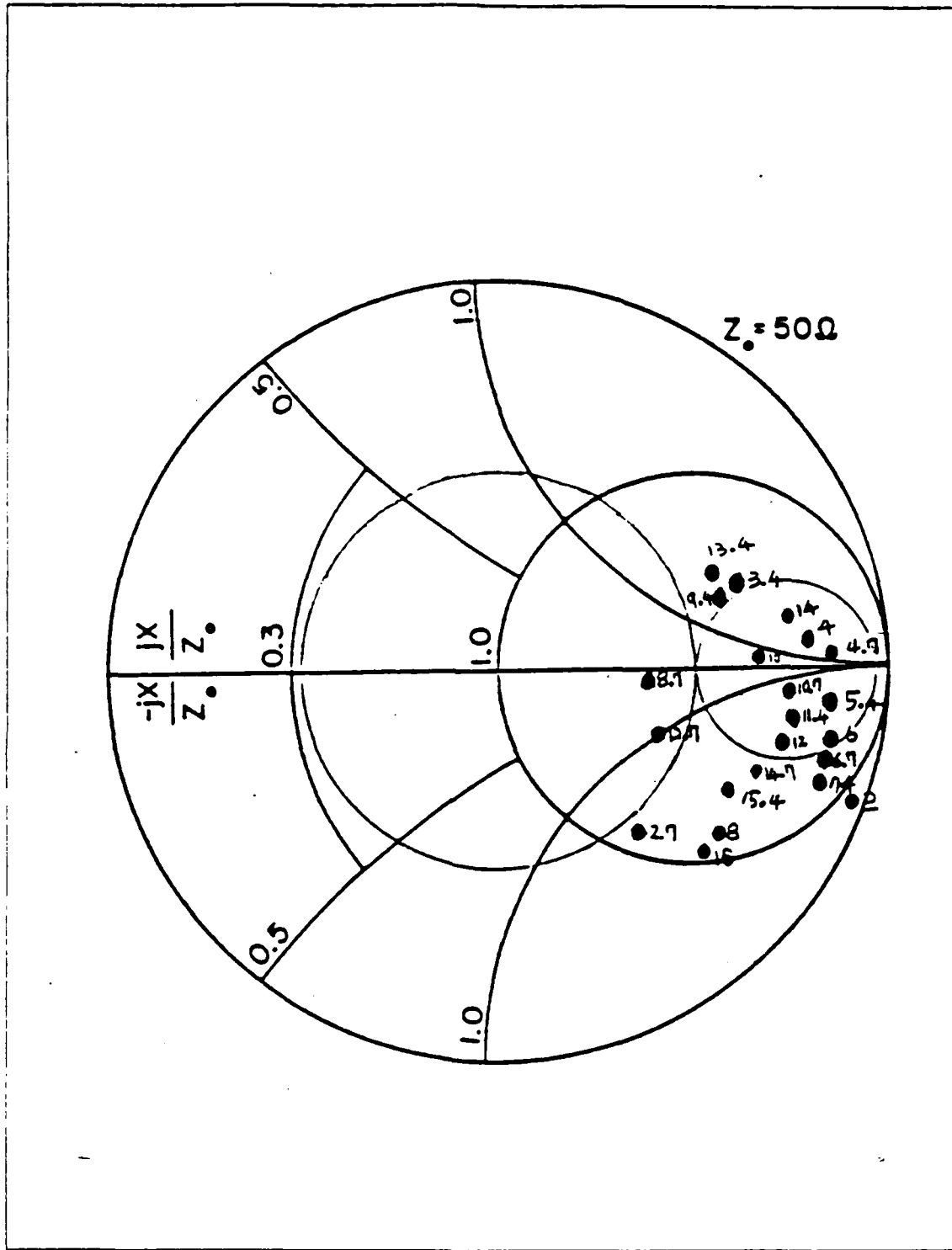


Figure 3.25 Model 4 Impedance Plot in Frequency 2-16 MHz  
for 4 Basic Feeds:  $Z_0 = 50\text{ Ohm}$ .

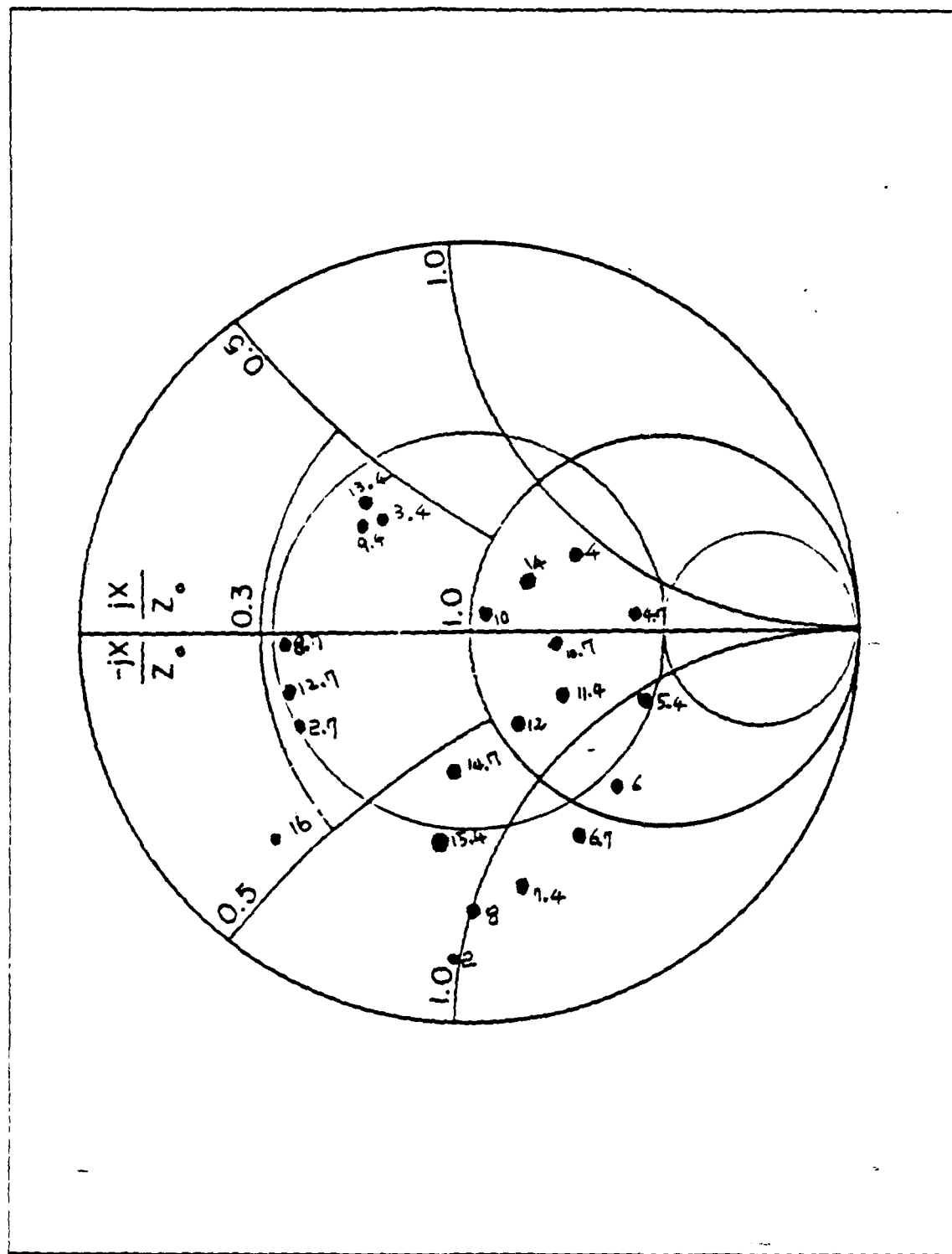


Figure 3.26 Model 4 Impedance Plot in Frequency 2-16 MHz  
for 4 Base Feeds:  $Z_0 = 300 \text{ Ohm}$ .

## IV. SUMMARY

This thesis developed six computer models for survivable shipboard HF communication antennas using two FFG-45 frigate masts. The sub-mast, 9 meters high, was modeled as a survivable HF communication antenna for the frequency range 2-10MHz. Both wire grid and surface patch models were developed with some additional wires used for feeding energy to the mast, and two models using different patch methods, four external shunt feeds and one internal shunt feed, were added. The main-mast, 18 meters high, was modeled as a survivable HF communication antenna for the frequency range 2-16 MHz. Both a wire grid and a surface patch model were developed with some additional wires used for feeding energy to the mast. All six models were exercised using the NEC program over a perfect ground plane. The simulated mast models were used to determine the input impedances and radiation patterns of survivable shipboard HF communication antennas.

### A. CONCLUSIONS

For the simulated mast survivable antennas, sources must be symmetrically located for desired omnidirectional azimuth radiation patterns.

Portions of feed wires to mast surfaces must not be placed closer than half of a patch width, or numerical instability occurs.

Generally, when characteristic impedance is 50 Ohms, the survivable shipboard mast antenna models are hard to match into the 3:1 VSWR region for the entire frequency range. Therefore, appropriate characteristic impedances must be selected to broaden the 3:1 VSWR regions.

Wire grids inherently have more inductance and less capacitance per square unit because current in wires is concentrated and produces higher magnetic fields. Also, smaller surface areas of wires provide less area for charge accumulation, hence lower capacitance. This affects calculated input impedance values.

For the simulated mast survivable antennas, input impedance is the impedance seen by the voltage source used to drive the antennas. The input impedance is the most important parameter in determining shipboard antenna performance. For wire grid mast computer models, the grid density does affect the impedance of a computer model. Grid heights are different from the grid widths for Model 2 and Model 4. The

grid density is not the only parameter affecting the computer model's impedance. The type of voltage source, the number and length of segments, the number and size of feed segments, and the radius of the wires also affect the impedance.

Because the surface patch computer model cannot be built without additional wire feed structures, the parameters affecting the surface patch computer model antenna performance are similar to those for wire grid models. Patch area, patch size, the position of patch centers, and separation between the surface and the feed wire structure also affect the impedance, but in the NEC surface patch model, surface currents are evaluated only at one point, the center of the patch. Also, the patch parameters which are used by NEC include the area and a surface normal vector orientation only, not patch shape.

The radiation patterns define the gain. This thesis checked the spatial distribution of phi ( $\phi$ ) and theta ( $\theta$ ), the polarized electric field components radiated in the far-field zone of the antennas.

The results of this investigation indicate that survivable simulated masts driven by the surface patch models and the wire grid models for the different patch methods such as base feed or external shunt feed do possess radiation patterns and impedance characteristics which make them feasible designs.

Model 1, the sub-mast surface patch model driven by four external shunt feeds, has the impedance characteristic that the 3:1 VSWR matchable region is 6-10 MHz by use of a series of reactance components with the 200 ohm characteristic impedance. Model 1's radiation patterns with the four external shunt feeds are similar to those of a same height whip antenna. The azimuth patterns are omnidirectional and do not have side lobes for the frequency range of interest. Directivity also increases as the frequency increases.

Model 2, the sub-mast wire grid model driven by the four base feeds, has the impedance characteristic that the 3:1 VSWR region is 6-10 MHz without use of a series reactance and is 4-10 MHz by use of a series reactance when the characteristic impedance is 150 Ohms. The results of Model 2 driven by the different patch methods gave different impedance characteristics on the 3:1 VSWR criteria. Model 2's radiation patterns for four base feeds are similar to those of a monopole whip antenna of same height. The azimuth patterns are omnidirectional and do not have side lobes for the target frequency range.

When the results of Model 1 were compared to those of Model 2A with the same feed method, radiation patterns were very similar for the entire designed frequency range, but Model 2A has better VSWR characteristics. Therefore, for the mast model with relatively low height, a wire grid computer model is recommended.

Model 3, the main-mast surface patch model driven by the four external shunt feeds, has impedance characteristics for a 3:1 VSWR region of 6-13 MHz without use of series reactances and is increased to 4-16 MHz by use of series reactances when the characteristic impedance is 150 Ohm. Model 3's azimuth patterns are omnidirectional and almost those of a monopole whip antenna of the same height for the low HF frequency range, but are more directional as frequency increases. Model 3's elevation patterns do not have a side lobe for the low HF frequency range, but have side lobes as frequency increases near 16 MHz.

Model 4, the main-mast wire grid model, has impedance characteristics with 3:1 VSWR regions of 2.7-5.4 and 8.0-14.7 MHz without use of series reactance and is increased to almost the entire frequency range, 2.7-15.4 MHz, by use of series reactances when the characteristic impedance is 300 Ohms. Model 4's azimuth patterns are omnidirectional for the whole frequency range, but elevation patterns show large side lobes at 45 degrees and 135 degrees at 16 MHz.

The results of this investigation reveal that the simulated mast survivable antennas have in common the characteristic that they require four symmetric feed points for successful operation.

When the sub-mast computer model antennas were compared with the main-mast computer model antennas, it was obvious that height of the mast is a most important factor in determining acceptability of survivable mast antennas. The taller mast gives better gain, patterns, input impedance characteristics, and 3:1 VSWR criteria than the shorter mast. But the increased height of a mast decreases the survivability of the driven mast antenna.

In summary, the wire grid models of masts used as antennas proved easier to use in parameter variation studies than surface patch models. Both mast geometries show definite promise when excited as radiating structures and are recommended for interim use as survivable antennas for lower HF frequency ranges.

## B. RECOMMENDATIONS

Many aspects of this study warrant further investigation:

- Determine the antenna's responses at higher frequencies for each model.

- Vary the height of the feed wire attachment point for the surface patch computer and also for the wire grid model.
- Try reducing the height of the simulated main-mast to increase the survivability of the antenna during combat, while still retaining useful antenna performance.
- Consider ways of reducing the separation between the mast surfaces and the feed wires to overcome the NEC limitation cited for Models 1 and 3.
- Develop survivable shipboard communication antenna models by the excitation of stacks, etc.
- Try an increased number of segments in vicinity of feed points in the case of wire grid models with unsymmetrical feeds, which suffered poor average power gain.
- Develop the main-mast wire grid model using four external shunt feeds around the mast and the one internal shunt feed installed inside of the mast. This was investigated during this thesis for the sub-mast only.
- Finally, build and test the scale, physical models of the survivable mast antennas for comparison to the computer model and to provide validation of the various numerical modeling options.

## APPENDIX A GEOMETRY DATA SETS

### a. Model 1 Geometry Data Set

```
CM      MODEL 1 SUB-MAST SURFACE PATCH MODEL
CM      HEIGHT      = 9 METERS
CM      WIDTH       = 3 METERS
CM      SOURCES LENGTH = 1.4 METERS
CM      SOURCES HEIGHT = 4.5 METERS
CM      FOUR EXTERNAL SHUNT FEEDS
CE
SM 2,2,1.5,-1.5,9,1.5,1.5,9
SC 0,0,-1.5,1.5,9
SM 2,2,1.5,-1.5,0,1.5,1.5,0
SC 0,0,1.5,1.5,3
SM 2,2,1.5,1.5,0,-1.5,1.5,0
SC 0,0,-1.5,1.5,3
SM 2,2,-1.5,1.5,0,-1.5,-1.5,0
SC 0,0,-1.5,-1.5,3
SM 2,2,-1.5,-1.5,0,1.5,-1.5,0
SC 0,0,1.5,-1.5,3
SP 0,1,1.5,-1.5,3,1.5,1.5,3
SC 0,1,1.5,1.5,6
SP 0,1,1.5,1.5,3,-1.5,1.5,3
SC 0,1,-1.5,1.5,6
SP 0,1,-1.5,-1.5,3
SC 0,1,1.5,-1.5,6
SP 0,1,1.5,-1.5,3,1.5,-1.5,3
SC 0,1,1.5,-1.5,6
SM 2,2,1.5,-1.5,6,1.5,1.5,6
SC 0,0,1.5,1.5,9
SM 2,2,1.5,1.5,6,-1.5,1.5,6
SC 0,0,-1.5,1.5,9
SM 2,2,-1.5,1.5,6,-1.5,-1.5,6
SC 0,0,-1.5,-1.5,9
SM 2,2,-1.5,-1.5,6,1.5,-1.5,6
SC 0,0,1.5,-1.5,9
GW 1,1,1.5,0,4.5,2.9,0,4.5,0,05
GW 2,1,-1.5,0,4.5,-2.9,0,4.5,0,05
GW 3,1,0,1.5,4.5,0,2.9,4.5,0,05
GW 4,1,0,-1.5,4.5,0,-2.9,4.5,0,05
GW 5,3,2.9,0,0,2.9,0,4.5,0,05
GW 6,3,-2.9,0,0,-2.9,0,4.5,0,05
GW 7,3,0,2.9,0,0,2.9,4.5,0,05
GW 8,3,0,-2.9,0,0,-2.9,4.5,0,05
GE 1
GN 1
FR 0,0,0,0,9
EX 0,5,1,00,1
EX 0,6,1,00,1
EX 0,7,1,00,1
EX 0,8,1,00,1
RP 0,91,3,1501,0,0,1,45
PL 3, 2, 0, 4
RP 0, 1, 361, 1000, 90, 0, 0, 1      STD. HORIZONTAL PATTERN CUT
PL 3, 1, 0, 4
RP 0, 181, 1, 1000, -90, 0, 1, 0      STD. VERTICAL PATTERN CUT
EN
```

b. Model 2 Geometry Data Set

```

CM      MODEL 2 SUB-MAST WIRE GRID MODEL
CM      HEIGHT = 9 METERS
CM      WIDTH  = 3 METERS
CM      FOUR BASE FEEDS
CE
GW 1,2,1.5,-1.5,1.5,1.5,1.5,1.5,0.05
GW 2,2,1.5,-1.5,3,1.5,1.5,3,0.05
GW 3,2,1.5,-1.5,4.5,1.5,1.5,4.5,0.05
GW 4,2,1.5,-1.5,6,1.5,1.5,6,0.05
GW 5,2,1.5,-1.5,7.5,1.5,1.5,7.5,0.05
GW 6,2,1.5,-1.5,9,1.5,1.5,9,0.05
GW 7,2,1.5,1.5,1.5,-1.5,1.5,1.5,0.05
GW 8,2,1.5,1.5,3,-1.5,1.5,3,0.05
GW 9,2,1.5,1.5,4.5,-1.5,1.5,4.5,0.05
GW 10,2,1.5,1.5,6,-1.5,1.5,6,0.05
GW 11,2,1.5,1.5,7.5,-1.5,1.5,7.5,0.05
GW 12,2,1.5,1.5,9,-1.5,1.5,9,0.05
GW 13,2,-1.5,-1.5,1.5,-1.5,1.5,1.5,0.05
GW 14,2,-1.5,-1.5,6,-1.5,1.5,6,0.05
GW 17,2,-1.5,-1.5,4.5,-1.5,1.5,4.5,0.05
GW 15,2,-1.5,-1.5,3,-1.5,1.5,3,0.05
GW 16,2,-1.5,-1.5,7.5,-1.5,1.5,7.5,0.05
GW 18,2,-1.5,-1.5,9,-1.5,1.5,9,0.05
GW 19,2,-1.5,-1.5,1.5,1.5,-1.5,1.5,0.05
GW 21,2,-1.5,-1.5,3,1.5,-1.5,3,0.05
GW 20,2,-1.5,-1.5,4.5,1.5,-1.5,4.5,0.05
GW 22,2,-1.5,-1.5,6,1.5,-1.5,6,0.05
GW 23,2,-1.5,-1.5,7.5,1.5,-1.5,7.5,0.05
GW 24,2,-1.5,-1.5,9,1.5,-1.5,9,0.05
GW 25,6,1.5,-1.5,0,1.5,-1.5,9,0.05
GW 26,6,1.5,1.5,0,1.5,1.5,9,0.05
GW 27,6,-1.5,-1.5,0,-1.5,-1.5,9,0.05
GW 28,6,-1.5,1.5,0,-1.5,1.5,9,0.05
GE 1
GN 1
FR 0,0,0,0,2
EX 0,25,1,00,1
EX 0,26,1,00,1
EX 0,27,1,00,1
EX 0,28,1,00,1
RP 0,91,3,1501,0,0,1,45
PL 3, 2, 0, 4
RP 0, 1, 361, 1000, 90, 0, 0, 1    STD. HORIZONTAL PATTERN CUT
PL 3, 1, 0, 4
RP 0, 181, 1, 1000, -90, 0, 1, 0   STD. VERTICAL PATTERN CUT
EN

```

c. Model 2A Geometry Data Set

```

CM      MODEL 2A SUB-MAST WIRE GRID MODIFIED MODEL
CM      HEIGHT = 9 METERS
CM      WIDTH  = 3 METERS
CM      FOUR EXTERNAL SHUNT FEEDS
CE
GW 1,2,1.5,-1.5,1,1.5,1.5,1,0.05
GW 2,2,1.5,-1.5,2,1.5,1.5,2,0.05
GW 3,2,1.5,-1.5,3,1.5,1.5,3,0.05
GW 4,2,1.5,-1.5,4,1.5,1.5,4,0.05
GW 5,2,1.5,-1.5,5,1.5,1.5,5,0.05
GW 6,2,1.5,-1.5,6,1.5,1.5,6,0.05
GW 7,2,1.5,-1.5,7,1.5,1.5,7,0.05
GW 8,2,1.5,-1.5,8,1.5,1.5,8,0.05
GW 9,2,1.5,-1.5,9,1.5,1.5,9,0.05
GW 10,2,1.5,1.5,1,-1.5,1.5,1,0.05
GW 11,2,1.5,1.5,2,-1.5,1.5,2,0.05
GW 12,2,1.5,1.5,3,-1.5,1.5,3,0.05

```

GW 13,2,1.5,1.5,4,-1.5,1.5,4,0.05  
 GW 14,2,1.5,1.5,5,-1.5,1.5,5,0.05  
 GW 15,2,1.5,1.5,6,-1.5,1.5,6,0.05  
 GW 16,2,1.5,1.5,7,-1.5,1.5,7,0.05  
 GW 17,2,1.5,1.5,8,-1.5,1.5,8,0.05  
 GW 18,2,1.5,1.5,9,-1.5,1.5,9,0.05  
 GW 19,2,-1.5,1.5,1,-1.5,-1.5,1,0.05  
 GW 20,2,-1.5,1.5,2,-1.5,-1.5,2,0.05  
 GW 22,2,-1.5,1.5,3,-1.5,-1.5,3,0.05  
 GW 23,2,-1.5,1.5,4,-1.5,-1.5,4,0.05  
 GW 24,2,-1.5,1.5,5,-1.5,-1.5,5,0.05  
 GW 25,2,-1.5,1.5,6,-1.5,-1.5,6,0.05  
 GW 26,2,-1.5,1.5,7,-1.5,-1.5,7,0.05  
 GW 27,2,-1.5,1.5,8,-1.5,-1.5,8,0.05  
 GW 28,2,-1.5,1.5,9,-1.5,-1.5,9,0.05  
 GW 29,2,-1.5,-1.5,1,1.5,-1.5,1,0.05  
 GW 30,2,-1.5,-1.5,2,1.5,-1.5,2,0.05  
 GW 31,2,-1.5,-1.5,3,1.5,-1.5,3,0.05  
 GW 32,2,-1.5,-1.5,4,1.5,-1.5,4,0.05  
 GW 33,2,-1.5,-1.5,5,1.5,-1.5,5,0.05  
 GW 34,2,-1.5,-1.5,6,1.5,-1.5,6,0.05  
 GW 35,2,-1.5,-1.5,7,1.5,-1.5,7,0.05  
 GW 36,2,-1.5,-1.5,8,1.5,-1.5,8,0.05  
 GW 37,2,-1.5,-1.5,9,1.5,-1.5,9,0.05  
 GW 38,9,1.5,-1.5,0,1.5,-1.5,9,0.05  
 GW 39,9,1.5,1.5,0,1.5,1.5,9,0.05  
 GW 40,9,-1.5,-1.5,0,-1.5,-1.5,9,0.05  
 GW 41,9,-1.5,1.5,0,-1.5,1.5,9,0.05  
 GW 42,2,3,0,0,3,0,4,0.05  
 GW 43,2,-3,0,0,-3,0,4,0.05  
 GW 44,2,0,3,0,0,3,4,0.05  
 GW 45,2,0,-3,0,0,-3,4,0.05  
 GW 46,1,1.5,0,4,3,0,4,0.05  
 GW 47,1,-1.5,0,4,-3,0,4,0.05  
 GW 48,1,0,1.5,4,0,3,4,0.05  
 GW 49,1,0,-1.5,4,0,-3,4,0.05  
 GW 50,2,1.5,0,9,-1.5,0,9,0.05  
 GW 51,2,0,1.5,9,0,-1.5,9,0.05  
 GW 52,9,0,1.5,0,0,1.5,9,0.05  
 GW 53,9,0,-1.5,0,0,-1.5,9,0.05  
 GW 54,9,1.5,0,0,1.5,0,9,0.05  
 GW 56,9,-1.5,0,0,-1.5,0,9,0.05  
 GE 1  
 GN 1  
 FR 0,0,0,0,2  
 EX 0,42,1,00,1  
 EX 0,43,1,00,1  
 EX 0,44,1,00,1  
 EX 0,45,1,00,1  
 RP 0,91,3,1501,0,0,1,45  
 PL 3, 2, 0, 4  
 RP 0, 1, 361, 1000, 90, 0, 0, 1      STD. HORIZONTAL PATTERN CUT  
 PL 3, 1, 0, 4  
 RP 0, 181, 1, 1000, -90, 0, 1, 0      STD. VERTICAL PATTERN CUT  
 EN

#### d. Model 2B Geometry Data Set

CM MODEL 2B SUB-MAST WIRE GRID MODIFIED MODEL  
 CM HEIGHT = 9 METERS  
 CM WIDTH = 3 METERS  
 CM ONE INTERNAL SHUNT FEED  
 CE  
 GW 1,2,1.5,-1.5,1.5,1.5,1.5,1.5,0.05  
 GW 2,2,1.5,-1.5,3,1.5,1.5,3,0.05  
 GW 3,2,1.5,-1.5,4,5,1.5,1.5,4,5,0.05  
 GW 4,2,1.5,-1.5,6,1.5,1.5,6,0.05  
 GW 5,2,1.5,-1.5,7,5,1.5,1.5,7,5,0.05

GW 6,2,1.5,-1.5,9,1.5,1.5,9,0.05  
 GW 7,2,1.5,1.5,1.5,-1.5,1.5,1.5,0.05  
 GW 8,2,1.5,1.5,3,-1.5,1.5,3,0.05  
 GW 9,2,1.5,1.5,4.5,-1.5,1.5,4.5,0.05  
 GW 10,2,1.5,1.5,6,-1.5,1.5,6,0.05  
 GW 11,2,1.5,1.5,7.5,-1.5,1.5,7.5,0.05  
 GW 12,2,1.5,1.5,9,-1.5,1.5,9,0.05  
 GW 13,2,-1.5,-1.5,1.5,-1.5,1.5,1.5,0.05  
 GW 14,2,-1.5,-1.5,6,-1.5,1.5,6,0.05  
 GW 17,2,-1.5,-1.5,4.5,-1.5,1.5,4.5,0.05  
 GW 15,2,-1.5,-1.5,3,-1.5,1.5,.05  
 GW 16,2,-1.5,-1.5,7.5,-1.5,1.5,.5,0.05  
 GW 18,2,-1.5,-1.5,9,-1.5,1.5,9,0.05  
 GW 19,2,-1.5,-1.5,1.5,1.5,-1.5,1.5,0.05  
 GW 21,2,-1.5,-1.5,3,1.5,-1.5,3,0.05  
 GW 20,2,-1.5,-1.5,4.5,1.5,-1.5,4.5,0.05  
 GW 22,2,-1.5,-1.5,6,1.5,-1.5,6,0.05  
 GW 23,2,-1.5,-1.5,7.5,1.5,-1.5,7.5,0.05  
 GW 24,2,-1.5,-1.5,9,1.5,-1.5,9,0.05  
 GW 25,6,1.5,-1.5,0,1.5,-1.5,9,0.05  
 GW 26,6,1.5,1.5,0,1.5,1.5,9,0.05  
 GW 27,6,-1.5,-1.5,0,-1.5,-1.5,9,0.05  
 GW 28,6,-1.5,1.5,0,-1.5,1.5,9,0.05  
 GW 30,2,1.5,0,4.5,-1.5,0,4.5,0.05  
 GW 31,2,0,1.5,4.5,0,-1.5,4.5,0.05  
 GW 32,3,0,0,0,0,0,4.5,0.05  
 GE 1  
 GN 1  
 FR 0,0,0,0,10  
 EX 0,32,1,00,1  
 RP 0,91,3,1501,0,0,1,45  
 PL 3, 2, 0, 4  
 RP 0, 1, 361, 1000, 90, 0, 0, 1      STD. HORIZONTAL PATTERN CUT  
 PL 3, 1, 0, 4  
 RP 0, 181, 1, 1000, -90, 0, 1, 0      STD. VERTICAL PATTERN CUT  
 EN

### e. Model 3 Geometry Data Set

CM MODEL 3 MAIN-MAST SURFACE PATCH MODEL  
 CM HEIGHT = 18 METERS  
 CM BELOW WIDTH = 4 METERS  
 CM ABOVE WIDTH = 2 METERS  
 CM SOURCES HEIGHT = 9 METERS  
 CM SOURCES LENGTH = 3 METERS  
 CM FOUR EXTERNAL SHUNT FEEDS  
 CE  
 SP 0,3,2,-2,0,2,-0.666667,0  
 SC 0,3,1,666667,-0.555556,6,1,666667,-1,666667,6  
 SC 0,3,1,333333,-0.444445,12,1,333333,-1.333333,12  
 SC 0,3,1,-333333,18,1,-1,18  
 SP 0,3,2,-0.666667,0,2,0.666667,0  
 SC 0,3,1,666667,0.555556,6,1,666667,-0.555556,6  
 SC 0,3,1,333333,0.444445,12,1,333333,-0.444445,12  
 SC 0,3,1,-333333,18,1,-0.333333,18  
 SP 0,3,2,0,666667,0,2,2,0  
 SC 0,3,1,666667,1,666667,6,1,666667,0.555556,6  
 SC 0,3,1,333333,1,333333,12,1,333333,0.444445,12  
 SC 0,3,1,1,18,1,0,333333,18  
 SP 0,3,2,2,0,666667,2,0  
 SC 0,3,0,555556,1,666667,6,1,666667,1,666667,6  
 SC 0,3,0,444445,1,333333,12,1,333333,1.333333,12  
 SC 0,3,-333333,1,18,1,1,18  
 SP 0,3,0,666667,2,0,-0.666667,2,0  
 SC 0,3,-0.555556,1,666667,6,0.555556,1,666667,6  
 SC 0,3,-0.444445,1,333333,12,0.444445,1.333333,12  
 SC 0,3,-333333,1,18,0.333333,1,18  
 SP 0,3,-0.666667,2,0,-2,2,0

SC 0,3,-1.666667,1.666667,6,-0.555556,1.666667,6  
 SC 0,3,-1.333333,1.333333,12,-0.444445,1.333333,12  
 SC 0,3,-1,1,18,-0.333333,1,18  
 SP 0,3,-2,2,0,-2,0.666667,0  
 SC 0,3,-1.666667,0.555556,6,-1.666667,1.666667,6  
 SC 0,3,-1.333333,0.444445,12,-1.333333,1.333333,12  
 SC 0,3,-1,-333333,18,-1,1,18  
 SP 0,3,-2,0.666667,0,-2,-0.666667,0  
 SC 0,3,-1.666667,-0.555556,6,-1.666667,0.555556,6  
 SC 0,3,-1.333333,-0.444445,12,-1.333333,0.444445,12  
 SC 0,3,-1,-333333,18,-1,0.333333,18  
 SP 0,3,-2,-0.666667,0,-2,-2,0  
 SC 0,3,-1.666667,-1.666667,6,-1.666667,-0.555556,6  
 SC 0,3,-1.333333,-1.333333,12,-1.333333,-0.444445,12  
 SC 0,3,-1,-1,18,-1,-0.333333,18  
 SP 0,3,-2,-2,0,-0.666667,-2,0  
 SC 0,3,-0.555556,-1.666667,6,-1.666667,-1.666667,6  
 SC 0,3,-0.444445,-1.333333,12,-1.333333,-1.333333,12  
 SC 0,3,-333333,-1,18,-1,-1,18  
 SP 0,3,-0.666667,-2,0,0.666667,-2,0  
 SC 0,3,0.555556,-1.666667,6,-0.555556,-1.666667,6  
 SC 0,3,0.444445,-1.333333,12,-0.444445,-1.333333,12  
 SC 0,3,333333,-1,18,-0.333333,-1,18  
 SP 0,3,0.666667,-2,0,2,-2,0  
 SC 0,3,1.666667,-1.666667,6,0.555556,-1.666667,6  
 SP 0,3,1.333333,-1.333333,12,0.444445,-1.333333,12  
 SC 0,3,1,-1,18,0.333333,-1,18  
 SP 0,1,1,-1,18,1,1,18  
 SC 0,1,-1,1,18  
 GW 17,4,0,0,18,0,0,24,0,3  
 GW 1,2,1.17460,-0.78307,14.85714,4.17460,-0.78307,14.85714,0.05  
 GW 2,2,1.17460,0.78307,14.85714,4.17460,0.78307,14.85714,0.05  
 GW 3,1,2.67460,-0.78307,14.85714,2.67460,0.78307,14.85714,0.05  
 GW 4,1,4.17460,-0.78307,14.85714,4.17460,0.78307,14.85714,0.05  
 GW 5,2,-1.17460,-0.78307,14.85714,-4.17460,-0.78307,14.85714,0.05  
 GW 6,2,-1.17460,0.78307,14.85714,-4.17460,0.78307,14.85714,0.05  
 GW 7,1,-2.67460,-0.78307,14.85714,-2.67460,0.78307,14.85714,0.05  
 GW 8,1,-4.17460,-0.78307,14.85714,-4.17460,0.78307,14.85714,0.05  
 GW 9,2,1.50617,0,8.888888,4.50617,0,8.888888,0.05  
 GW 10,2,0,1.50617,8.888888,0,4.50617,8.888888,0.05  
 GW 11,2,-1.50617,0,8.888888,-4.50617,0,8.888888,0.05  
 GW 12,2,0,-1.50617,8.888888,0,-4.50617,8.888888,0.05  
 GW 13,6,4.50617,0,8.888888,4.50617,0,0,0.05  
 GW 14,6,0,4.50617,8.888888,0,4.50617,0,0,0.05  
 GW 15,6,-4.50617,0,8.888888,-4.50617,0,0,0.05  
 GW 16,6,0,-4.50617,8.888888,0,-4.50617,0,0,0.05  
 GE 1  
 GN 1  
 FR 0,0,0,0,11  
 EX 0,13,6,00,1  
 EX 0,15,6,00,1  
 EX 0,14,6,00,1  
 EX 0,16,6,00,1  
 RP 0,91,3 1501,0,0,1,45  
 PL 3,2,0,4  
 RP 0,1,361,1000,90,0,0,1 STD. HORIZONTAL PATTERN CUT  
 PL 3,1,0,4  
 RP 0,181,1,1000,-90,0,1,0 STD. VERTICAL PATTERN CUT  
 EN

#### f. Model 4 Geometry Data Set

CM MODEL 4 MAIN-MAST WIRE GRID MODEL  
 CM HEIGHT = 18 METERS  
 CM BELOW WIDTH = 4 METERS  
 CM ABOVE WIDTH = 2 METERS  
 CE FOUR BASE FEEDS  
 GW 1,12,2,-2,0,1,-1,18,0.05

GW 2,12,2,2,0,1,1,18,0.05  
 GW 3,12,-2,-2,0,-1,-1,18,0.05  
 GW 4,12,-2,2,0,-1,1,18,0.05  
 GW 5,2,1,0,18,-1,0,18,0.05  
 GW 6,2,0,1,18,0,-1,18,0.05  
 GW 7,3,0,0,18,0,0,24,0.3  
 GW 8,2,1,8333333,-1,8333333,3,1,8333333,1,8333333,3,0.05  
 GW 9,2,1,8333333,1,8333333,3,-1,8333333,1,8333333,3,0.05  
 GW 10,2,-1,8333333,1,8333333,3,-1,8333333,-1,8333333,3,0.05  
 GW 11,2,-1,8333333,-1,8333333,3,1,8333333,-1,8333333,3,0.05  
 GW 12,2,1,6666667,-1,6666667,6,1,6666667,1,6666667,6,0.05  
 GW 13,2,1,6666667,1,6666667,6,-1,6666667,1,6666667,6,0.05  
 GW 14,2,-1,6666667,1,6666667,6,-1,6666667,-1,6666667,6,0.05  
 GW 15,2,-1,6666667,-1,6666667,6,1,6666667,-1,6666667,6,0.05  
 GW 16,2,1,5,1,5,9,-1,5,1,5,9,0.05  
 GW 17,2,-1,5,1,5,9,-1,5,1,5,9,0.05  
 GW 18,2,-1,5,-1,5,9,1,5,-1,5,9,0.05  
 GW 19,2,1,5,-1,5,9,1,5,1,5,9,0.05  
 GW 20,2,1,3333333,-1,3333333,12,1,3333333,1,3333333,12,0.05  
 GW 21,2,1,3333333,1,3333333,12,-1,3333333,1,3333333,12,0.05  
 GW 22,2,-1,3333333,1,3333333,12,-1,3333333,-1,3333333,12,0.05  
 GW 23,2,-1,3333333,-1,3333333,12,1,3333333,-1,3333333,12,0.05  
 GW 24,2,1,1666667,-1,1666667,15,1,1666667,1,1666667,15,0.05  
 GW 25,2,1,1666667,1,1666667,15,-1,1666667,1,1666667,15,0.05  
 GW 26,2,-1,1666667,1,1666667,15,-1,1666667,-1,1666667,15,0.05  
 GW 27,2,-1,1666667,-1,1666667,15,1,1666667,-1,1666667,15,0.05  
 GW 28,2,1,-1,18,1,1,18,0.05  
 GW 29,2,1,1,18,-1,1,18,0.05  
 GW 30,2,-1,1,18,-1,-1,18,0.05  
 GW 31,2,-1,-1,18,1,-1,18,0.05  
 GW 32,2,1,-1,18,4,-0.5,18,0.05  
 GW 33,2,1,1,18,4,0.5,18,0.05  
 GW 34,2,2.5,-0.75,18,2.5,0.75,18,0.05  
 GW 35,2,4,-0.5,18,4,0.5,18,0.05  
 GW 36,2,-1,-1,18,-4,-0.5,18,0.05  
 GW 37,2,-1,1,18,-4,0.5,18,0.05  
 GW 38,2,-2.5,-0.75,18,-2.5,0.75,18,0.05  
 GW 39,2,-4,-0.5,18,-4,0.5,18,0.05  
 GE 1  
 GN 1  
 FR 0,0,0,0,15.4  
 EX 0,1,1,00,1  
 EX 0,2,1,00,1  
 EX 0,3,1,00,1  
 EX 0,4,1,00,1  
 RP 0,91,3,1501,0,0,1,45  
 PL 3, 2, 0, 4  
 RP 0, 1, 361, 1000, 90, 0, 0, 1 STD. HORIZONTAL PATTERN CUT  
 PL 3, 1, 0, 4  
 RP 0, 181, 1, 1000, -90, 0, 1, 0 STD. VERTICAL PATTERN CUT  
 EN

**APPENDIX B**  
**MODEL 2 RESULTS FOR DIFFERENT FEED METHODS.**

TABLE 16  
MODEL 2 INPUT IMPEDANCE IN FREQUENCY 2-10 MHZ FOR  
FOUR BASE FEEDS

Frequency in MHz	Resistance in Ohms (R)	Reactance in Ohms (jX)
2	6.60	- 655.50
3	16.01	- 382.45
4	31.74	- 266.63
5	56.90	- 116.68
6	96.77	- 30.55
7	158.54	+ 0.23
8	246.97	+ 67.55
9	347.54	+ 39.99
10	407.81	- 56.49

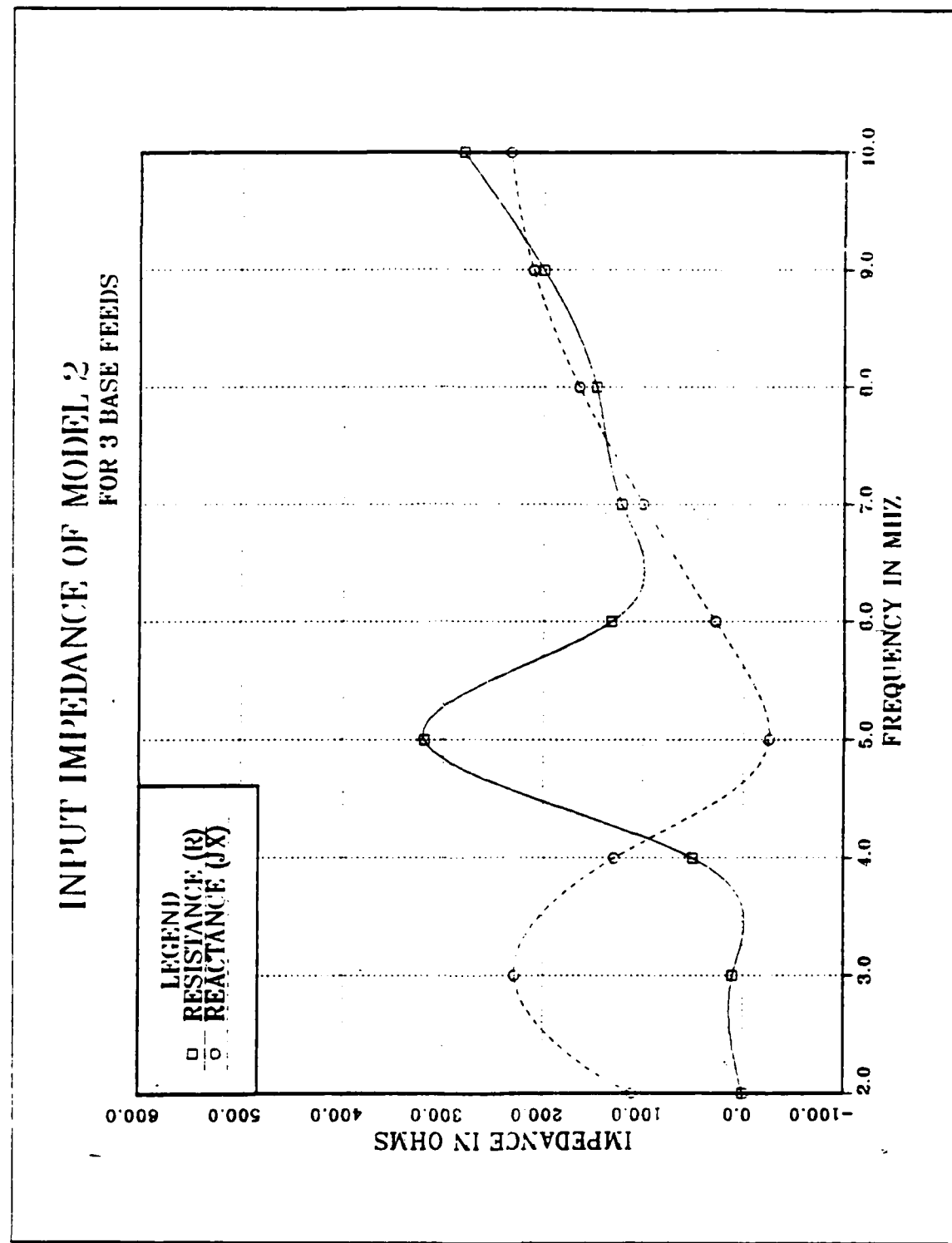


Figure B.1 Model 2 Input Impedance in Frequency 2-10 MHz  
for 3 Base Feeds.

TABLE 17  
MODEL 2 INPUT IMPEDANCE IN FREQUENCY 2-10 MHZ FOR  
THREE BASE FEEDS

Frequency in MHz	Resistance in Ohms (R)	Reactance in Ohms (jX)
2	0.21	+ 110.77
3	6.20	+ 228.10
4	28.36	+ 128.43
5	318.74	- 25.34
6	131.67	+ 27.70
7	121.47	+ 100.00
8	147.01	+ 164.25
9	199.47	+ 210.08
10	280.33	+ 233.34

INPUT IMPEDANCE OF MODEL 2  
FOR 2 DIAGONAL BASE FEEDS

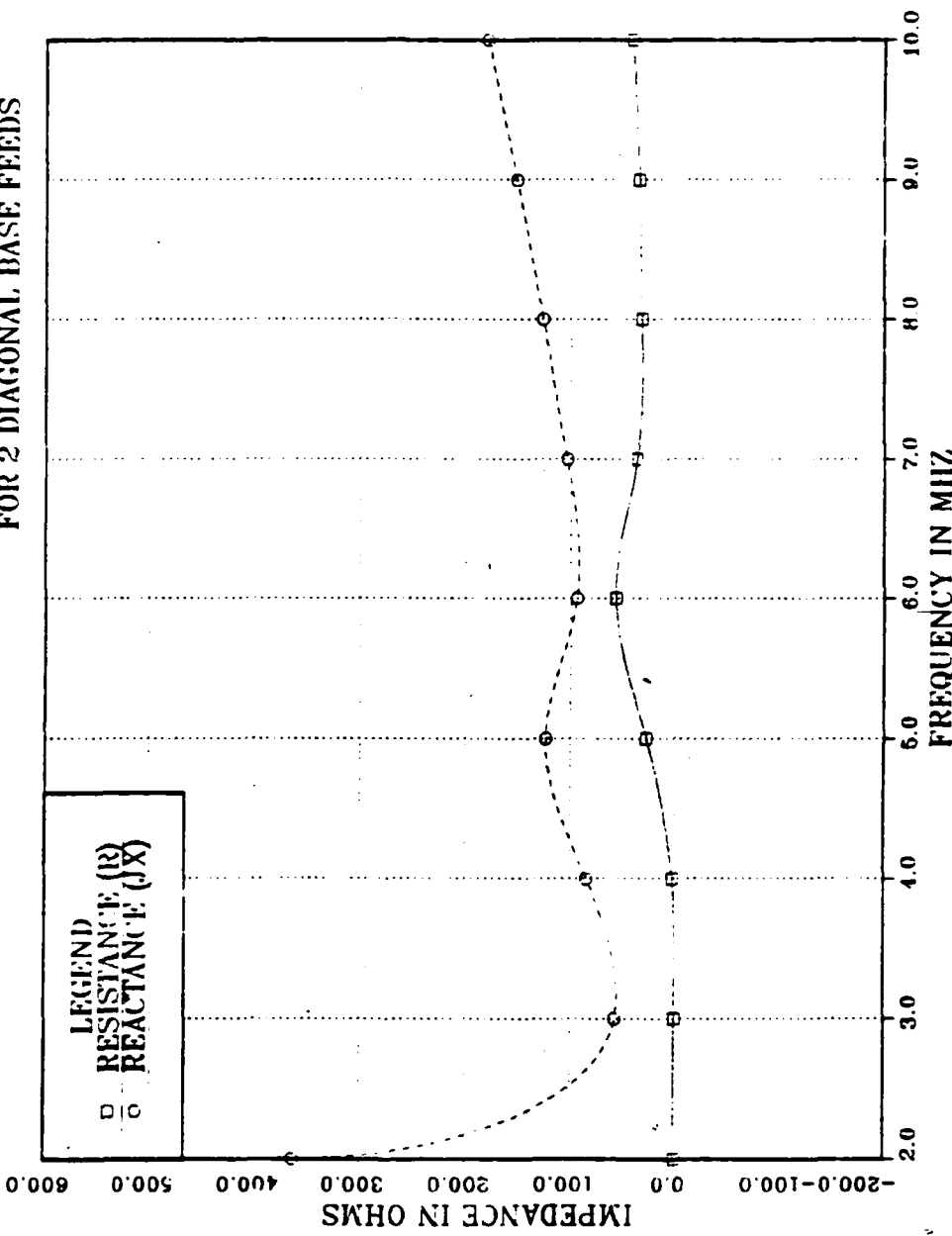


Figure B.2 Model 2 Input Impedance in Frequency 2-10 MHz  
for 2 Diagonal Base Feeds.

TABLE 18  
MODEL 2 INPUT IMPEDANCE IN FREQUENCY 2-10 MHZ FOR TWO  
DIAGONAL BASE FEEDS

Frequency in MHz	Resistance in Ohms (R)	Reactance in Ohms (jX)
2	0.01	+ 363.22
3	0.18	+ 57.06
4	2.20	+ 84.52
5	27.12	+ 123.80
6	56.71	+ 94.09
7	36.31	+ 103.71
8	32.15	+ 126.59
9	34.35	+ 151.63
10	40.76	+ 179.34

INPUT IMPEDANCE OF MODEL 2  
FOR 1 BASE FEED

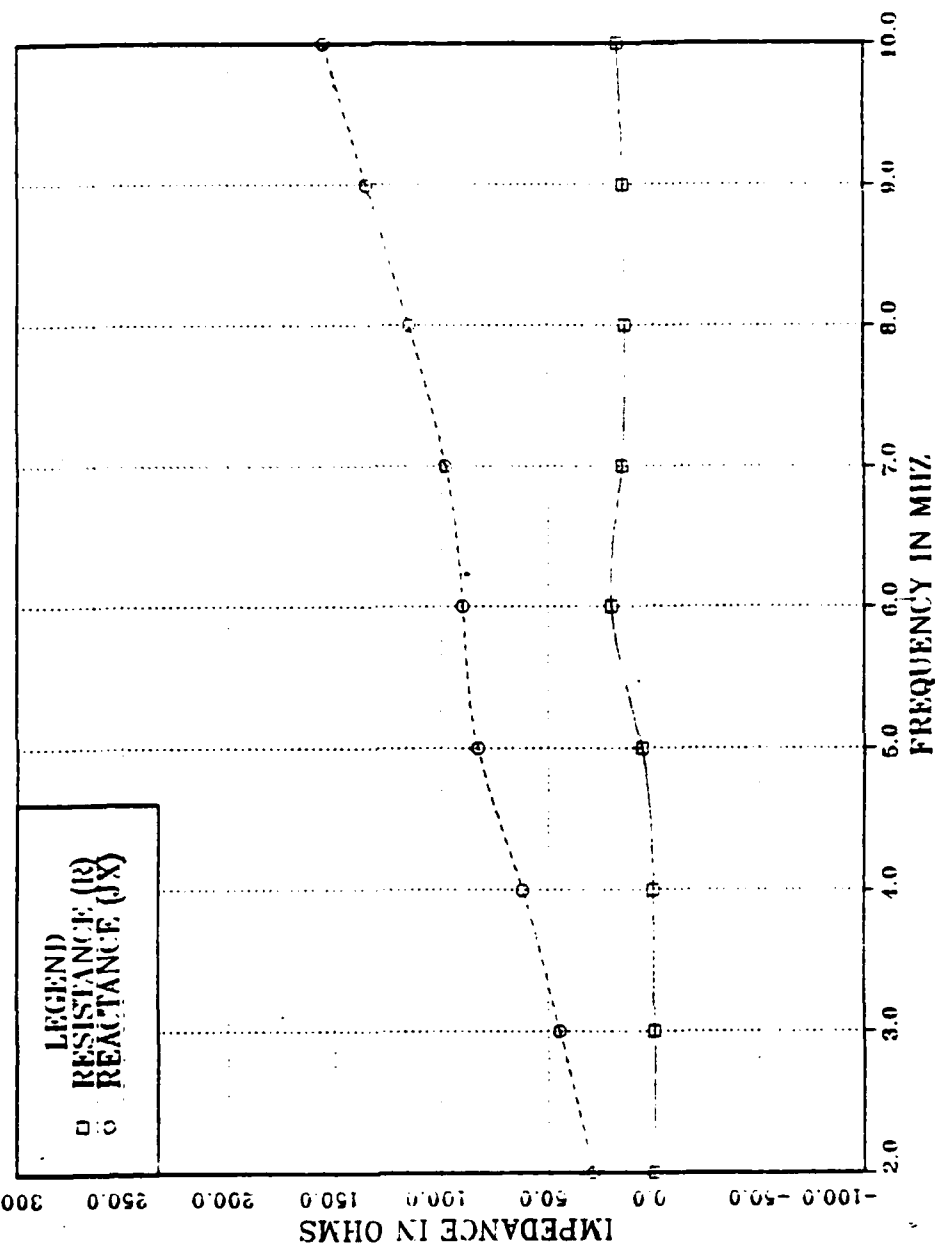


Figure B.3 Model 2 Input Impedance in Frequency 2-10 MHz  
for 1 Base Feed.

TABLE 19  
MODEL 2 INPUT IMPEDANCE IN FREQUENCY 2-10 MHZ FOR ONE  
BASE FEED

Frequency in MHz	Resistance in Ohms (R)	Reactance in Ohms (jX)
2	0.06	+ 28.87
3	0.07	+ 44.69
4	0.65	+ 62.03
5	6.07	+ 83.30
6	20.38	+ 90.13
7	15.42	+ 98.42
8	13.62	+ 115.41
9	14.55	+ 134.49
10	17.32	+ 155.37

INPUT IMPEDANCE OF MODEL 2A  
FOR 4 EXTERNAL SHUNT FEEDS

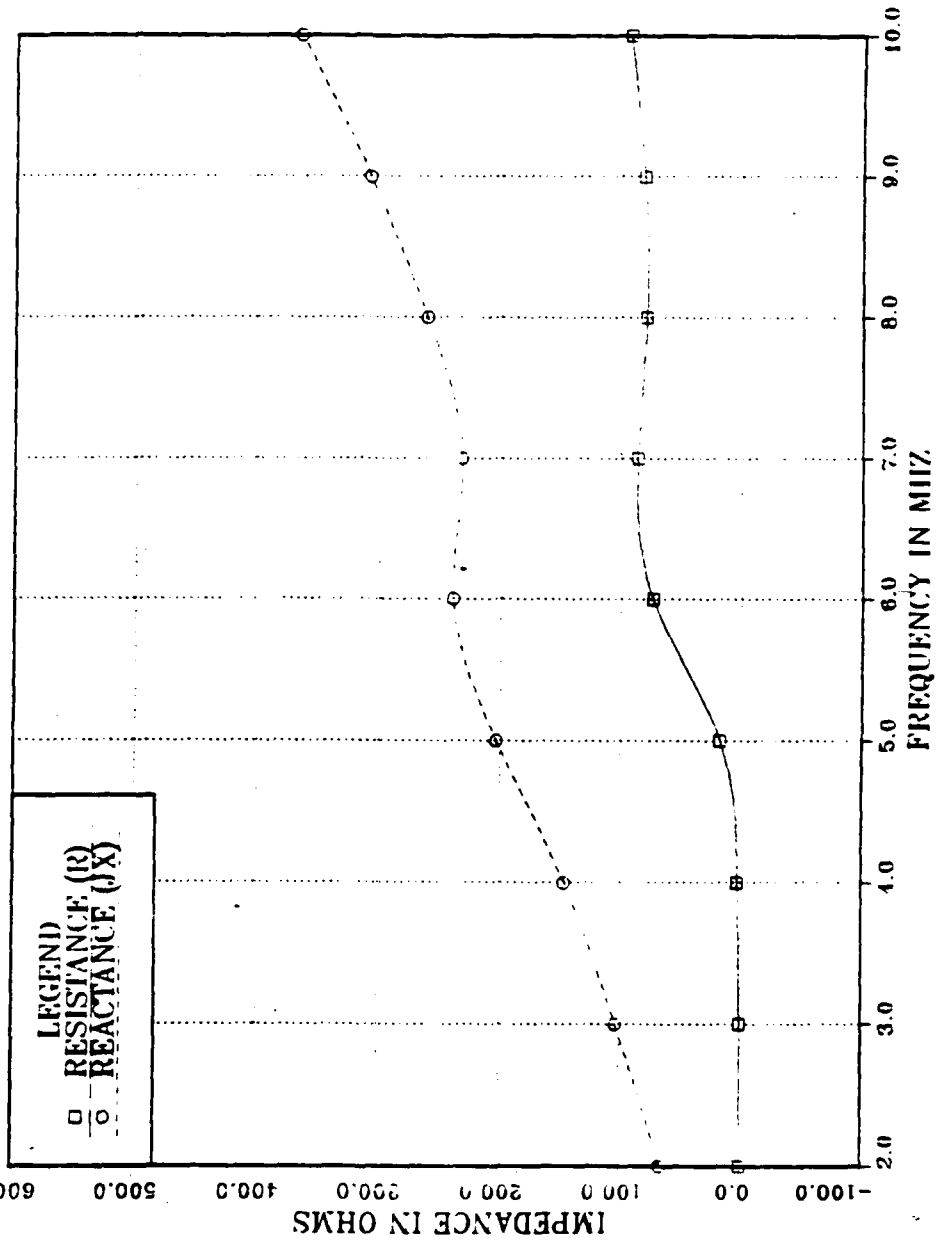


Figure B.4 Model 2A Input Impedance in Frequency 2-10 MHz  
for 4 External Shunt Feeds.

TABLE 20  
MODEL 2A INPUT IMPEDANCE IN FREQUENCY 2-10 MHZ FOR  
FOUR EXTERNAL SHUNT FEEDS

Frequency in MHz	Resistance in Ohms (R)	Reactance in Ohms (jX)
2	0.02	+ 65.89
3	0.29	+ 102.61
4	2.21	+ 146.08
5	17.07	+ 203.23
6	73.51	+ 239.17
7	86.17	+ 231.53
8	78.55	+ 260.59
9	80.87	+ 307.56
10	92.56	+ 366.22

MODEL 2 BY THREE BASE FEEDS

FREQUENCY = 2 MHZ

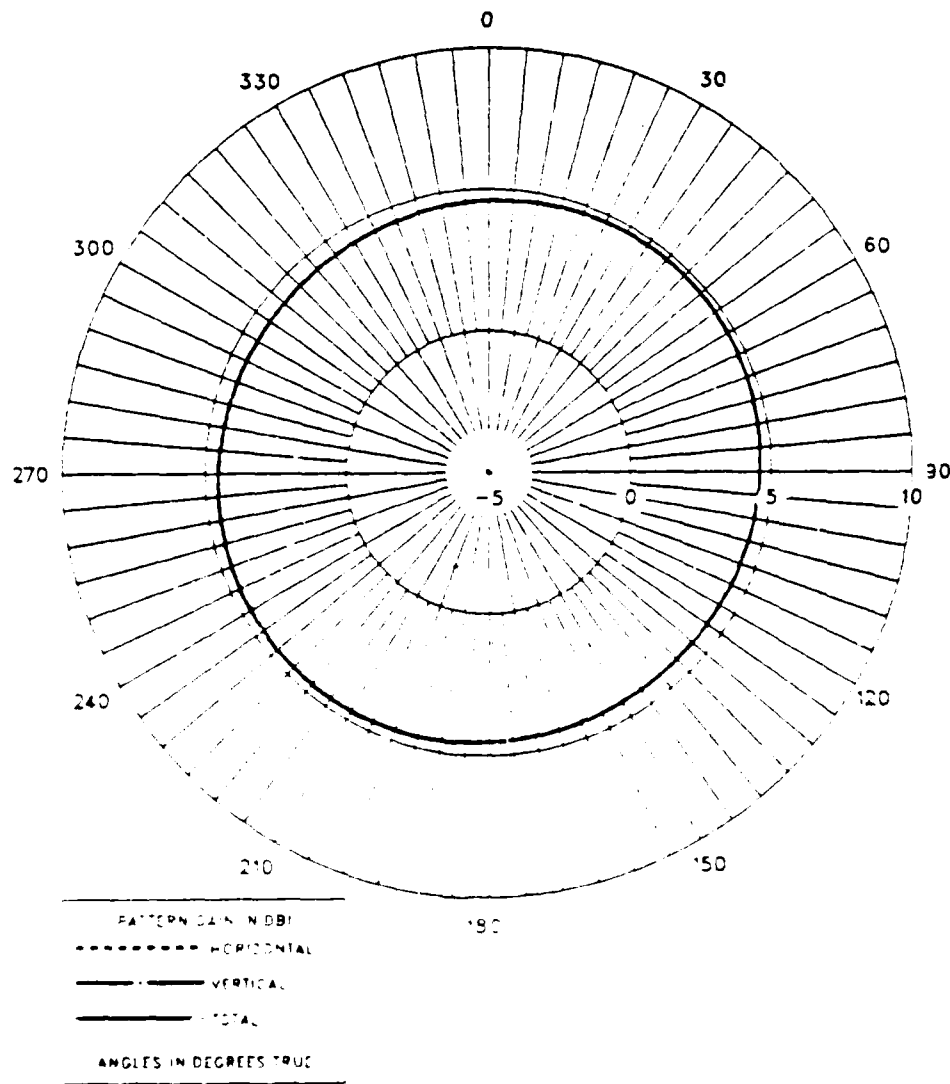
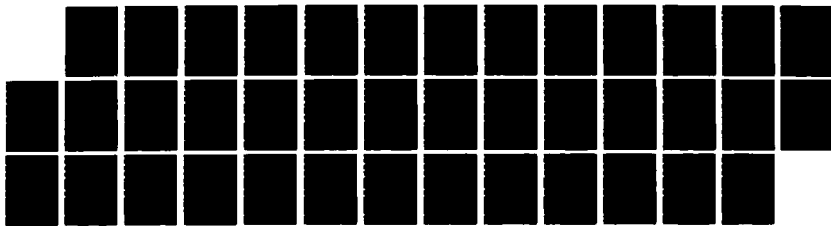
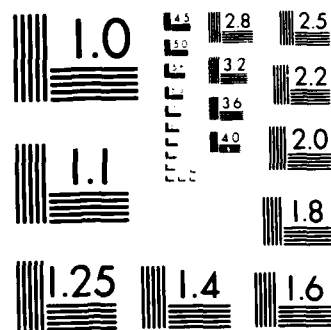


Figure B.5 Model 2 E-Field Azimuth Pattern at 2 MHz  
for 3 Base Feeds.

ND-A186 811 DESIGN OF SURVIVABLE SHIPBOARD HF MAST ANTENNA MODELS 272  
USING THE NUMERICAL ELECTROMAGNETICS CODE(U) NAVAL  
POSTGRADUATE SCHOOL MONTEREY CA I V CHOI SEP 87  
UNCLASSIFIED NPS62-87-015 F/G 9/1 NL





MICROCOPY RESOLUTION TEST CHART  
NATIONAL BUREAU OF STANDARDS 1963 A

MODEL 2 BY THREE BASE FEEDS

FREQUENCY = 10 MHZ

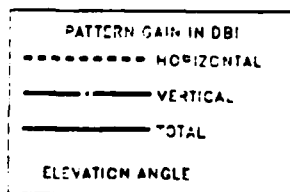
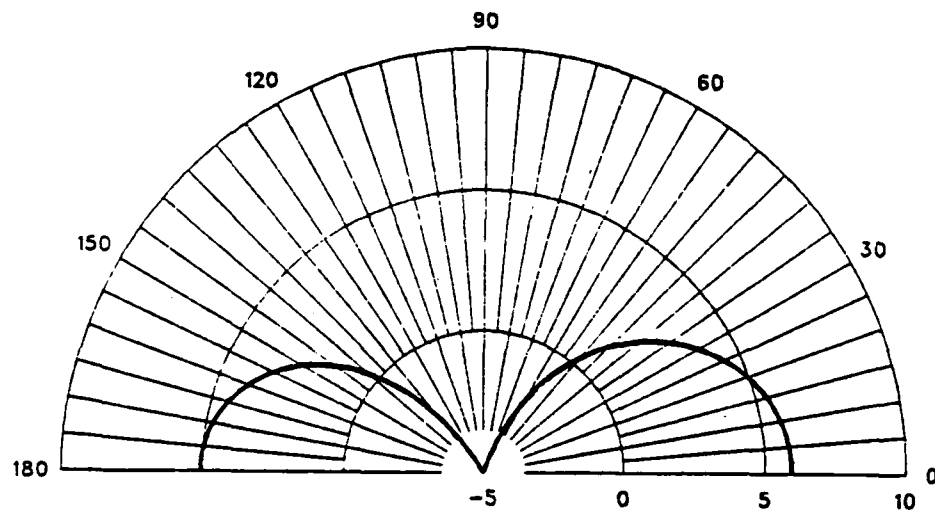


Figure B.6 Model 2 E-Field Elevation Pattern at 10 MHz  
for 3 Base Feeds.

MODEL 2 BY THREE BASE FEEDS

FREQUENCY = 10 MHZ

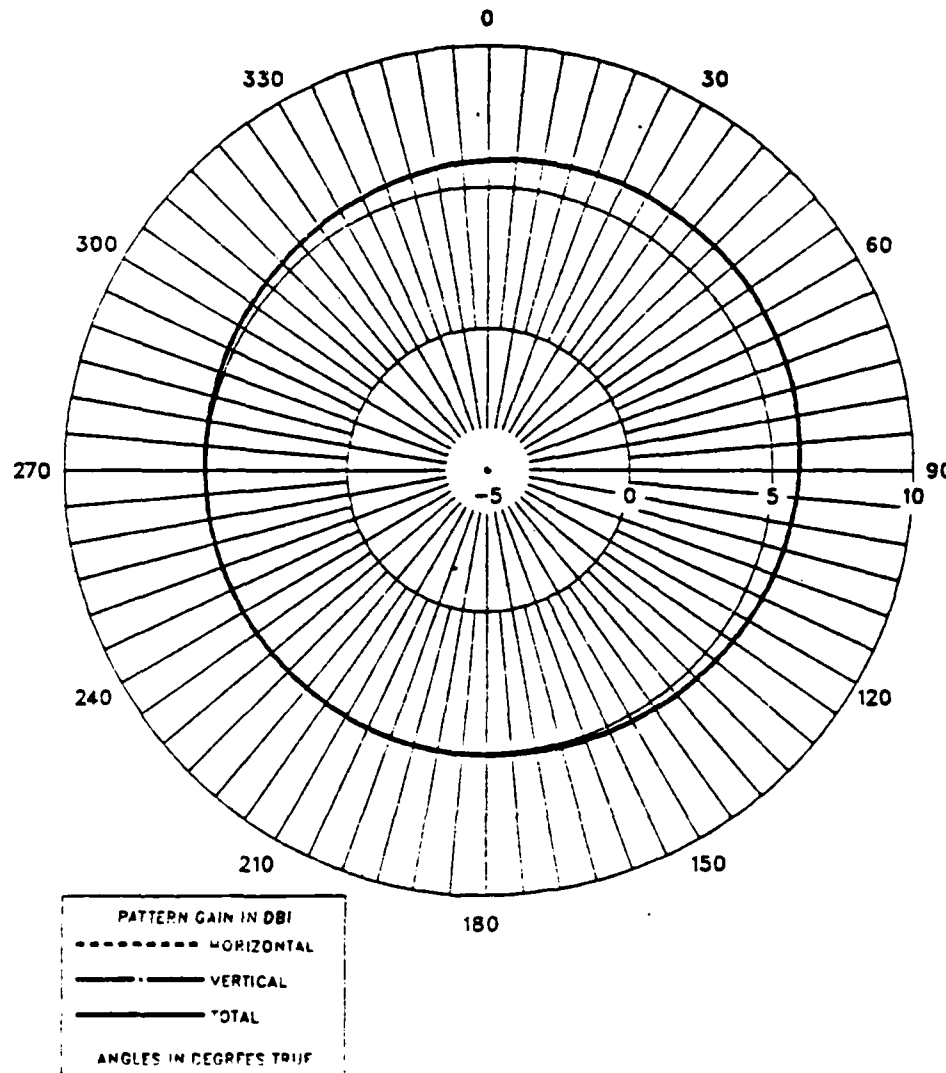


Figure B.7 Model 2 E-Field Azimuth Pattern at 10 MHz  
for 3 Base Feeds.

MODEL 2 BY ONE BASE FEED

FREQUENCY = 2 MHZ

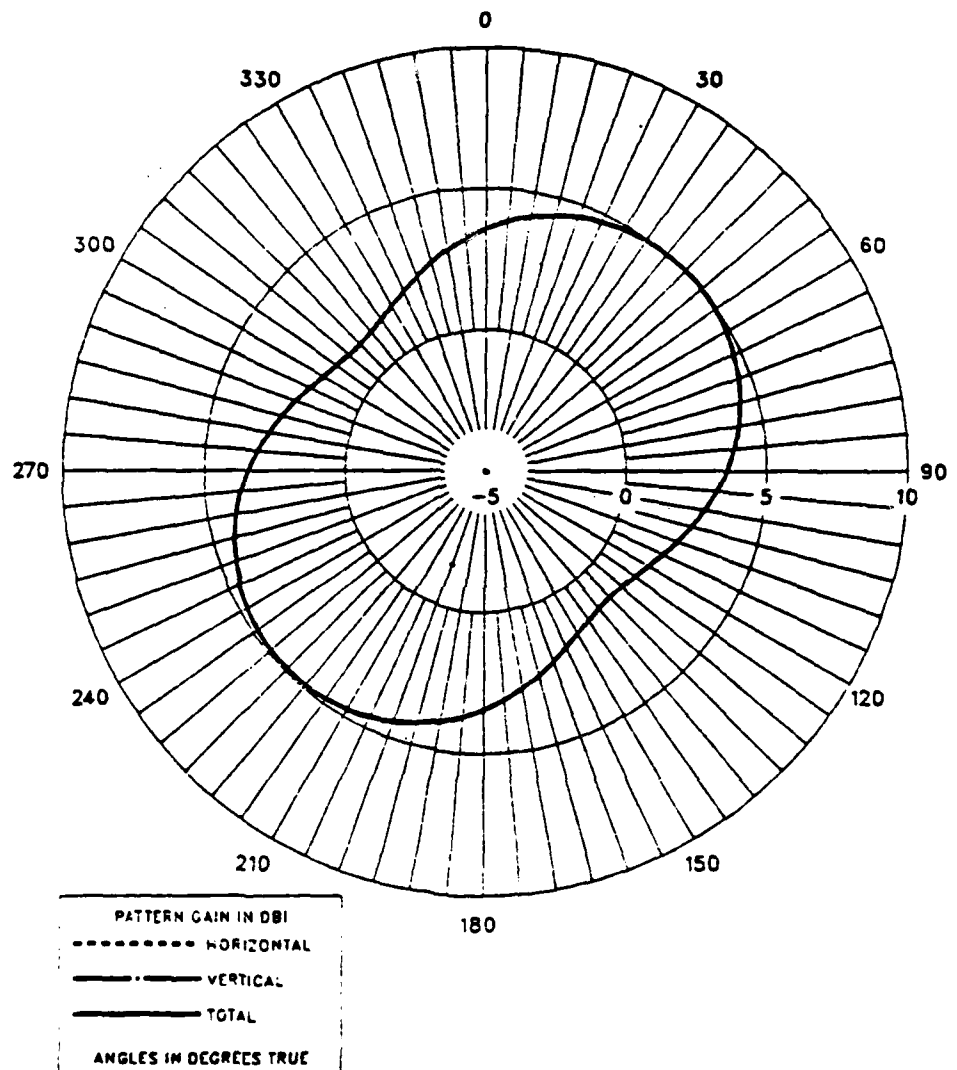
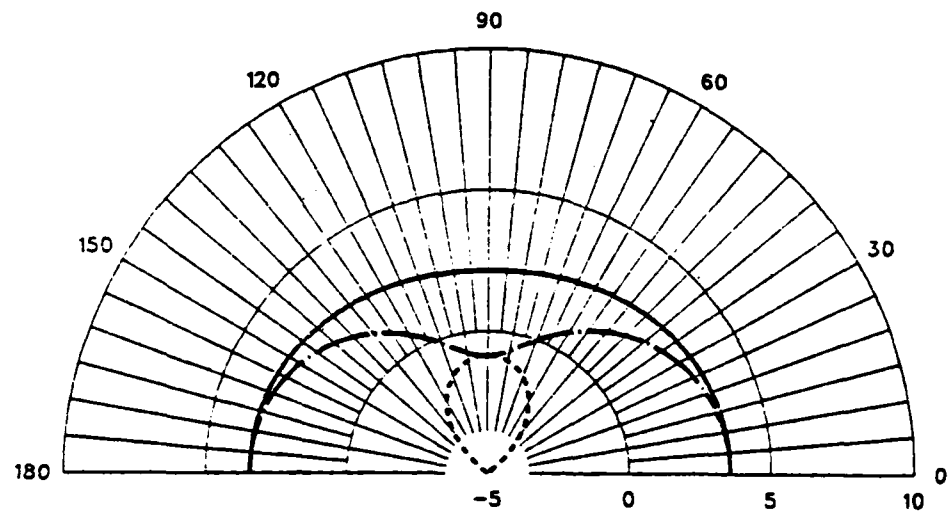


Figure B.8 Model 2 E-Field Azimuth Pattern at 2 MHz  
for 1 Base Feed.

MODEL 2 BY ONE BASE FEED

FREQUENCY = 2 MHZ



PATTERN GAIN IN DBi  
----- HORIZONTAL  
----- VERTICAL  
----- TOTAL  
ELEVATION ANGLE

Figure B.9 Model 2 E-Field Elevation Pattern at 2 MHz  
for 1 Base Feed.

MODEL 2 BY ONE BASE FEED

FREQUENCY = 10 MHZ

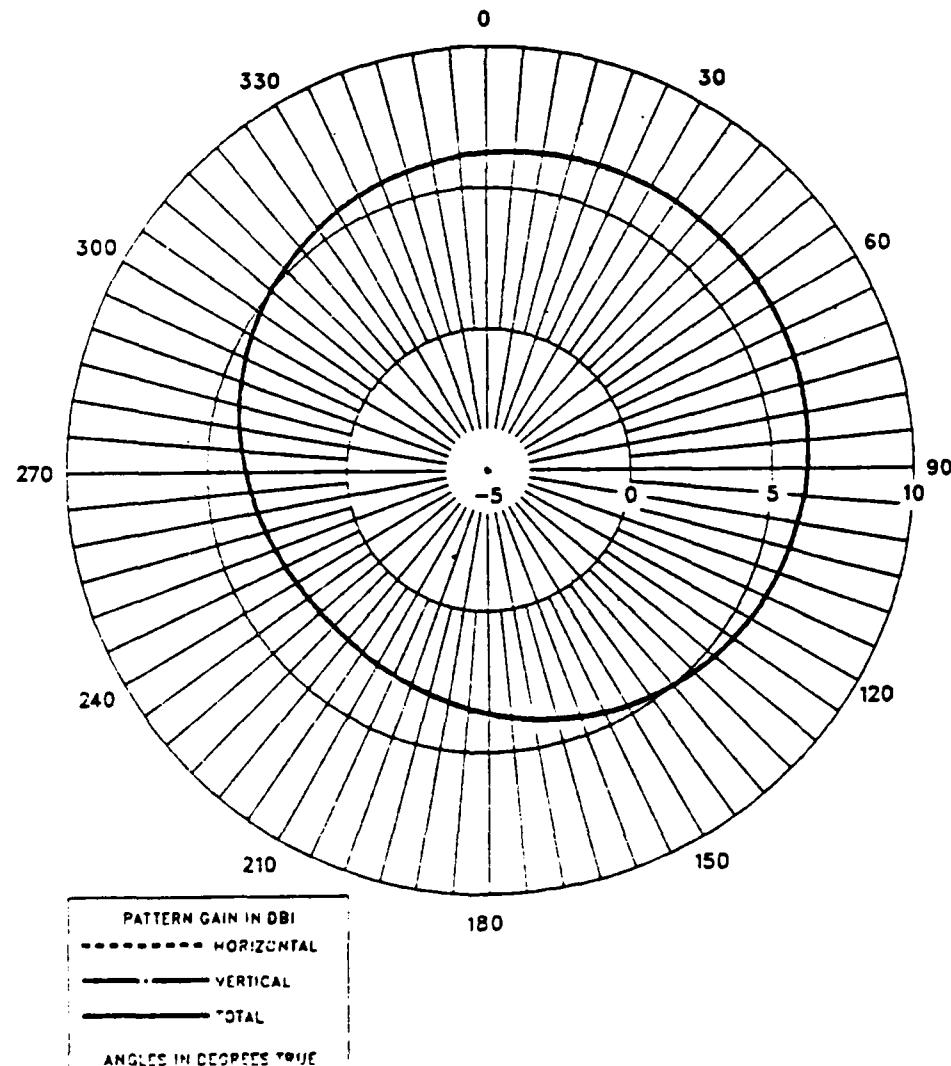
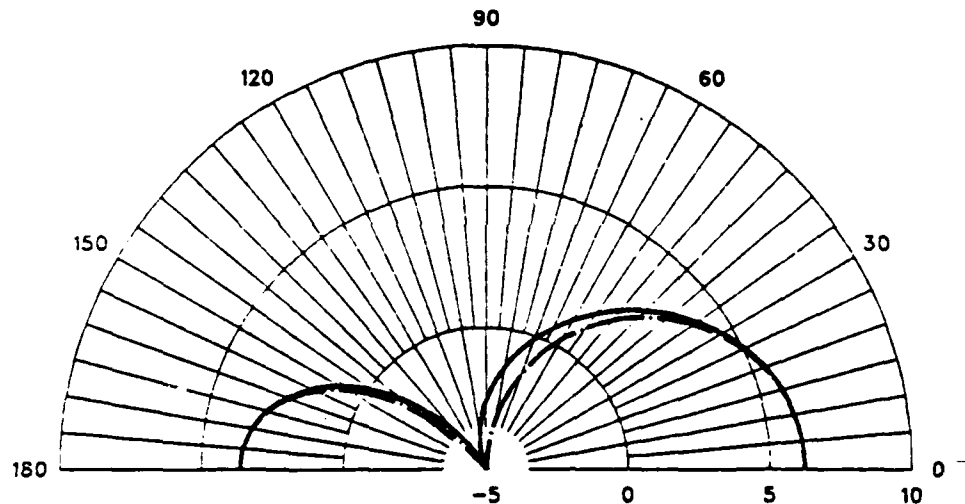


Figure B.10 Model 2 E-Field Azimuth Pattern at 10 MHz  
for 1 Base Feed.

MODEL 2 BY ONE BASE FEED

FREQUENCY = 10 MHZ



PATTERN GAIN IN DBI  
----- HORIZONTAL  
— VERTICAL  
— TOTAL  
ELEVATION ANGLE

Figure B.11 Model 2 E-Field Elevation Pattern at 10 MHz  
for 1 Base Feed.

MODEL 2A BY FOUR EXTERNAL SHUNT FEEDS

FREQUENCY = 2 MHZ

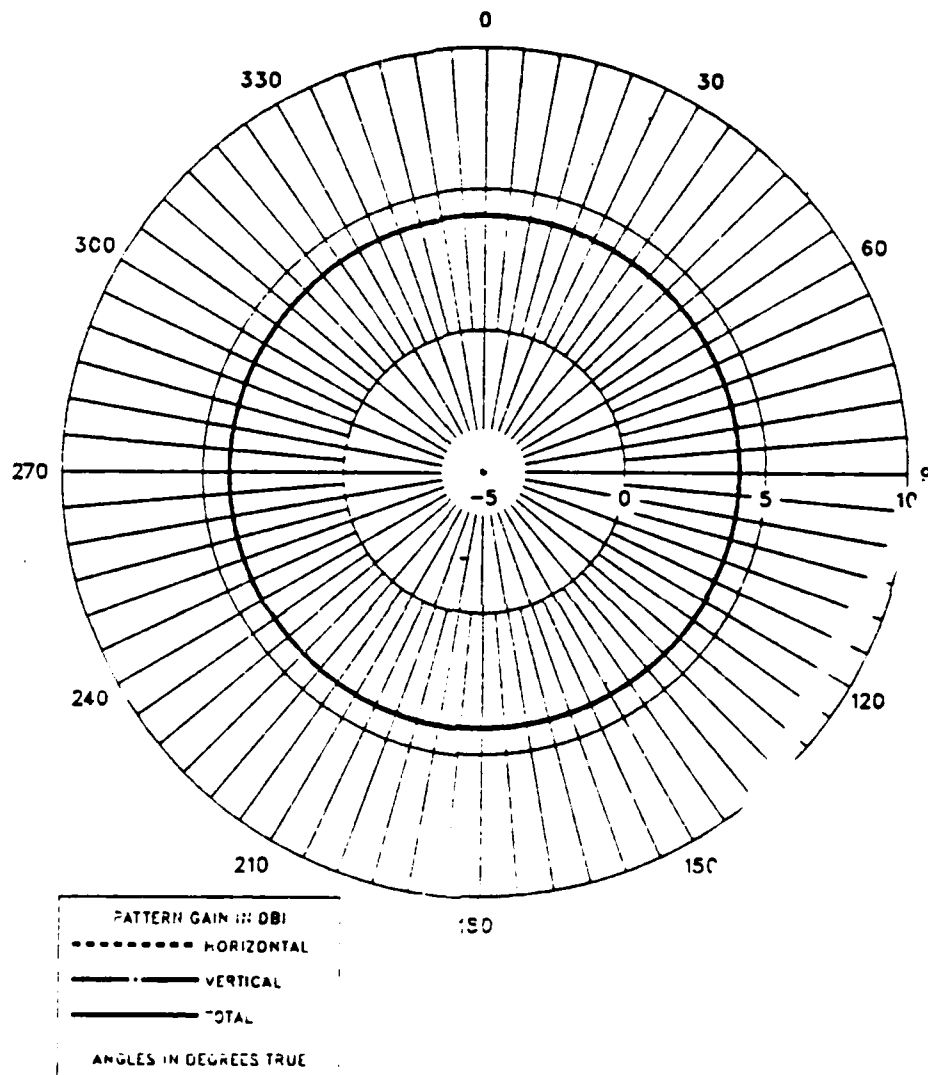


Figure B.12 Model 2A E-Field Azimuth Pattern at 2 MHz  
for 4 External Shunt Feeds.

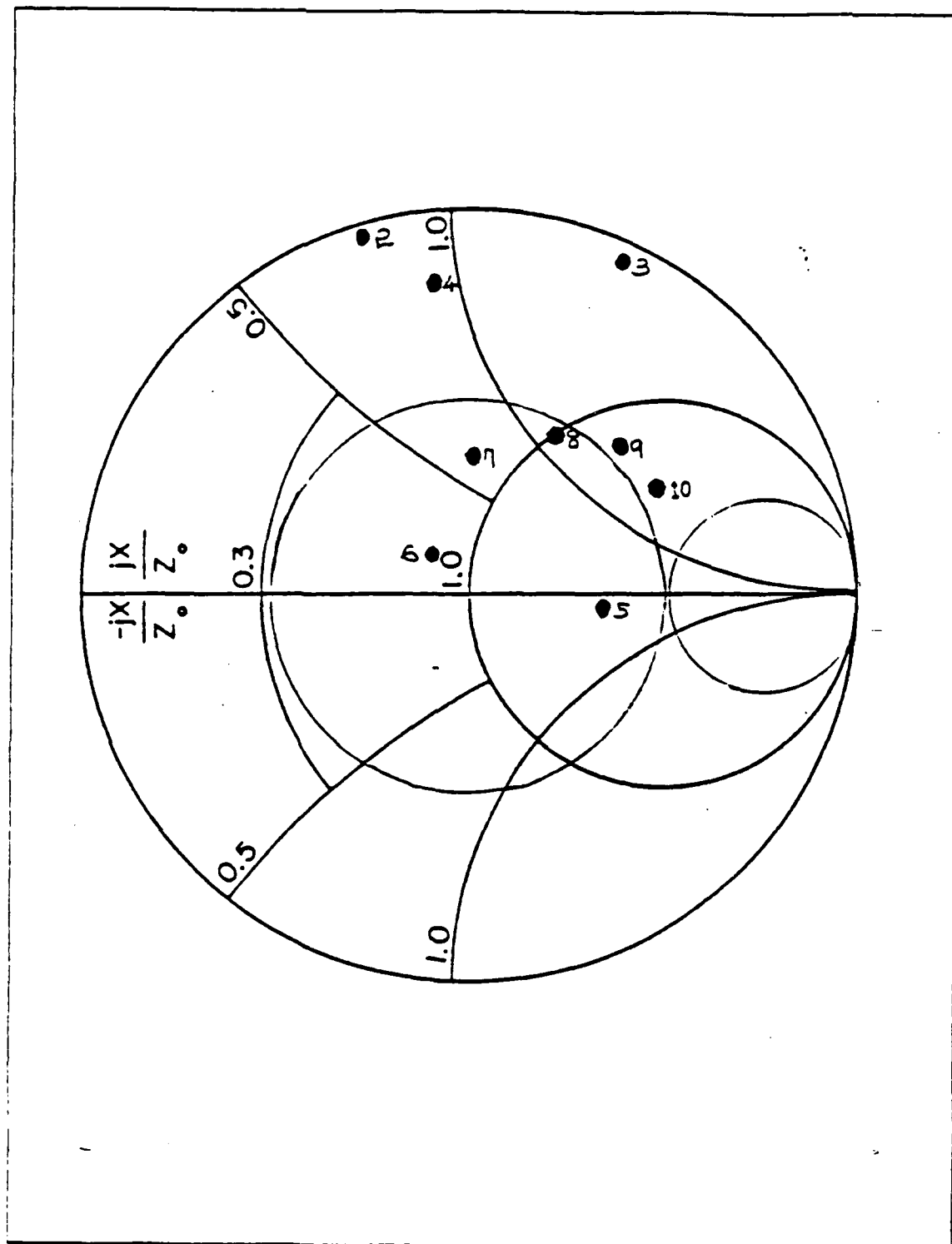


Figure B.13 Model 2 Impedance Plot in Frequency 2-10 MHz  
for 3 Base Feeds:  $Z_0 = 150$  Ohm.

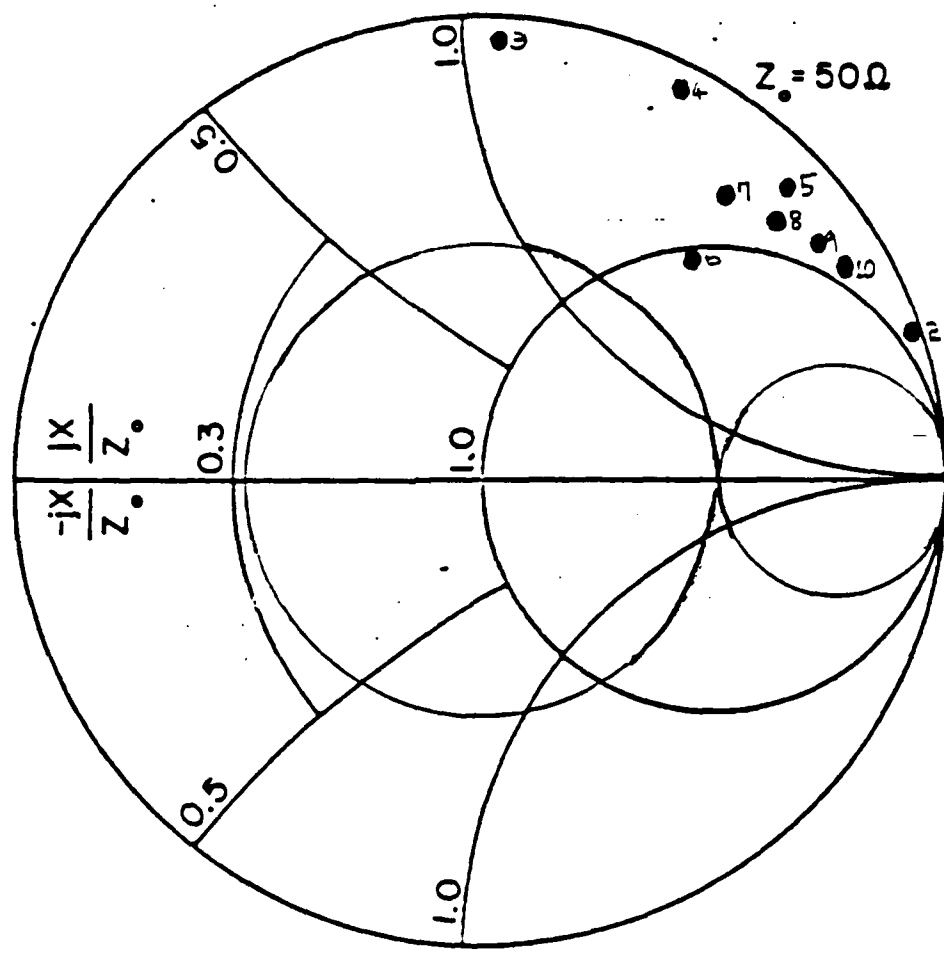


Figure B.14 Model 2 Impedance Plot in Frequency 2-10 MHz  
for 2 Diagonal Base Feeds:  $Z_0 = 50$  Ohm.

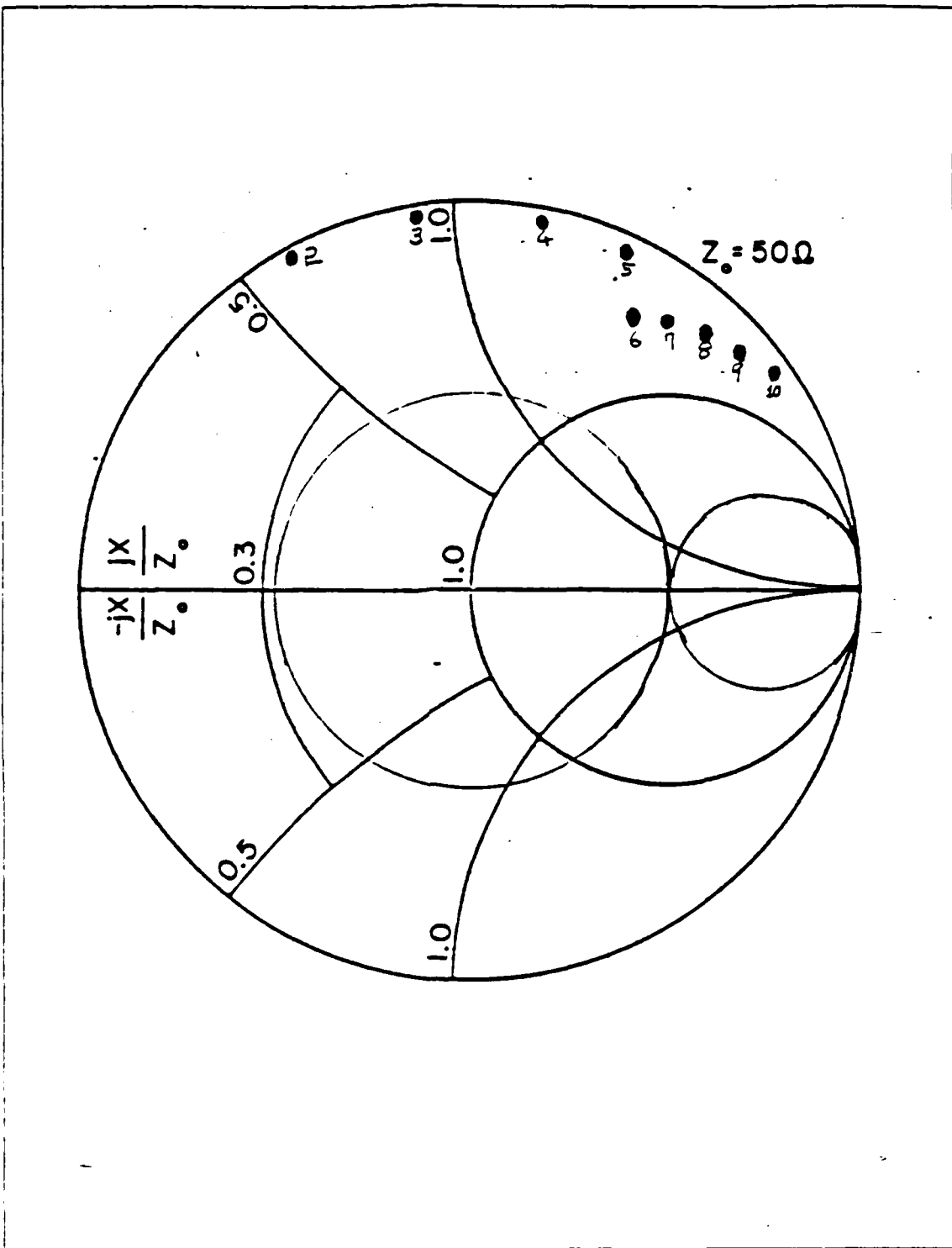


Figure B.15 Model 2 Impedance Plot in Frequency 2-10 MHz  
for 1 Base Feed:  $Z_0 = 50 \Omega$ .

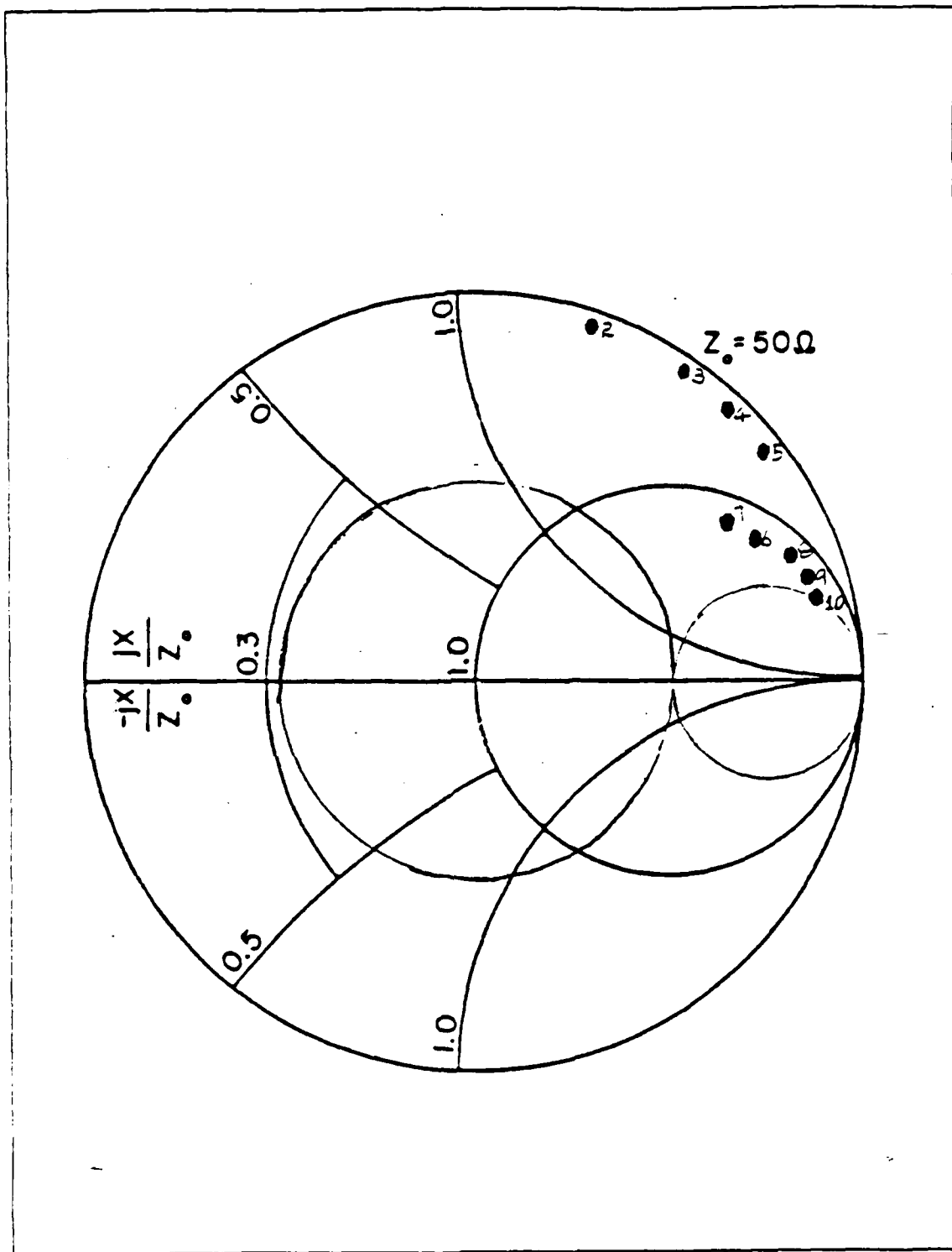


Figure B.16 Model 2A Impedance Plot in Frequency 2-10 MHz  
for 4 External Shunt feeds:  $Z_0 = 50 \Omega$ .

**APPENDIX C**  
**MODEL 3 RESULTS FOR DIFFERENT FEED METHODS.**

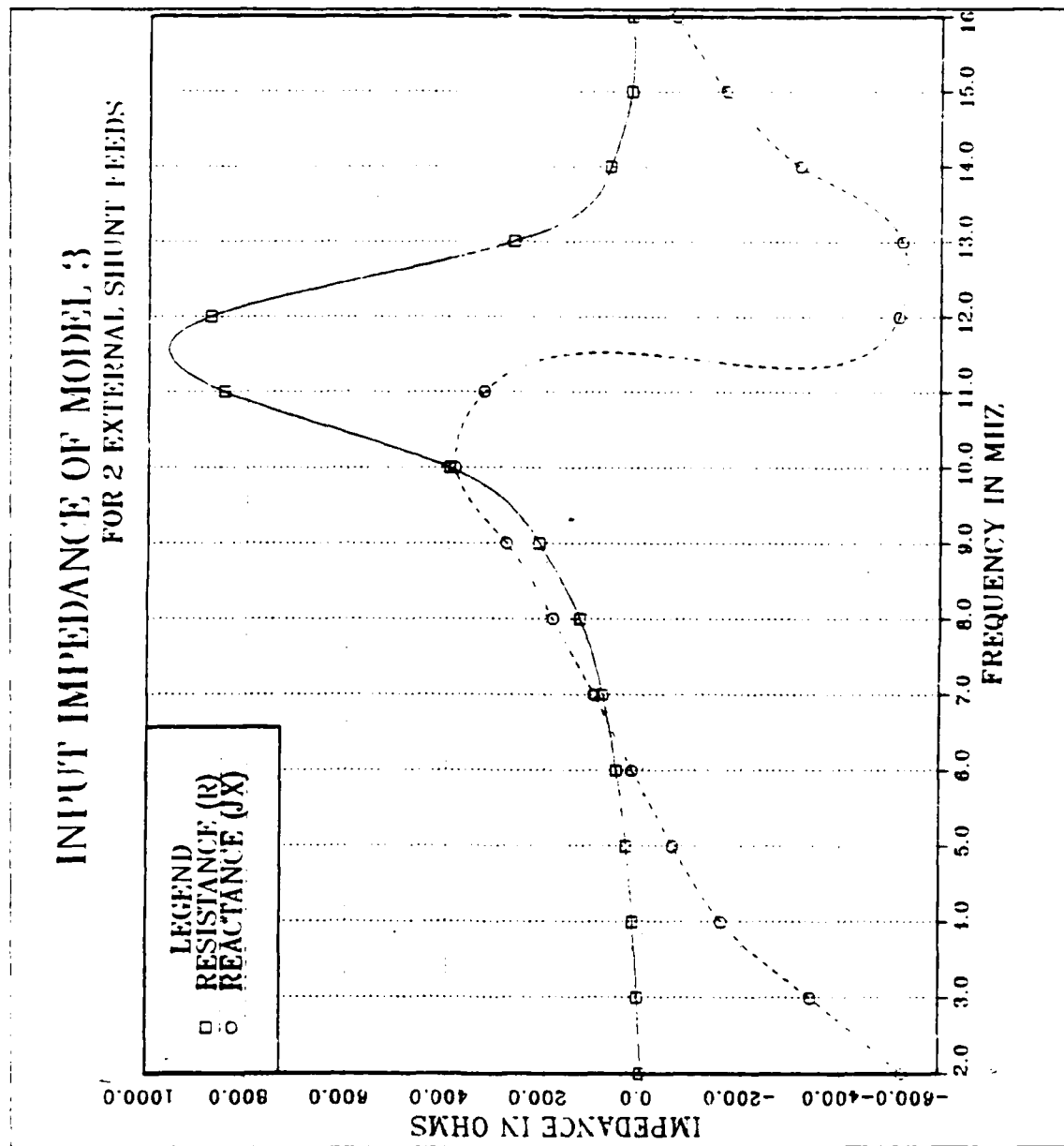


Figure C.1 Model 3 Input Impedance in Frequency 2-16 MHz  
for 2 External Shunt Feeds.

TABLE 21  
MODEL 3 INPUT IMPEDANCE IN FREQUENCY 2-16 MHZ FOR  
FOUR EXTERNAL SHUNT FEEDS

Frequency in MHz	Resistance in Ohms (R)	Reactance in Ohms (jX)
2	8.74	- 685.74
3	19.90	- 399.70
4	36.06	- 240.04
5	58.13	- 130.90
6	87.48	- 48.72
7	125.84	+ 1.00
8	177.78	+ 64.48
9	234.80	+ 157.50
10	303.80	+ 102.00
11	370.90	+ 74.80
12	427.46	+ 9.84
13	438.30	- 55.00
14	435.79	- 166.98
15	332.20	- 257.84
16	196.60	+ 255.80

TABLE 22  
MODEL 3 INPUT IMPEDANCE IN FREQUENCY 2-16 MHZ FOR TWO  
EXTERNAL SHUNT FEEDS

Frequency in MHz	Resistance in Ohms (R)	Reactance in Ohms (jX)
2	5.16	- 526.64
3	11.80	- 340.00
4	21.48	- 159.36
5	35.18	- 60.63
6	54.74	+ 22.77
7	83.85	+ 102.14
8	130.55	+ 185.78
9	214.81	+ 281.47
10	397.13	+ 386.25
11	846.55	+ 327.20
12	875.57	- 515.55
13	267.90	- 522.73
14	72.26	- 315.93
15	30.20	- 164.04
- 16	29.21	- 60.42

MODEL 3 BY TWO EXTERNAL SHUNT FEEDS

FREQUENCY = 16 MHZ

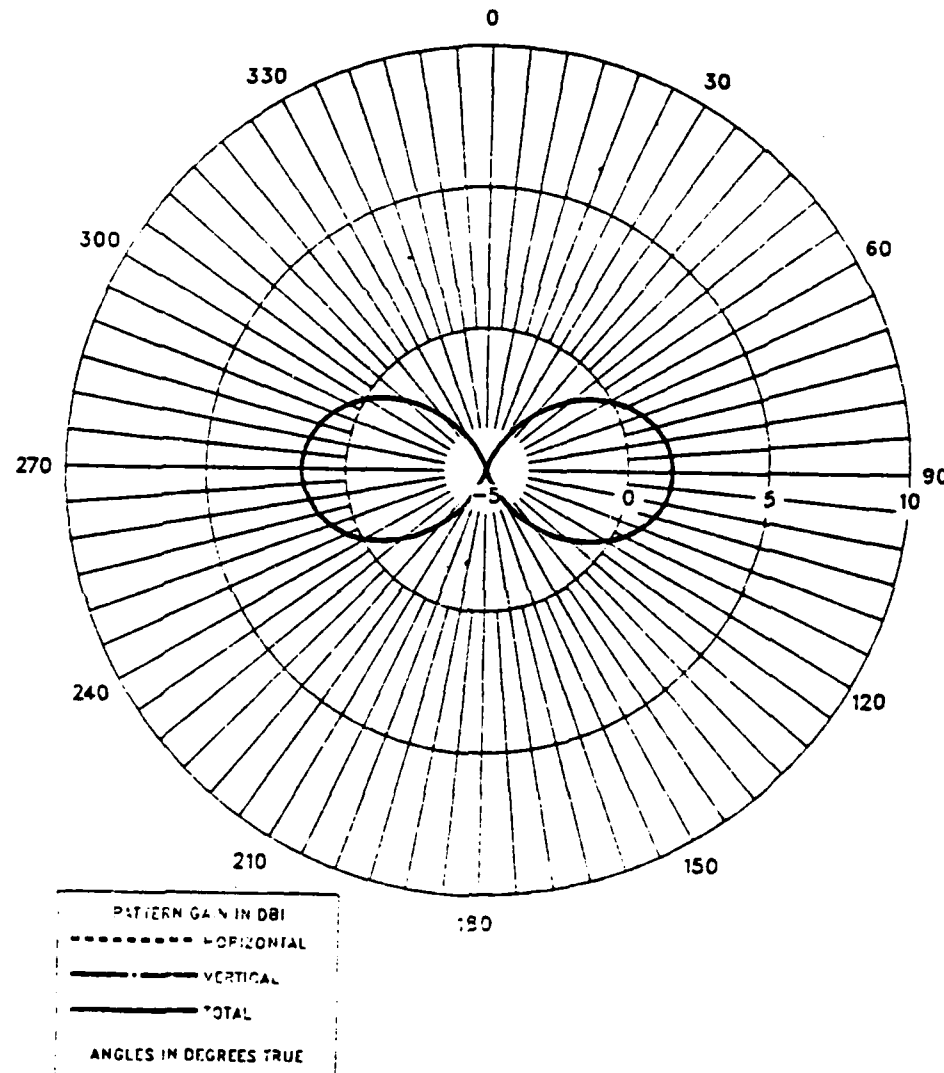
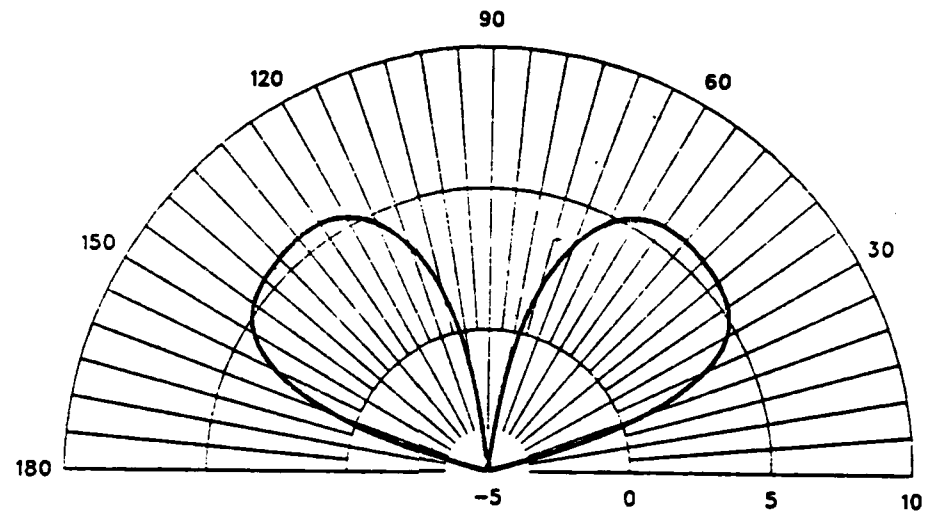


Figure C.2 Model 3 E-Field Azimuth Pattern at 16 MHz  
for 2 External Shunt Feeds.

MODEL 3 BY TWO EXTERNAL SHUNT FEEDS

FREQUENCY = 16 MHZ



PATTERN GAIN IN DBI  
----- HORIZONTAL  
— VERTICAL  
— TOTAL  
ELEVATION ANGLE

Figure C.3 Model 3 E-Field Elevation Pattern at 16 MHz  
for 2 External Shunt Feeds.

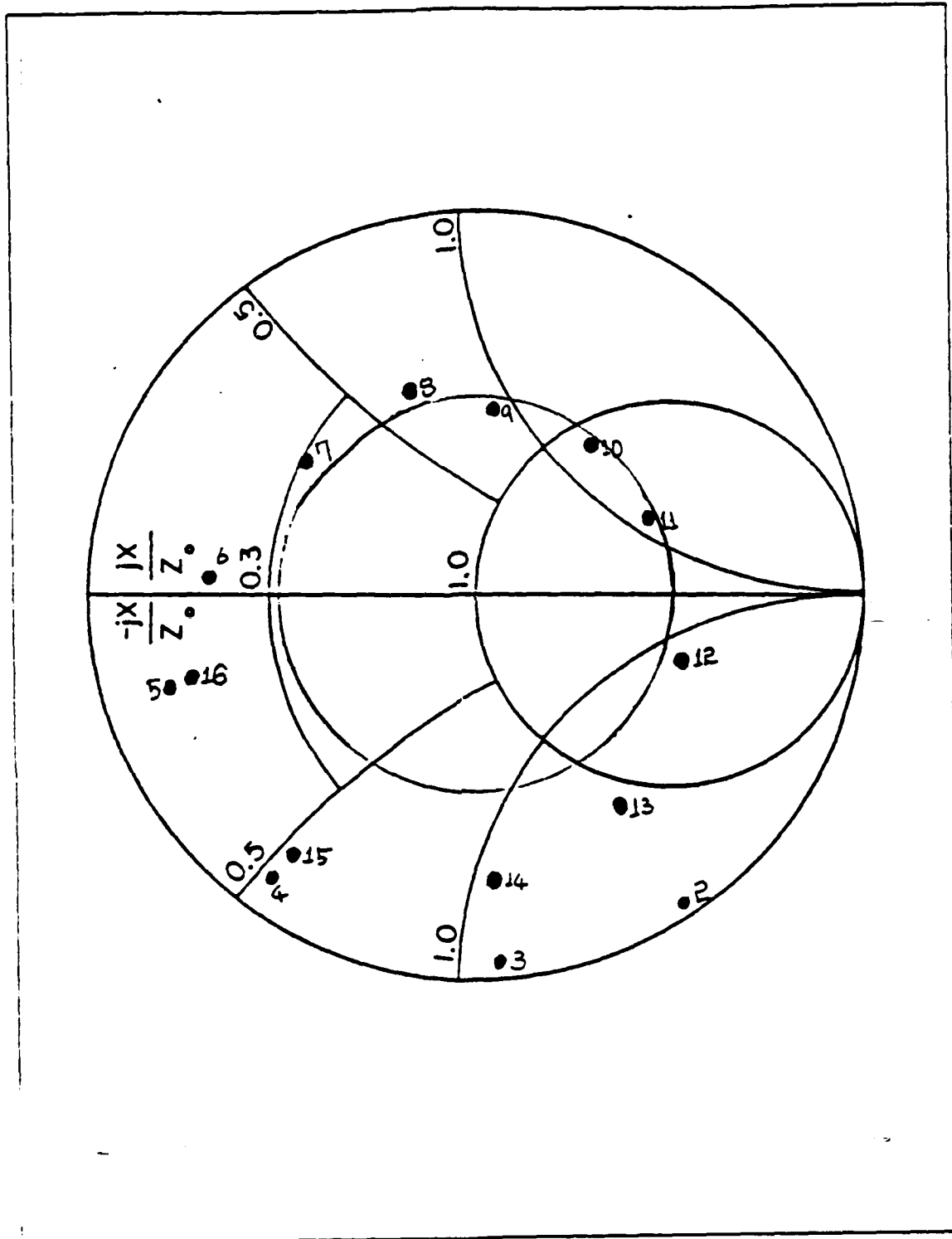


Figure C.4 Model 3 Impedance Plot in Frequency 2-16 MHz  
for 2 External Shunt Feeds:  $Z_0 = 300 \text{ Ohm}$ .

**APPENDIX D**  
**MODEL 4 RESULTS FOR DIFFERENT FEED METHODS.**

**TABLE 23**  
**MODEL 4 INPUT IMPEDANCE IN FREQUENCY 2-8 MHZ FOR FOUR  
 BASE FEEDS**

Frequency in MHz	Resistance in Ohms (R)	Reactance in Ohms (jX)
2.0	39.55	- 289.17
2.7	97.85	- 68.97
3.4	212.60	+ 103.31
4.0	421.67	+ 160.53
4.7	716.73	+ 57.63
5.4	685.01	- 350.07
6.0	321.25	- 436.35
6.7	196.68	- 366.25
7.4	104.54	- 299.84
- 8.0	62.80	- 122.93

TABLE 24  
MODEL 4 INPUT IMPEDANCE IN FREQUENCY 8-16 MHZ FOR  
FOUR BASE FEEDS

Frequency in MHz	Resistance in Ohms (R)	Reactance in Ohms (jX)
8.0	62.80	- 122.93
8.7	118.48	- 2.05
9.4	212.95	+ 82.92
10.0	327.64	+ 20.67
10.7	414.12	- 47.54
11.4	325.57	- 181.53
12.0	190.88	- 174.59
12.7	107.48	- 50.25
13.4	175.76	+ 99.22
14.0	362.34	+ 96.56
14.7	391.18	- 166.38
15.4	123.52	- 204.82
16.0	43.88	- 123.64

INPUT IMPEDANCE OF MODEL 4  
FOR 3 BASE FEEDS

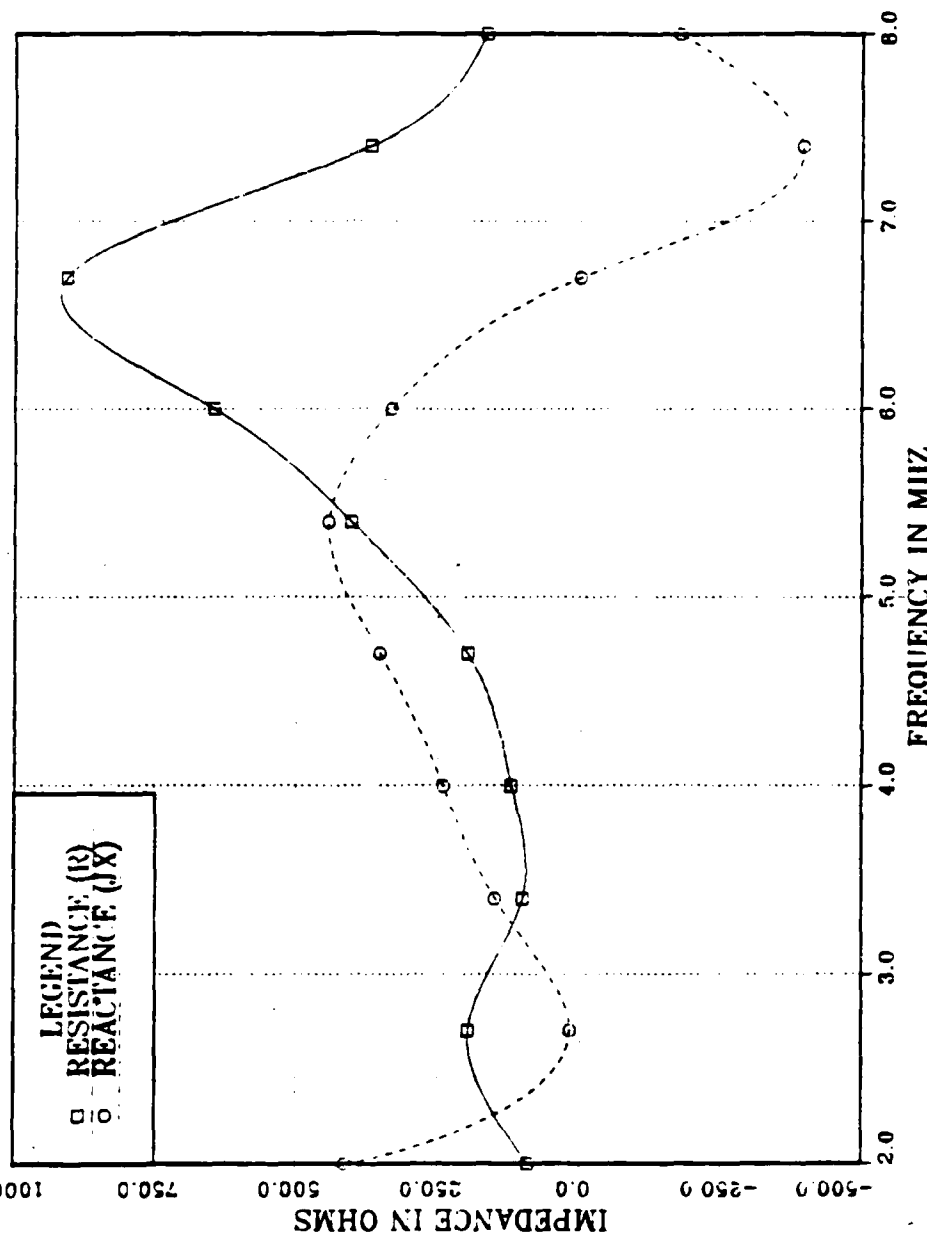


Figure D.1 Model 4 Input Impedance in Frequency 2-8 MHz  
for 3 Base Feeds.

TABLE 25  
MODEL 4 INPUT IMPEDANCE IN FREQUENCY 2-8 MHZ FOR  
THREE BASE FEEDS

Frequency in MHz	Resistance in Ohms (R)	Reactance in Ohms (jX)
2.0	92.46	+ 413.16
2.7	196.53	+ 18.38
3.4	102.82	+ 149.74
4.0	121.15	+ 240.77
4.7	198.51	+ 353.32
5.4	402.55	+ 443.10
6.0	644.75	+ 331.79
6.7	907.80	+ 0.26
7.4	369.65	- 393.91
8.0	165.51	- 177.27

INPUT IMPEDANCE OF MODEL 4  
FOR 3 BASE FEEDS

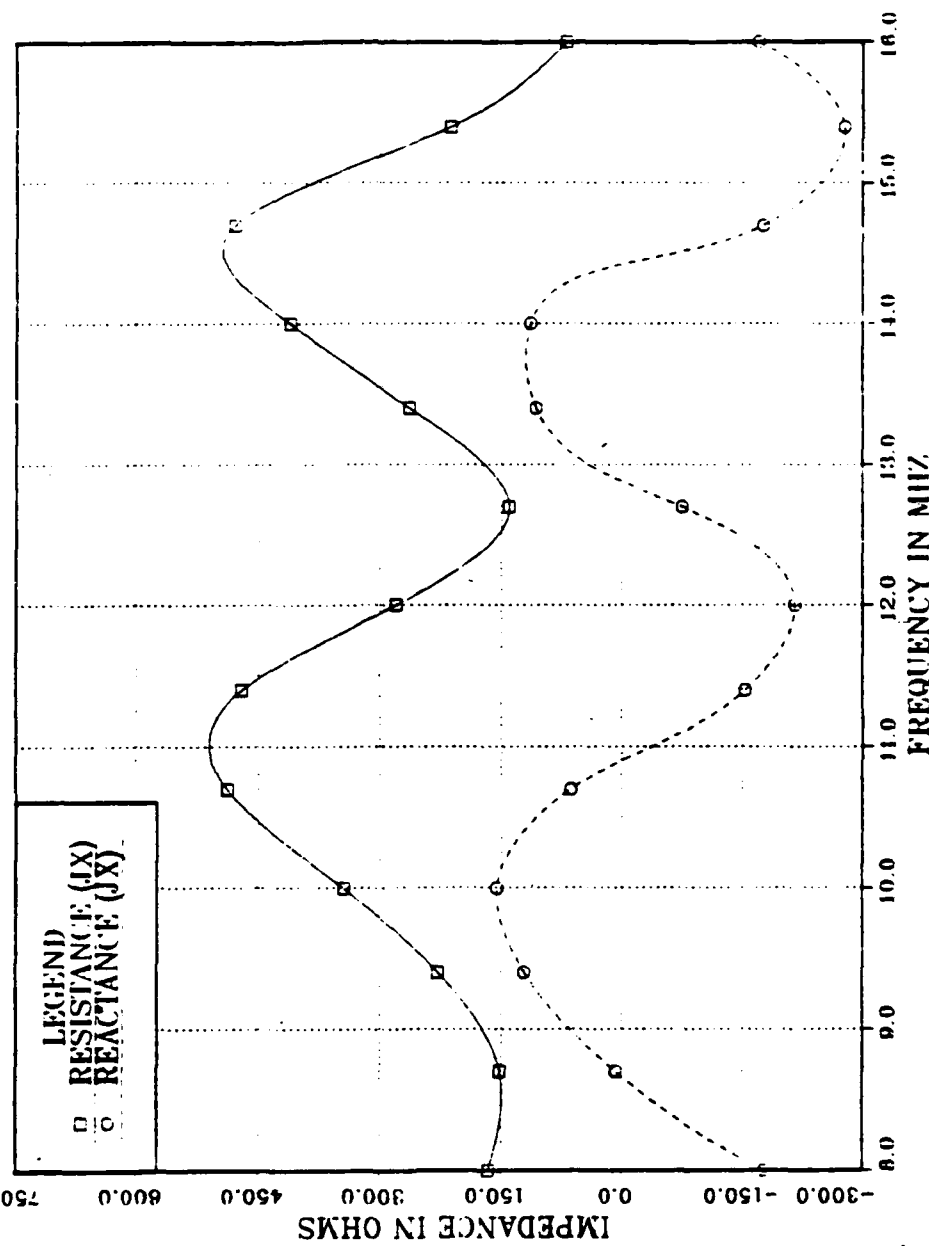


Figure D.2 Model 4 Input Impedance in Frequency 8-16 MHz  
for 3 Base Feeds.

TABLE 26  
MODEL 4 INPUT IMPEDANCE IN FREQUENCY 8-16 MHZ FOR  
THREE BASE FEEDS

Frequency in MHz	Resistance in Ohms (R)	Reactance in Ohms (jX)
8.0	165.51	- 177.27
8.7	151.91	+ 7.46
9.4	227.57	+ 121.10
10.0	345.40	+ 155.54
10.7	487.81	+ 63.24
11.4	470.29	- 153.69
12.0	279.99	- 216.53
12.7	138.39	- 75.23
13.4	263.70	+ 107.00
14.0	411.29	+ 114.22
14.7	479.30	- 176.18
15.4	213.41	- 277.80
16.0	68.89	- 170.41

INPUT IMPEDANCE OF MODEL 4  
FOR 1 BASE FIELD

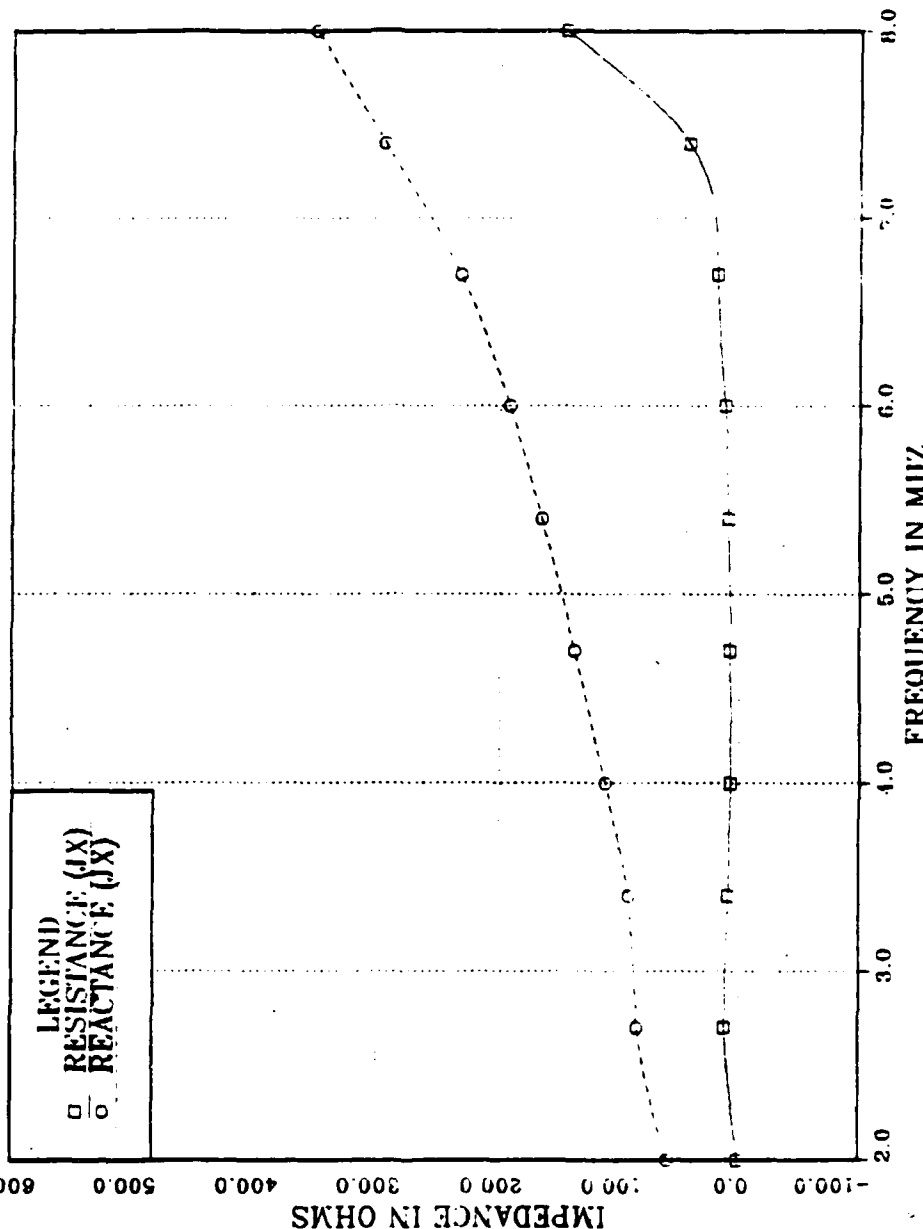


Figure D.3 Model 4 Input Impedance in Frequency 2-8 MHz  
for 1 Base Feed.

TABLE 27  
MODEL 4 INPUT IMPEDANCE IN FREQUENCY 2-8 MHZ FOR ONE  
BASE FEED

Frequency in MHz	Resistance in Ohms (R)	Reactance in Ohms (jX)
2.0	0.43	+ 59.51
2.7	11.35	+ 83.61
3.4	8.60	+ 91.86
4.0	6.77	+ 111.68
4.7	7.23	+ 136.68
5.4	9.10	+ 164.45
6.0	12.10	+ 192.00
6.7	19.04	+ 232.70
7.4	41.70	+ 293.44
8.0	145.00	+ 349.88

INPUT IMPEDANCE OF MODEL 4  
FOR 1 BASE FEED

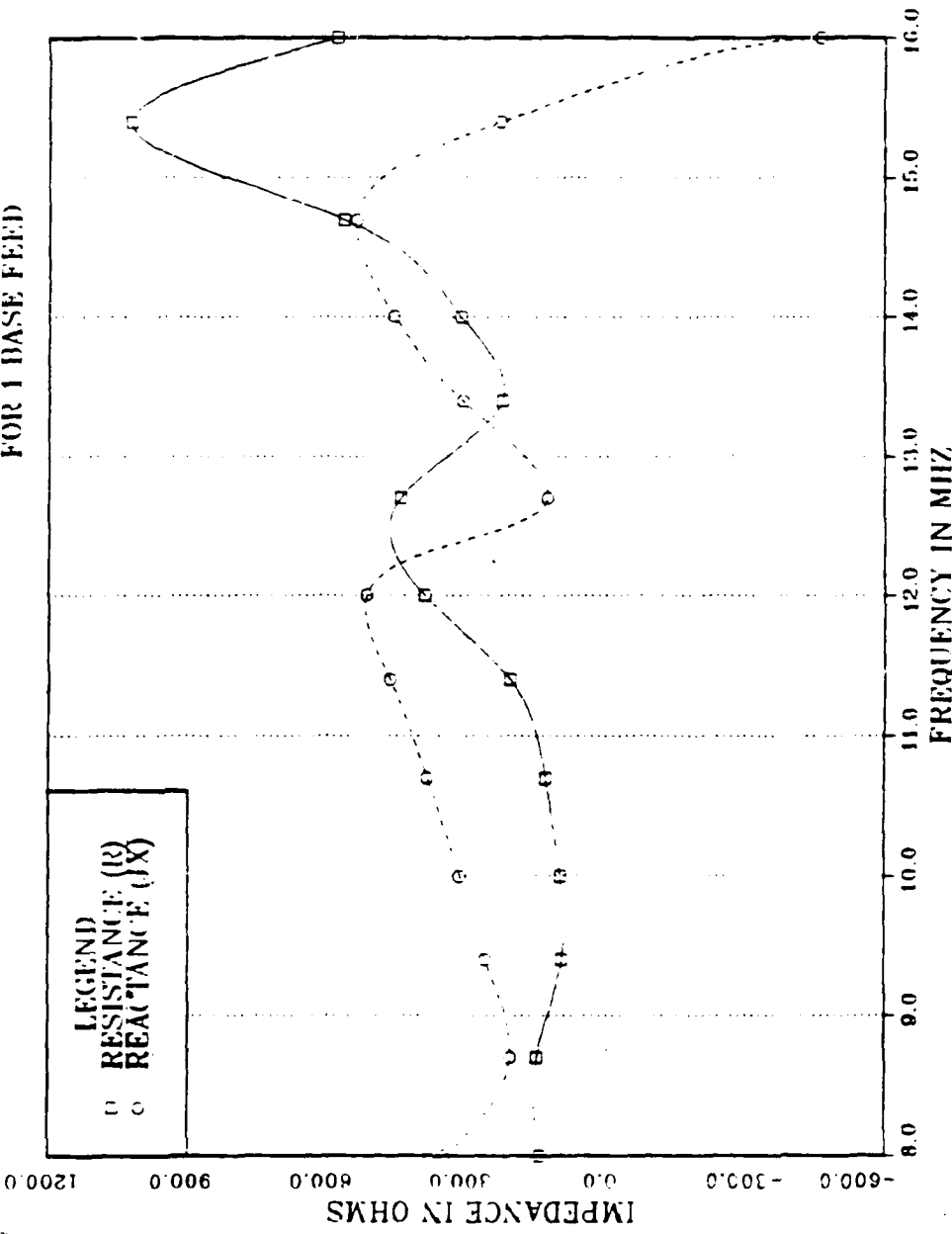


Figure D.4 Model 4 Input Impedance in Frequency 8-16 MHz  
for 1 Base Feed.

TABLE 28  
MODEL 4 INPUT IMPEDANCE IN FREQUENCY 8-16 MHZ FOR ONE  
BASE FEED

Frequency in MHz	Resistance in Ohms (R)	Reactance in Ohms (jX)
8.0	145.00	+ 349.88
8.7	150.36	+ 208.31
9.4	95.87	+ 261.40
10.0	99.70	+ 316.62
10.7	131.10	+ 386.07
11.4	209.30	+ 468.90
12.0	392.50	+ 516.78
12.7	443.91	+ 128.18
13.4	225.70	+ 311.35
14.0	314.20	+ 457.55
14.7	566.60	+ 540.30
15.4	1022.30	+ 228.20
16.0	580.00	- 461.60

MODEL 4 BY THREE BASE FEEDS

FREQUENCY = 16 MHZ

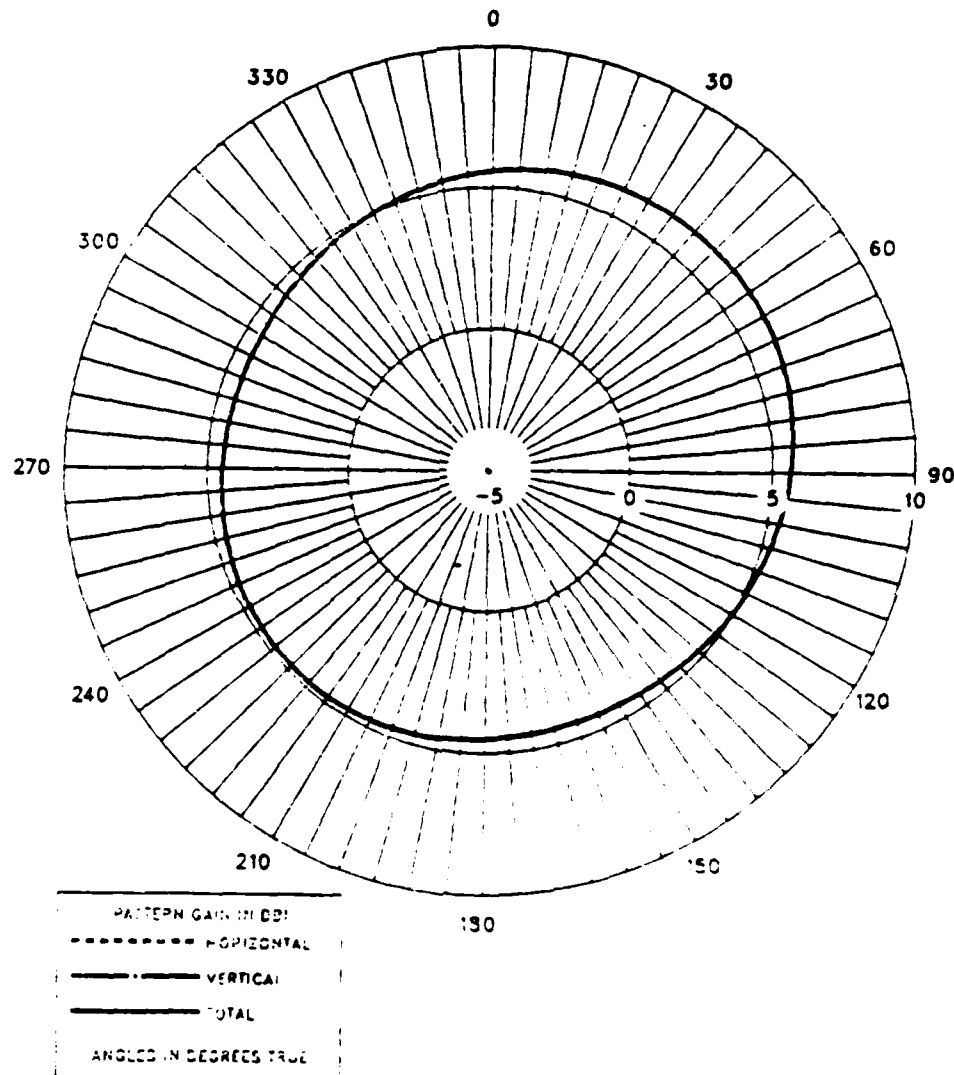
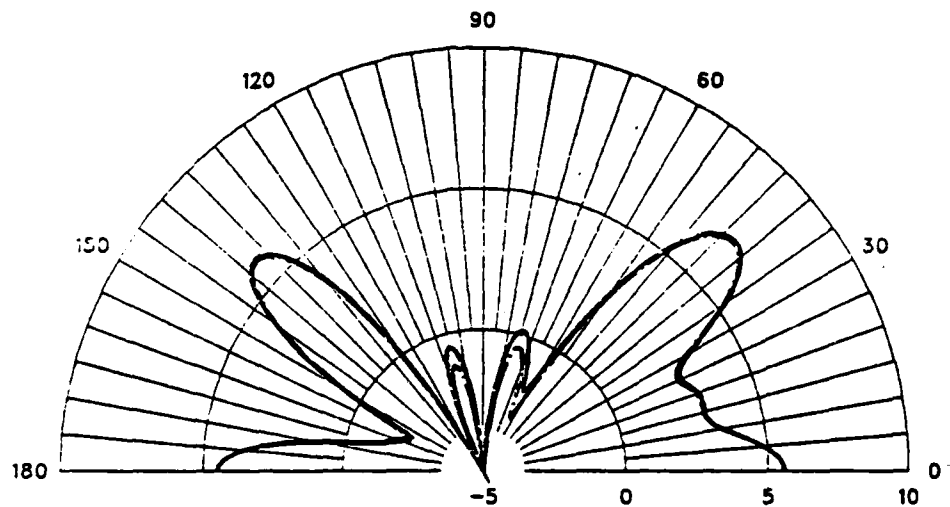


Figure D.5 Model 4 E-Field Azimuth Pattern at 16 MHz  
for 3 Base Feeds.

MODEL 4 BY THREE BASE FEEDS

FREQUENCY = 16 MHZ



PATTERN SHOWN IN DBI
----- ORIZONAL
— VERTICAL
— TOTAL
ELEVATION ANGLE

Figure D.5 Model 4 E-Field Elevation Pattern at 16 MHz  
for 3 Base Feeds.

MODEL 4 BY ONE BASE FEED

FREQUENCY = 16 MHZ

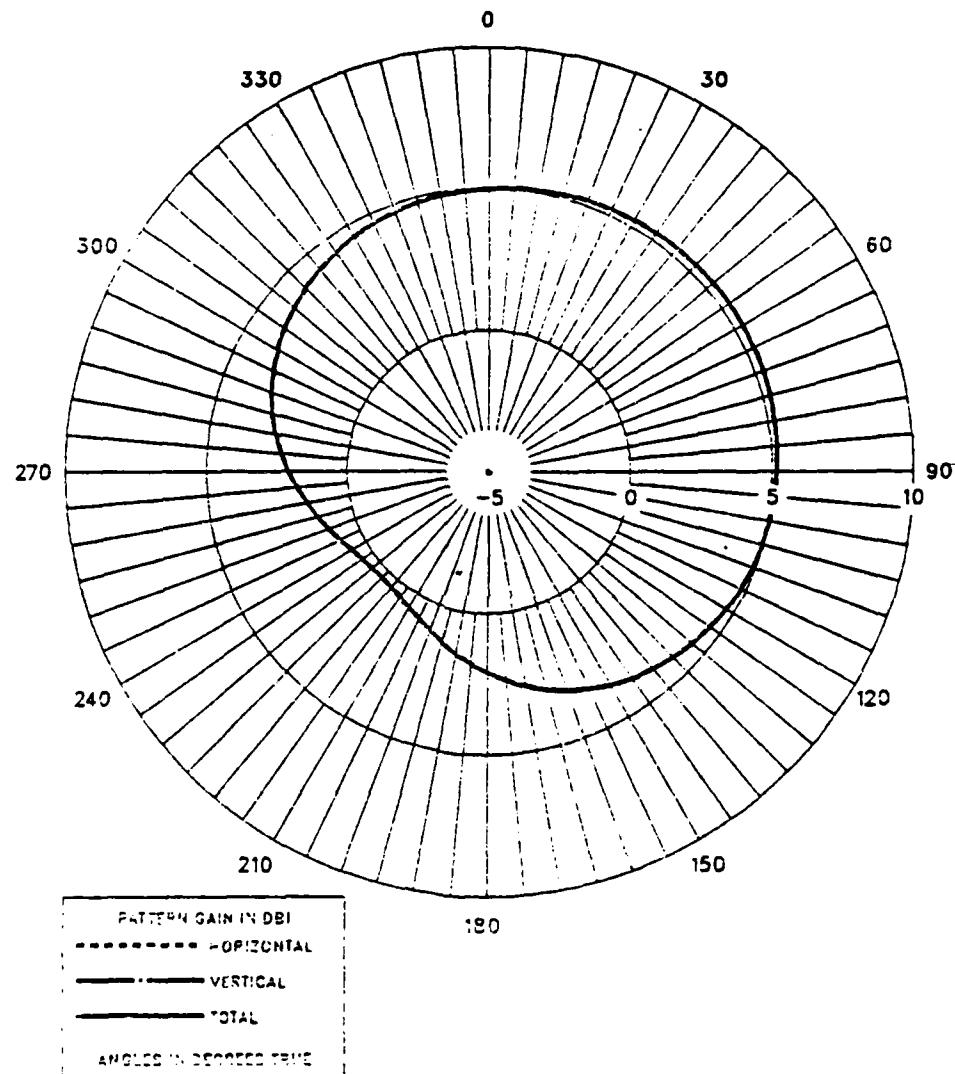


Figure D.6 Model 4 E-Field Azimuth Pattern at 16 MHz  
for 1 Base Feed.

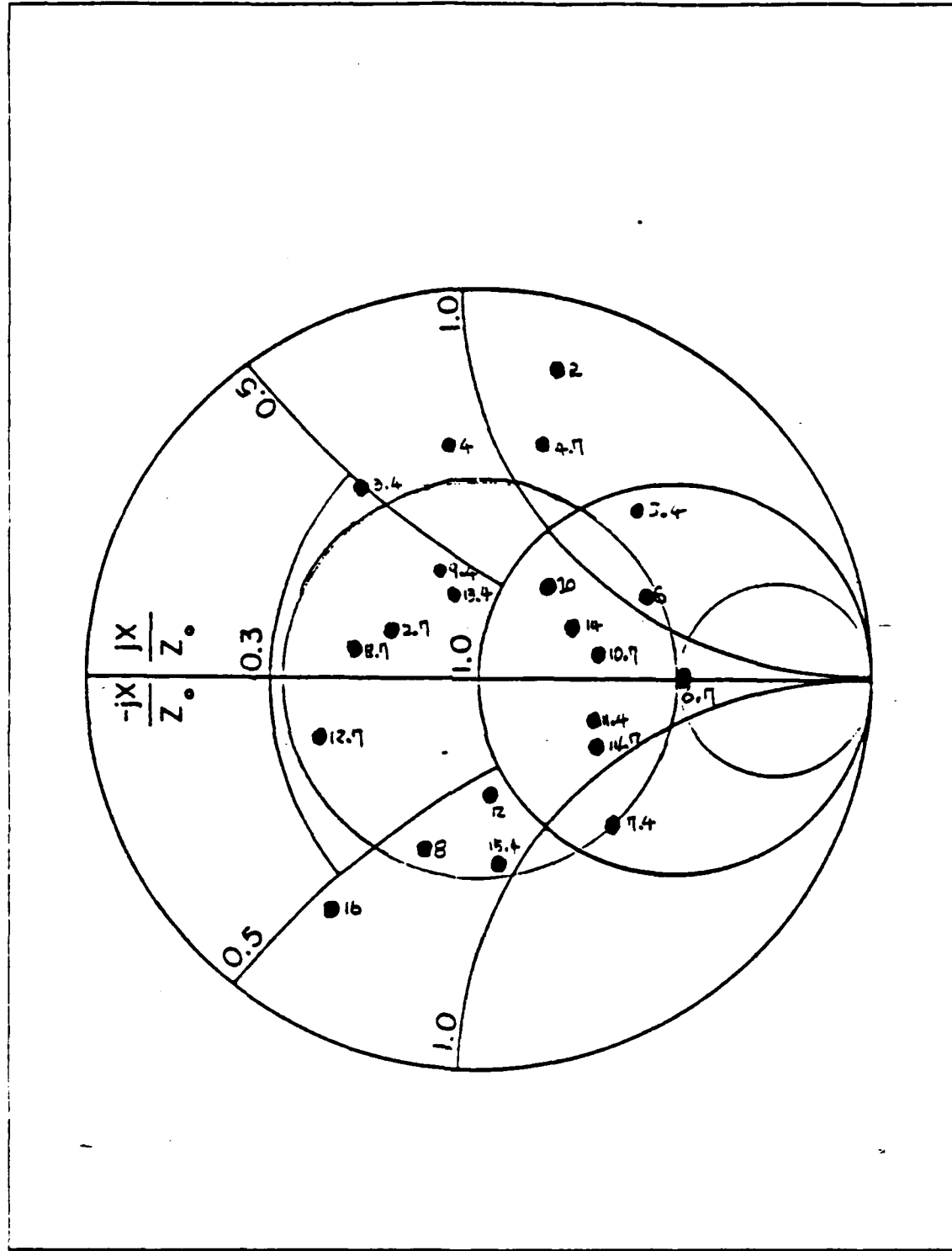


Figure D.7 Model 4 Impedance Plot in Frequency 2-16 MHz  
for 3 Base Feeds;  $Z_0 = 300 \text{ Ohm}$ .

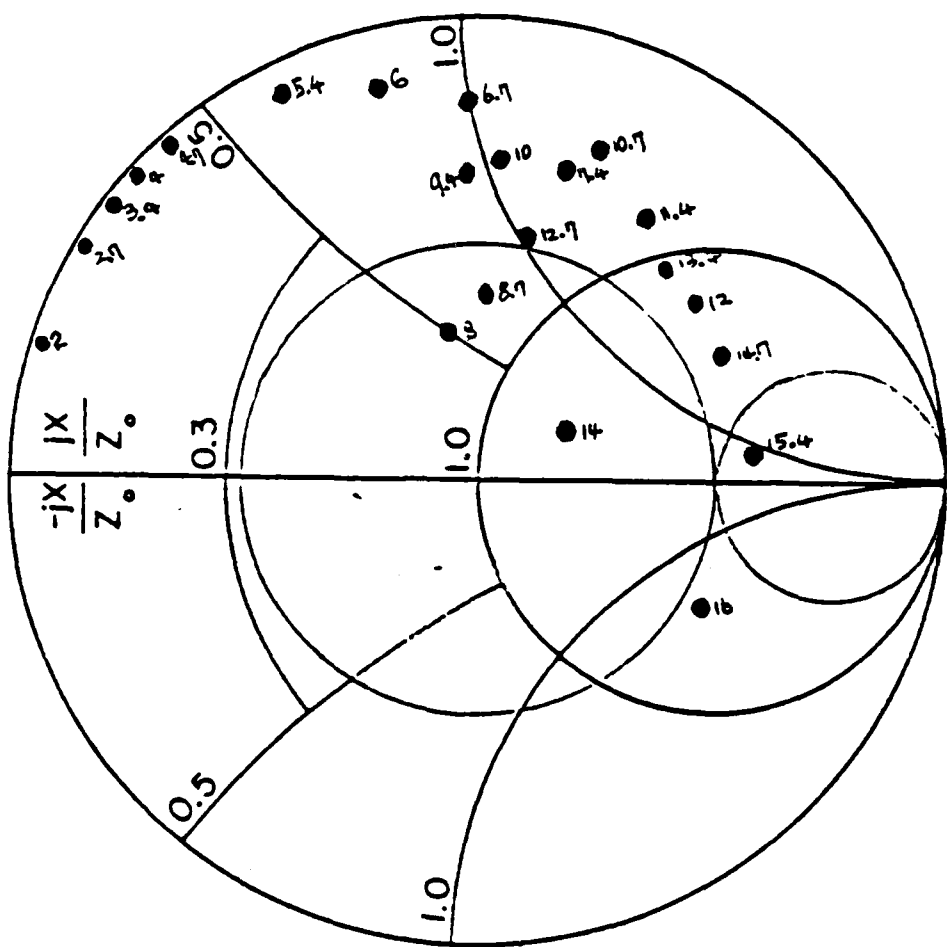


Figure D.8 Model 4 Impedance Plot in Frequency 2-16 MHz  
for 1 Base Feed:  $Z_0 = 300 \text{ Ohm}$ .

## LIST OF REFERENCES

1. Stutzman, W. L. and Thiele, G. A., *Antenna Theory and Design*, John Wiley & Sons., Chapter 7, 1981.
2. Naval Ocean Systems Center Technical Document 116, Volume 2, *Numerical Electromagnetics Code (NEC) - Methods of Moments*, G. J. Burke and A. J. Pogio, Lawrence Livermore Laboratory, January 1981.
3. Thomson D. D., *Electromagnetic Near-field Computations for a Broadcast Monopole using the Numerical Electromagnetics Code (NEC)*, M.S.E.E. Thesis, Naval Postgraduate School, Monterey, California, September 1983.
4. Tertocha James C., *A Feasibility Study of a Shipboard Combat Survivable HF Antenna Design*, M.S.E.E. Thesis, Naval Postgraduate School, Monterey, California, March 1986.
5. Lyberopoulos George L., *Numerical Models of New HF Shipboard Communication Antenna Systems for Improved Survivability*, M.S.E.E. Thesis, Naval Postgraduate School, Monterey, California, June 1986.
6. Neiva Mario Cabral, *Broadband Techniques Applied to Shipboard HF Slot Antennas*, M.S.E.E. Thesis, Naval Postgraduate School, Monterey, California, June 1986.
7. Vorrias Ioannis G., *Shipboard Combat Survivable HF Antenna Designs*, M.S.E.E. Thesis, Naval Postgraduate School, Monterey, California, December 1986.
8. Theofanopoulos Constantinos, *Performance Evaluation of a Half-Wave Resonant Slot Antenna over Perfect Ground Using Numerical Electromagnetics Code*, M.S.E.E. Thesis, Naval Postgraduate School, Monterey, California, March 1987.
9. Naval Electronic Systems Command, *FFG-45 thru. FFG-55 Communication Antenna Configuration Data*, pp. 10-13, Washington, DC. 20360, July 1984.
10. Naval Postgraduate School Report MVS-01, *User's Guide to MVS at NPS*, by J. Favorite, p. 29, November 1983.

## INITIAL DISTRIBUTION LIST

	No. Copies
1. Defense Technical Information Center Cameron Station Alexandria, VA 22304-6145	2
2. Library, Code 0142 Naval Postgraduate School Monterey, CA 93943-5002	2
3. Department Chairman, Code 62 Dept. of Electrical and Computer Engineering Naval Postgraduate School Monterey, CA 93943-5000	1
4. Prof. Richard W. Adler, Code 62AB Dept. of Electrical and Computer Engineering Naval Postgraduate School Monterey, CA 93943-5000	5
5. Prof. Hung Mou, Lee, Code 62LH Dept. of Electrical and Computer Engineering Naval Postgraduate School Monterey, CA 93943-5000	1
6. Choi, Il Yong 356 Shin li Dongtan meon Hwaseong kun Gyungki do 170-83 Republic of Korea	8
7. Naval Academy Library Jinhae City, Gyungnam 602-00 Republic of Korea	2
8. LCDR Baek, Chil Ki SMC 1646 Naval Postgraduate School Monterey, CA 93943-5000	1
9. LT Lee, Hoon Sub SMC 1935 Naval Postgraduate School Monterey, CA 93943-5000	1
10. LT Shin, Dong Yong SMC 1732 Naval Postgraduate School Monterey, CA 93943-5000	1

- |     |   |   |
|-----|---|---|
| 11. | Captain Lee, Jun<br>SMC 1215<br>Naval Postgraduate School<br>Monterey, CA 93943-5000                      | 1 |
| 12. | Al Christman Roger Radcliff<br>Ohio University, Clipping Res. Labs<br>Athens, OH 45701                    | 1 |
| 13. | Harold Askins<br>NESEC Charleston<br>4600 Goer Rd.<br>N. Charleston, SC 29406                             | 1 |
| 14. | W. P. Averill CAPT<br>U. S. Naval Academy,<br>Department of Electrical Engineering<br>Annapolis, MD 21402 | 1 |
| 15. | J. K. Breakall<br>Lawrence Liv. Nat'l. Lab.<br>P. O. Box 5504, L-156<br>Livermore, CA 94550               | 1 |
| 16. | I. C. Olson, NOSC Code 822(T)<br>271 Catalina Blvd.<br>San Diego, CA 92152                                | 1 |
| 17. | Mr. Jim Logan, NOSC Code 822(T)<br>271 Catalina Blvd.<br>San Diego, CA 92152                              | 1 |
| 18. | John W. Rockway, NOSC Code 822(T)<br>271 Catalina Blvd.<br>San Diego, CA 92152                            | 1 |
| 19. | E. Thowless, NOSC Code 822(T)<br>271 Catalina Blvd.<br>San Diego, CA 92152                                | 1 |
| 20. | W. F. Flanigan, NOSC Code 825<br>271 Catalina Blvd.<br>San Diego, CA 92152                                | 1 |
| 21. | R. Raschke, GE Elec. Co., BLDG 3, RM 3312<br>- P. O. Box 2500<br>Daytona Beach, FL 32015                  | 1 |
| 22. | J. J. Reaves JR., Naval Elec. Sys. Eng. Cntr.<br>4600 Marriot Dr.<br>N. Charleston, SC 29413              | 1 |
| 23. | Alfred Resnick, Capital Cities Comm. ABC Radio<br>1345 Ave. of Americas 26th Floor<br>New York, NY 10105  | 1 |

- |     |   |   |
|-----|---|---|
| 24. | M. Selkellick, Code 825<br>David Taylor Naval Ship Research<br>Development Center<br>Betheseda, MD 20084-5000               | 1 |
| 25. | D. Faust<br>Evring Research Institue<br>1455 W 820<br>Provo, UT 84601   | 1 |
| 26. | Robert Latorre<br>Lawrence Liv. Nat'l. Lab.<br>P. O. Box 5504, L-156<br>Livermore, CA 94550                                 | 1 |
| 27. | Ron Corry<br>USAISEA ASBH-SET-P<br>Fort Huachuca, AZ 85613-5300   | 1 |
| 28. | Bill Alvarez<br>USAISEA ASBH-SET-P<br>Fort Huachuca, AZ 85613-5300  | 1 |
| 29. | Janet McDonald<br>USAISEA ASBH-SET-P<br>Fort Huachuca, AZ 85613-5300  | 1 |
| 30. | Dr. Tom Tice<br>Department of Electrical and Computer Engrg.<br>Arizona State University<br>Tempe, AZ 85287                 | 1 |
| 31. | Dr. Roger C. Rudduck<br>Ohio State University<br>Electrophysics Laboratory<br>1320 Kinnear RD.<br>Colombus, OH 43212        | 1 |
| 32. | Commander Naval Space and<br>Naval Warfare Systems Command<br>Attention: Dick Pride<br>PDW 110-243<br>Washington D.C. 20363 | 1 |
| 33. | Naval Sea System Command<br>Attention: P. Law<br>C61X41<br>Washington D.C. 20362  | 1 |
| 34. | James Tertocha<br>C-15 Fenbvtowne Apts.<br>Delran, NJ 08075   | 1 |

- |     |  |   |
|-----|--|---|
| 35. | Director Research Administration, Code 012<br>Naval Postgraduate School<br>Monterey, CA 93943-5000 | 1 |
| 36. | Moray King<br>Evrin Research Institute<br>1455 W 820 N<br>Provo, UT 84601                          | 1 |
| 37. | H. Kobavashi<br>1607 Cliff Dr.<br>Edgewater, MD 21037  | 1 |
| 38. | Dan Baran<br>IITRI<br>185 Admiral Cochrance DR.<br>Annapolis, MD 21401                             | 1 |
| 39. | Brenton Campbell<br>ILL Inst. of Technology<br>185 Admiral Cochrance DR.<br>Annapolis, MD 21401    | 1 |
| 40. | Dawson Coblin<br>Lockheed M & S Co.<br>O/6242; B/130/ Box 3504<br>Sunnyvale, CA 94088-3504         | 1 |
| 41. | Dr. A. J. Ferraro<br>Penn: State University<br>Inosphere Res. Lab.<br>University Park, PA 16802    | 1 |
| 42. | Dr. S. J. Kubina<br>Concordia University<br>7141 Sherbrooke St West<br>Montreal, Que H4B1R6        | 1 |
| 43. | E. K. Miller<br>Rockwell Science Center<br>Box 1085<br>Thousand Oaks, CA 91365                     | 1 |
| 44. | Donald Wehner, NOSC code 744<br>271 Catalina Blvd.<br>San Diego, CA 92152                          | 1 |
| 45. | LCDR Youn, Duck Sang<br>SMC 1254<br>Naval Postgraduate School<br>Monterey, CA 93943-5000           | 1 |

46. LT Joo, Hyung Kyu  
SMC 1593  
Naval Postgraduate School  
Monterey, CA 93943-5000 1
47. LCDR Lee, Sang Sik  
Dept. of Electrical Engineering  
Naval Academy, Jinhae City, Gyungnam 602-00  
Republic of Korea 1

END

FEB.

1988

DTIC